MINISTRY OF EDUCATION AND SCIENCE OF UKRAINE
KHERSON STATE AGRARIAN AND ECONOMIC UNIVERSITY

M. H. Chekanovych

PRESTRESSED CONCRETE STRUCTURES: DURING-TENSIONING METHOD

Monograph

Odesa • 2026 • Oldi+

UDC 624.012.36+691.328.2+693.956
C51

Рецензенти:

B. H. Demchyna – Doctor of Technical Sciences, Professor at Lviv Polytechnic National University;

I. M. Dobrianskyi – Doctor of Technical Sciences, Professor at Ivano-Frankivsk National Technical University of Oil and Gas

Recommended for publication by the Academic Council of Kherson State Agrarian and Economic University (Protocol No. 7 dated March 27, 2025)

Chekanovych M. H.

C51 Prestressed Concrete Structures: During-Tensioning Method : monograph / M. H. Chekanovych ; Kherson State Agrarian and Economic University. – Odesa : Oldi+, 2024. – 160 c.

ISBN 978-617-8559-95-3

This monograph presents a method for prestressing reinforced concrete structures by applying stress to a freshly laid concrete mix. The technological processes required for implementing this method are examined in detail.

The book outlines a methodology for calculating the strength of compressed concrete with a matrix-frame structure. It provides equations that describe the stress state of reinforcement steel as continuous mathematical functions across its entire load-bearing range. Additionally, it offers an analytical derivation of stress-strain state equations for normal sections of reinforced concrete structures with solid circular and annular cross-sections, based on accepted assumptions.

A practical example of producing prestressed reinforced concrete structures using this during-tensioning method is discussed, along with quality control considerations.

This book is intended for professionals in the construction industry and may also be useful for postgraduate and university students specializing in construction.

UDC 624.012.36+691.328.2+693.956

ISBN 978-617-8559-95-3

ЗМІСТ

PREFACE

In the early third millennium, the artificial environment is characterized by the widespread use of concrete as a building material. The dominant position of cement concrete in construction is explained by the availability of unlimited raw materials in the Earth's crust, their relatively low cost, and the good physical and mechanical properties of concrete. Additionally, the continuous efforts of scientists and practitioners to improve high-strength concrete and enhance its physical and mechanical properties ensure its leading position among construction materials.

The ultimate result of numerous improvements is the rational use of concrete in building elements and structures. The combination of the beneficial properties of concrete and steel in reinforced concrete elements has secured the prominence of this material in load-bearing structures. The introduction of prestressing in reinforced concrete elements has allowed for relatively inexpensive, crack-resistant, and durable structures for buildings and facilities.

In the first half of the twentieth century, two fundamental methods of prestressing rebars and concrete compression were proposed: **"pre-tensioning"** and **"post-tensioning"**. Today, hundreds of approaches exist to implement these methods. Most of them have been well studied, and some of the best have been practically applied. Almost all of these approaches share one common feature: they involve transferring the prestress force of steel onto already hardened, high-strength concrete.

The potential for developing new, more efficient prestressing methods within the narrow framework of a single force transfer principle has largely been exhausted. According to most experts, this has led to a slowdown in progress in this field. In this situation, further development requires a qualitative transition to fundamentally new principles of prestressed concrete that would set a precedent for the rapid growth of ideas and innovations.

While working on this problem, the author proposed creating prestressing even at the stage when the cement concrete components are

still in the mixture form. That is, instead of waiting for the concrete to harden, the pre-compression force is applied directly to the fresh mix. In this process, the concrete mix is compacted and hardens under pressure, significantly increasing the concrete's strength in the structure. The rebar prestress is preserved due to the fact that, after compaction of a specially selected concrete mix, a sufficiently strong and rigid skeleton is formed from its solid constituents, and to it are the prestressed rebars fully or partially anchored.

Thus, a dual effect is achieved in a single technological operation: compacting the concrete mix through compression and tensioning the steel. As a result, the structure achieves high crack resistance and superior strength.

The practical implementation of the principle of transferring prestress force to freshly placed concrete requires the development of new technological solutions, including innovative, movable formwork systems capable of withstanding compression. Today, this new technology has been successfully developed and introduced into production and has been used in manufacturing large-scale reinforced concrete bridge elements.

CHAPTER 1
PRESTRESSED REINFORCED CONCRETE STRUCTURES AND THEIR PROPERTIES

1.1. Methods of Creating Prestress in Reinforced Concrete Structures

The first attempts to create prestressed reinforced concrete structures date back to the late 18th century. In 1886, a patent application (USA 875999) was filed in the United States, followed by a similar proposal in 1888 by W. Doering in Germany (DRP 535.48). These patents introduced reinforced concrete elements with prestressed reinforcement to prevent cracking in the tensile zone of concrete.

The concept of counteracting external loads with internal prestress was first expressed by G. Mendl in the Viennese journal *Zeitschrift d. Oster. Ing. u. Arch. Ver* in 1896.

In 1905, I. G. Lund from Norway proposed placing pre-stretched steel rods with threaded ends in floor slabs to prevent concrete cracking [1, 2]. In 1906, M. Kenen in Berlin conducted experiments with prestressed reinforcement encased in concrete. These tests demonstrated a significant increase in the load required to initiate cracking.

In 1908, K. R. Steiner suggested preventing early bonding between reinforcement and concrete, allowing the steel rods to be tensioned only after the concrete had gained sufficient strength (USA patent 903909). In 1910, Ziseler in Germany [3] and Sigwart in Switzerland applied steel wire wrapping under tension around concrete pipes, with Sigwart using a prestress of 62.5 MPa.

In the same year, 1910, K. Bach and O. Graf reported in their research [4] on the use of reinforcement subjected to a stress of 60 MPa in experiments. The curved placement of prestressed reinforcement followed by concreting was patented by V. Wilson in British patent No. 103681 in 1916.

In 1919, K. Wettstein (Bohemia) was the first to use thin wire, with a diameter of 0.3–1.2 mm and high initial tension, as prestressed reinforcement. By 1921, he had already demonstrated that thin high-strength wire could self-anchor in concrete [5]. In 1922, W. H. Hewett from the United States successfully eliminated tensile stress in circular reinforced concrete tanks by applying wire tension [6].

Between 1923 and 1925, R. H. Dill in the United States proposed a method for producing prestressed beams by tensioning high-strength steel wire after the concrete had hardened. To prevent early bonding, he suggested applying a protective coating to the wire. Dill's approach is considered a precursor to the modern post-tensioning method, where prestress is transferred to fully hardened concrete (Figure 1.1).

In 1927, Rich Ferber patented (DRP 557331) a technique for placing unbonded steel reinforcement in concrete, allowing post-hardening tensioning. He suggested coating steel with paraffin or installing metal or cardboard sleeves, a concept now used in modern tendon ducts. The latter, as is known, has been reflected in modern conduit formers for reinforcement.

During that period, most prestressing methods provided only temporary strengthening, improving crack resistance in the early stages. Over time, the prestress diminished, and structures behaved like conventional reinforced concrete. This was due to relaxation in the reinforcement, shrinkage, and creep of concrete, leading to losses in prestress force.

Prestressed reinforced concrete became widely used only after 1928, when E. Freyssinet convincingly demonstrated in French patents 680547 and 36703 that reinforcement needed to have a tensile strength above 400 MPa and a high yield limit. His work focused on pre-tensioning on fixed supports before casting (pretensioning) (Figure 1.1).

For the production of prestressed concrete pipes, E. Freyssinet suggested simultaneous compaction of concrete through pressure and transverse reinforcement tensioning [8, 9]. By 1938–1939, Germany had industrialized the manufacture of such pipes, using internal pressure to stretch circumferential reinforcement. Here, excessive internal pressure was created to tension the wound reinforcement wire.

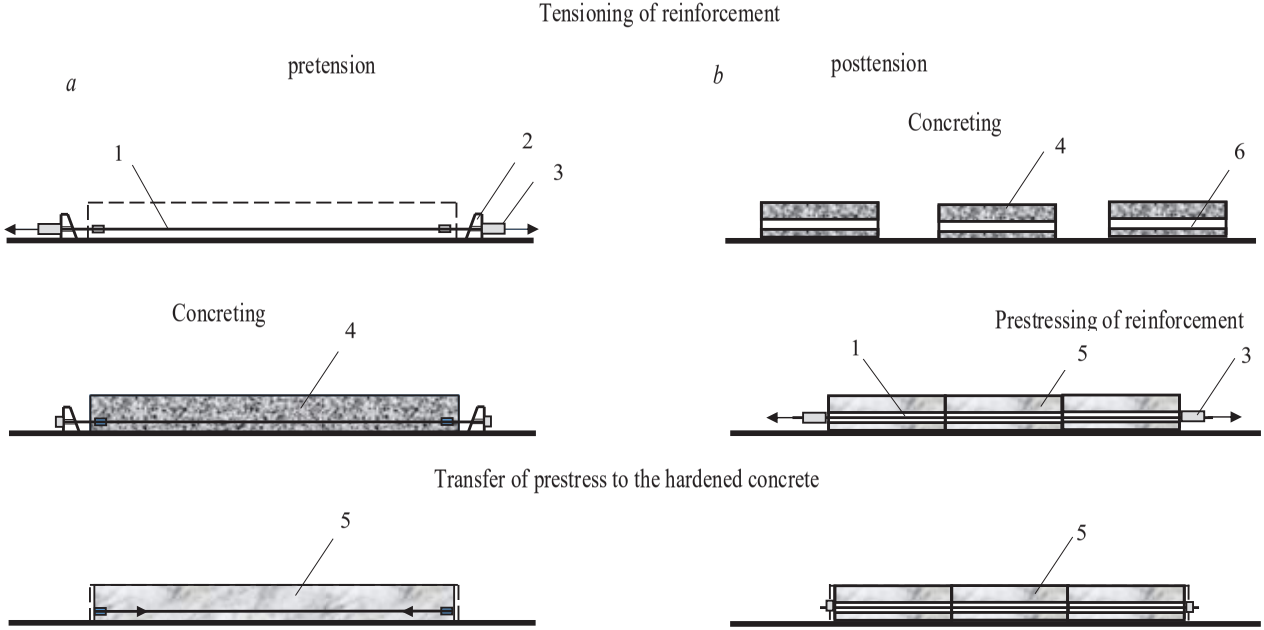

Figure 1.1. Diagram of prestress formation in reinforced concrete elements:
***a** – Pretensioning method; **b** – Post-tensioning method:*
1 – Reinforcement; 2 – Abutment; 3 – Jack; 4 – Concrete mix; 5 – Hardened concrete; 6 – Duct; 7 – Anchor

As a result, the pipe diameter increased by an amount corresponding to the elongation of the circumferential reinforcement. High-quality compaction of the concrete mixture was ensured by the application of radial pressure on the outer surface of the pipe. The ratio of external to internal pressure during production shifted over time in favor of the latter. It was recommended to carry out concrete compaction by pressing when the setting process had already begun.

In the 1939 work [10], F. Emperger proposed mixed reinforcement of reinforced concrete structures with partial prestressing. F. Emperger's idea became highly relevant for the further development of reinforced concrete element design. The concept of placing prestressed reinforcement in open ducts, followed by tensioning on hardened concrete and filling the duct with concrete, was introduced by P. Abeles (England) in 1942–1943.

In 1942, K. B. Bilner from the USA proposed a thermoelectric method for prestressing reinforcement. The distinctive feature of this method was coating the reinforcement bar with a thermoplastic material containing sulfur and tensioning it after the concrete had hardened by passing an electric current through the bar. In this process, the heated coating of the reinforcement softened and acted as a lubricant, helping to reduce prestress losses caused by friction in the reinforcement.

In the 1940s, the Bauer–Leonhardt method [11] was developed in Germany for the simultaneous tensioning of all prestressed reinforcement on hardened concrete. This method was used in the construction of several bridges [12; 13].

After 1945, several major works on prestressed concrete were published abroad, including those by I. Guyon, G. Magnel, E. Mörsch, F. Leonhardt, P. Abeles, H. Rüsch, T. Lin, L. Pacholík, G. Kani, and many others [14–21]. Similar to most foreign authors, Dr.-Ing. G. Kani, in his work [22], considered prestressed concrete as an independent material, obtained by transferring the prestressing force from the reinforcement to hardened, strong concrete.

The fundamental works of Professor F. Leonhardt, published in translation in 1957 and 1983 [23], made a significant contribution to the development and generalization of the results of earlier research on prestressed reinforced concrete. Notably, both by 1955 and 1980,

when these books were first published, the methods of prestressing reinforced concrete structures known in global practice remained within the framework of two techniques: tensioning the reinforcement against anchors (force-based method) before the concrete mixture had hardened, and tensioning the reinforcement on hardened concrete (Figure 1).

This is confirmed by data from A. Komendant's book [24], as well as the concluding materials of the International Federation for Prestressed Concrete (FIP) and the current International Federation for Structural Concrete (fib) [25–28]. In the book by Polish authors A. Ajdukiewicz and I. Mames [29], published in 1984, the creation of prestress in reinforced concrete structures is also noted to be carried out using these two aforementioned methods.

In all the cited works, regardless of the reinforcement tensioning method, prestressing was achieved by transferring the tensioning force from the reinforcement to the hardened concrete. Significant contributions to the development of efficient prestressed reinforced concrete structures were made by researchers such as A. A. Gvozdev, V. V. Mikhailov, S. A. Dmitriev, O.Ya. Berg, G. I. Berdichevsky, V. V. Baikov, A.Ya. Barashikov, A. P. Vasiliev, L. I. Storozhenko, T. M. Petzold, A. L. Shagin, A. I. Kozachevsky, and I. P. Shapoval. In the creation of new types of prestressed reinforcement and methods of tensioning, notable contributions were made by K. V. Mikhailov, N. N. Mulin, A. P. Korovkin, and E. G. Ratz. Research into the properties of prestressed concrete was advanced by S. V. Alexandrovsky, I. N. Akhverdov, F. I. Ivanov, I. I. Ulitsky, A. B. Golyshev, G. A. Klimov, A. E. Sheikin, V. M. Moskvin, and many others. In the field of bridge construction using prestressed reinforced concrete elements, significant achievements were made by N. M. Kolokolov, E. A. Troitsky, E. L. Shcherbakov, A. V. Zakharov, A. I. Druganova, Ya.D. Livshits, A. L. Tseitlin, and G. B. Fuks [30–46].

V. V. Mikhailov was the first to develop the method of continuous reinforcement (author's certificates No. 61894, 77326, 88356), which involved winding the reinforcement wire in a stressed state onto the supports of a stand or force-based form. Prestressing was achieved by passing the wire through blocks and devices of a tensioning

machine equipped with a tensioning station and a counterweight. The transfer of the prestressing force using this method was applied to the hardened concrete of the structure [31].

The problem of creating and calculating modern prestressed reinforced concrete structures has been addressed in the works of A. S. Zalesov, E. N. Kodysh, L. L. Lemysh, I. K. Nikitin [47], A. B. Golyshev, V.Ya. Bachinsky, V. I. Polishchuk, A. V. Kharchenko, I. V. Rudenko [48], V. N. Baikov and E. E. Sigalov [49], A. N. Kudzis [50, 51], A.Ya. Barashikov [52], G. B. Murashkin [53], E. M. Babich [54], O. A. Gershberg [55], L. K. Luksha [56], A. S. Dekhtyar [57], L. A. Murashko [58], L. I. Iosilevsky [59], A. E. Lopashto [60–63], Yu.A. Klimov [64], V. A. Sekhniashvili [65], V. M. Bondarenko and D. G. Suvorkin [66], B. V. Stefanovich [67], O. A. Volyansky [68], and many others. All these works highlight the possibility of prestressing reinforced concrete structures using either the "anchorage" method or the "hardened concrete" method. In both cases, the transfer of the prestressing force to the concrete occurs after it has gained sufficient transfer strength.

Recently, technologies aimed at reducing the production cycle of prestressed reinforced concrete structures and increasing their strength have been actively developed. These include methods that involve simultaneous pressing and tensioning of reinforcement, followed by the transfer of the prestressing force to hardened concrete. Under the supervision of Prof. G. V. Murashkin, a press mold was developed and tested for producing rectangular cross-section elements (author's certificate No. 1390034), with the transfer of prestressing force applied to hardened concrete. This method involves transverse pressing of the solid prismatic element by externally applying pressure to its lateral surfaces. This process achieves tensioning of the longitudinal reinforcement and compaction of the concrete mixture, ensuring high concrete strength in the finished product. It should be noted, however, that achieving high-quality transverse pressing for large volumetric elements is challenging, and controlling the prestressing force of the reinforcement is difficult to carry out.

A reinforced concrete element with a rectangular cross-section and a hollow core can be manufactured through simultaneous pressing and prestressing of transverse reinforcement, as proposed by

V. G. Matveev and G. I. Amelkin (author's certificate No. 1047697). According to the invention, the concrete mixture is compacted by expanding the inner core of the formwork, while the reinforcement is tensioned and fixed using anchoring supports. The transfer of the prestressing force from the reinforcement is applied to the hardened concrete. The use of rigid anchors within the structure allows for controlled application of the prestressing force on the reinforcement. However, it is challenging to determine the exact pressure exerted by the formwork on the concrete mixture. Additionally, leaving steel anchors within each finished structure is not always economically justified.

It should be noted that for both of the aforementioned methods of transverse pressing of structures, there is a high likelihood of deformation (bending) of the transverse reinforcement bars during compression. This necessitates the implementation of special technological measures, as well as enhanced quality control procedures.

Among the proposed methods, a notable one developed in Japan (application No. 49-29936) involves manufacturing prestressed reinforced concrete through pressing, where the reinforcement bars passing through the element are tensioned simultaneously with the compaction of the concrete mixture. According to the Japanese application, a movable plunger positioned on top of the formwork is used to compress the concrete mixture. As the plunger presses down, it simultaneously drives a wedge mechanism that tensions the reinforcement bars. After the concrete hardens and gains the required strength, the pressing force is released, and the reinforcement is freed. The use of wedge devices for tensioning and releasing the reinforcement has made the technology simple and reliable, ensuring the necessary control over the reinforcement tensioning force.

The original Japanese technical solution, like other known methods of mechanical surface pressing, is characterized by a relatively small thickness of the concrete layer that can be effectively compacted. This limitation is due to technical constraints, as generating the required pressing force would demand an unjustifiably high effort. As a result, the production of massive structures with a densely compacted concrete structure is challenging within the framework of this technical approach.

The idea of using prestressing for compressing concrete mixtures was reflected in the works of Prof. Ye.M. Babich [69, 70]. Experimental production of prestressed piles was carried out at the Rivne Reinforced Concrete Plant. During the forming process, one end of the reinforcement bar was secured to a movable punch, while the other end was fixed in the grips of a jack. The bar was placed inside a closed form filled with a concrete mixture. When the reinforcement was tensioned, the mixture was compressed by the punch in the form under a pressure of 6–7 MPa [69]. The results showed that, despite the vibrational impact during compression in the closed form, a plug of compacted concrete formed near the ends, while the middle section of the pile remained insufficiently compacted. Due to friction forces, particularly the friction of the mixture against the formwork walls and jamming of coarse aggregate within the form, the prestressing force was effectively transferred to the rigid formwork. As a result, the reinforcement tensioning corresponded to the well-known "abutment method."

The problem of transferring prestressing force to freshly placed concrete and ensuring its uniform compaction has remained unresolved until recently. It could not be effectively addressed within the framework of existing technological capabilities of formwork systems, equipment, and machinery.

In the context of the above, the development of prestressed long-span reinforced concrete structures with reinforcement tensioning and the transfer of prestressing force to freshly placed concrete emerges as a relevant challenge for the further advancement of prestressed reinforced concrete technology. This approach would enable the production of efficient, high-strength reinforced concrete elements using medium-grade cements and standard aggregates.

1.2. Influence of Prestressing on the Physical and Mechanical Properties of Concrete

Concrete compression in reinforced concrete structures can be applied before hardening (by pressing the concrete mixture) or after hardening (by transferring the prestressing force from the

reinforcement). Applying an external load to concrete can significantly affect its physical and mechanical properties (see Fig. 1.2) [41–140]. Below are the most notable studies in this field.

The use of pressing as a method of compacting concrete mixtures and increasing concrete strength has been known for a long time. As early as 1879 in France, during the construction of a 276-meter-long tunnel under the Oise River, pressure compaction of the concrete mix was employed [71]. Later, French scientists E. Roberts and L. Lesse [72] studied vibration pressing in the production of precast reinforced concrete elements.

In the 1930s, E. Freyssinet applied pressing during the production of reinforced concrete piles and pipes [73]. Later, other compaction techniques were developed, including:

- "How-Con" technology in England for forming large-scale slabs and panels [74].
- "PressVacuum Concrete" and "Press-Bet" technologies in Poland.
- The "Spiroll" extrusion method in Canada [26], later improved by the Roth company [75].

All these techniques aimed to increase the strength of concrete by compacting the mix during molding, achieving varying degrees of success.

Recently, new power rolling (press rolling) methods [76] have allowed for significant increases in concrete strength [77] even when using medium-grade cements. Studies by A. V. Satalkin [78], P. Lermit [79], I. Bolomey[80], G. Z. Lokhvitsky [81], and V. V. Mikhailov [82] in the 1930s–1950s confirmed the effectiveness of pressing and optimized concrete mix compositions and compression regimes.

In the 1960s–1970s, many international studies focused on the strength of pressed cement stone, mortar, and concrete. One significant study by T. Klyuz [83] investigated cylindrical concrete samples (80–94 mm diameter, 80 mm height) subjected to pressures of 24–71 MPa. By day 28, the maximum compressive strength of cement stone reached 206 MPa under 71 MPa compression (initial water-cement ratio 0.6). The maximum strength of concrete samples (composition 0.4:0.6:0.06 – C:S:G:W) reached 91 MPa under 32 MPa compression.

According to S. D. Lawrence [84], cement stone achieved a compressive strength of 375 MPa after 28 days under 672 MPa double compression, followed by curing in water at 293K.

The theory and practice of pressed concrete were further developed by A. A. Ananenko, I. N. Akhverdyan, E. M. Babich, Ya.M. Belkin, A.Ye. Desov, I. R. Yenukashvili, G. V. Murashkin, O. P. Mchedlov-Petrosyan, A. V. Svitonsky, A. L. Tsionsky, M. G. Elbakidze, and others. Studies indicated a significant increase in the strength of vibrated concrete when pressed, making it suitable for high-strength reinforced concrete structures [43, 87–96].

In recent years, multiple studies have investigated the effects of prolonged concrete compression [97–116]. Research shows that increasing the duration of concrete exposure to pressure can significantly enhance its strength. Experiments by G. V. Murashkin on granite aggregate concrete (composition 1:0.68:1.94, W/C = 0.38, pressure P = 5 MPa) demonstrated a steady strength increase over 28 days when compression duration increased from 15 seconds to 7 hours.

According to A. A. Varlamov, the optimal curing period under pressure without thermal treatment is 12–16 hours, as this timeframe ensures sufficient early strength for formwork removal. The strength gain of compressed concrete during the first 16 hours of hardening is 2.2 to 2.6 times higher compared to the initial strength.

Observations from reinforced concrete pipe [82, 87, 107, 108] production (pressing at ~3 MPa for 10–12 hours with heat treatment) indicate a stable 1.5–1.7 times increase in strength by day 28. Observations on the strength development of concrete hardened under pressure indicate that even after 28 days, its rate of strength gain is at least equal to that of conventional concrete.

Thus, research confirms that pressed concrete strength continues to grow with increased compression time, suggesting that precompression in structures where concrete remains under sustained pressure is highly effective.

The magnitude of compression pressure significantly affects concrete strength. Studies indicate [43, 110, 111] that increasing pressure raises concrete strength, though the rate of strength gain decreases over time.

Key factors limiting pressure include:

- Strength properties of aggregate materials (weaker aggregates may crack under pressure) [91, 112].
- Technological equipment constraints.
- Economic feasibility of applying excessive pressure [107, 113, 114].

Studies suggest an optimal pressing pressure range of 0.1–10 MPa, which can increase compressive strength by up to 2.3 times [43, 99–106].

Aggregate quality also plays a crucial role. Research by S. Nagataki [112] shows that a 18% decrease in coarse aggregate strength resulted in a 70% reduction in concrete compressive strength due to aggregate crushing under pressure.

Findings by I. R. Yenukashvili [91] suggest that aggregate grains may begin fracturing at pressures as low as 5 MPa. Therefore, aggregate strength should at least match the hardened cement paste strength after compression [43, 91, 111].

Studies by A. V. Satalkin reveal that compression timing and speed significantly affect concrete strength. Optimal load application coincides with the end of the induction period (between the start and end of cement gel setting) [78, 111].

Research by I.Zh. Khusainov shows that rapid loading improves the strength of semi-dry mixes [115]. For higher moisture content mixes, slower pressure application leads to better strength gains.

With an increase in the moisture content of the mixture, a slower increase in pressure is required to enhance the concrete's strength. In the production of reinforced concrete pipes, the optimal rate of pressure application, according to the studies by A. E. Popov, A. L. Tsionsky, S. I. Korzun, and R. M. Ruditser [107, 95, 116, 117], is approximately 0.1 MPa per minute.

From the presented data, it follows that the research findings of various authors confirm consistent trends in the influence of these technological factors on the strength properties of concrete curing under pressure (Fig. 1.2). In addition to strength, the deformation properties of concrete are crucial for determining the load-bearing capacity of compressed reinforced concrete structures.

According to the research by Ye. Babich and V. Kizima [101], compressing the mixture under a pressure of 5–6 MPa increased the

elastic modulus of concrete from 27.6 × 10³ MPa to 35.4 × 10³ MPa, alongside a 63% increase in prismatic strength. In the study [118] by I. Ye. Seskin, V. A. Esmond, and G. V. Murashkin, it was demonstrated that the higher the pressing pressure, the greater the elastic modulus of the concrete. Their experiments showed that after 630 days of curing, the modulus for regular concrete was 30.8 × 10³ MPa, whereas for concrete compressed under 3 MPa and 5 MPa, it reached 45.7 × 10³ MPa and 47.8 × 10³ MPa, respectively.

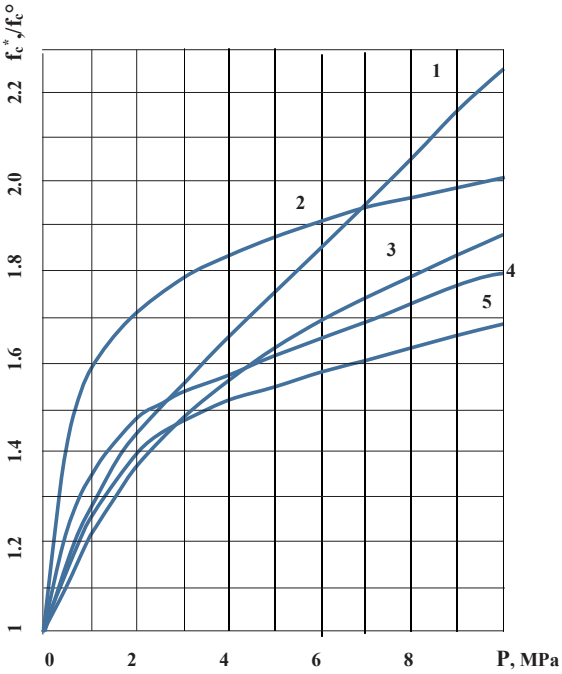

Figure 1.2. The effect of compression on concrete strengthening according to research data:
1 – [95]; 2 – [48]; 3 – [120]; 4 – [53]; 5 – [107]

The Poisson's ratio at a load equal to 20% of the prismatic strength was 0.13 for regular concrete and increased to 0.15 for concrete compressed at around 4 MPa. In I.Ye. Seskin's work [119], applying

6 MPa of pressure led to a maximum modulus increase of 38% by the seventh day of curing.

Research by A. A. Varlamov, A. L. Krishan, and V. G. Matveev [120] also confirmed an increase in the elastic modulus of compressed concrete by up to 35% compared to ordinary concrete. The enhancement of the initial elastic modulus due to compression is consistently noted by nearly all researchers.

The possibility of increasing the ultimate compression of concrete is indicated in the work of Ye.M. Babich [69]. In the research conducted by H. V. Murashkin [53], for concretes with a cement content of 500–700 kg per cubic meter and a large aggregate grain spacing factor ($\boldsymbol{\alpha}_{spacing} > 1.5$), an increase in the values of relative compression deformations corresponding to the maximum load – $\boldsymbol{\varepsilon}_{cf}$, and the ultimate load – $\boldsymbol{\varepsilon}_{cu}$, was obtained.

Specifically, for concrete compressed under a pressure of 3 MPa, the value of $\boldsymbol{\varepsilon}_{cf}$ was 315×10^{-5}, and $\boldsymbol{\varepsilon}_{cu}$ was 388×10^{-5}. The concrete testing was carried out in a steel cylinder with a height-to-diameter ratio of two. These testing conditions are unlikely to be considered close to standard, and further clarification of the parameters of compressed concrete is necessary.

Since the application of a load to the concrete mixture alters the water-cement ratio, causes structural changes, and generates an initial stress field, this affects the magnitude of both the inherent deformations and the creep deformations of compressed concrete.

According to the research by Ye.M. Babich [70], the values of shrinkage and creep deformations in compressed concrete are reduced by half compared to ordinary concrete.

The results of studies by V. G. Matveev, A. L. Krishan, A. A. Varlamov, and H. I. Amelkin [121] indicate that under a compression pressure of 3 MPa, the shrinkage and creep deformations of concrete decrease by 2 and 1.5 times, respectively. At a pressure of 6 MPa, shrinkage deformations are practically eliminated, while creep deformations are reduced by half.

Experimental and theoretical data on the inherent deformations and creep deformations of compressed concrete, obtained by H. V. Murashkin, are considered as the sum of decompression and shrinkage deformations of the concrete [53, 98].

Experiments [53], as well as other studies [107, 122–124], show that decompression deformations are functionally dependent on the magnitude of the compression pressure and are opposite in magnitude to shrinkage deformations.

According to H. V. Murashkin, the total value of decompression and shrinkage deformations of test samples on the 300th day of concrete curing is close to zero when the compression pressure is 6 MPa.

At earlier stages of concrete curing, decompression deformations dominate over shrinkage. For concrete compressed under a pressure of 3 MPa, a reduction of inherent deformations by nearly half is observed compared to ordinary concrete.

Regarding the creep deformations of compressed concrete, studies [53, 119, 124, 125] indicate that they depend on the composition of the concrete mix, the magnitude of the compression pressure, the timing and magnitude of the applied load, and other factors.

In these studies, the loading of compressed concrete samples and observations of creep deformations were carried out after decompression, starting from the seventh day.

According to experimental research results, the creep rate for concrete compressed at a pressure of 3 MPa decreased by 1.64 times at a load level of 0.3 and by 1.52 times at a load level of 0.7. For concrete compressed at double the pressure, i.e., 6 MPa, the reduction in creep rate was 2.36 and 2 times, respectively, at the same load levels.

The presented research results indicate a reduction in the creep deformations of hardened concrete with an increase in the compression pressure of the mixture. This finding is significant for the design of prestressed reinforced concrete structures.

At the same time, it should be noted that the conducted studies did not include continuous observations of the concrete deformation process starting from the moment of mixture compression. It is possible that during this initial period, significant deformations occur, related to contraction and other processes that take place during the hardening of compressed concrete.

Numerous studies on the properties of concrete subjected to compression after hardening have been conducted both in Ukraine and

abroad. Particular attention is drawn to research on early loading, as the influence of preloading on concrete characteristics increases with the reduction of the concrete's age at the time of loading [126–147].

Overall, early loading of concrete can be considered a specific case of long-term compressed concrete.

The experiments conducted by R. A. Melnyk [128] demonstrated that preliminary compression of hardened concrete at an early age intensified the growth of compressive strength by 20–25% and increased the modulus of elasticity by up to 6%.

Research on the influence of load levels on the mechanical properties of concrete by O. Ya. Berg [33, 129], I. N. Akhverdov [130, 131], Ye.M. Babich [69], and others is analyzed in the work of A. V. Satalkin [132], who reached the following conclusions:

a) Loading concrete at a certain intensity can lead to an improvement in its structure and enhancement of its properties, such as increased strength and water resistance, as well as reduced shrinkage and creep;

b) Improvement in structure and enhancement of properties under load are observed in concrete of any age and can be considered a general pattern inherent to materials capable of plastic deformation under stress.

According to research analysis, the optimal loading intensity for concrete is approximately 0.4 of its compressive strength.

In the experimental studies of pre-compressed concrete conducted by I. N. Akhverdov and I. V. Podmostko [131], an increase of up to 30% in the modulus of elasticity was observed for concrete with a compressive strength of 50 MPa when loaded at the age of three days. In contrast, when the same concrete was loaded at the age of three months, the increase in the modulus of elasticity did not exceed 9%. This highlights the effectiveness of applying load to concrete at the earliest stages.

According to the research conducted by L. P. Makarenko and G. A. Fenko [133], A. I. Semenov and S. I. Arzhanovsky [134], as well as A. P. Kudzis and V. M. Glebov [135], an increase in the compressive strength of concrete by 20–25% and in the modulus of elasticity by 15–20% can be achieved when the intensity of long-term concrete compression reaches 0.4–0.47 of the prism strength.

However, tests on compressed specimens in a series of experiments revealed a decrease in the tensile strength of concrete.

According to the studies by L. P. Makarenko [27], after long-term compression, the tensile strength of concrete decreased by 25–35%, while the ultimate tensile strain was reduced by 35–50%. As noted by the author, this reduction lowers the cracking moment in the tensile zone of beams.

Numerous experiments conducted by various researchers, including A. V. Satalkin and B. A. Senchenko [136, 137], V. A. Zedgenidze, V. M. Oplachko, and V. I. Polovets [138], O. B. Golishev and O. V. Melnychenko [139], D. R. Mailian [127], and Yu.A. Ivanova and L. I. Syrovatka [140, 144], have confirmed that under compression, concrete is capable of improving its structure and physico-mechanical properties. This can be effectively utilized to enhance the load-bearing capacity of reinforced concrete elements.

From the above, it follows that compressing freshly placed concrete mixture is more effective than early loading of hardened concrete and can significantly improve the physico-mechanical properties of concrete. It enhances compressive and tensile strength, increases the initial modulus of elasticity and the value of relative deformations (ε_{cf}), and reduces shrinkage and creep deformations. These improvements can be advantageously utilized in prestressed reinforced concrete structures.

1.3. Analysis of Methods for Calculating the Load-Bearing Capacity of Prestressed Reinforced Concrete Elements

The load-bearing capacity of reinforced concrete structures largely depends on the physical and mechanical properties of concrete and reinforcing steel. As demonstrated in the previous section, compression of the concrete mix and hardened concrete significantly affects strength and deformation characteristics. Numerous studies have been conducted to account for these changes when determining the load-bearing capacity of reinforced concrete elements.

Several works [145–150] propose predicting the long-term strength of hardened concrete for structural calculations.

• Yu.V. Zaitsev [147, 148] suggests normalizing the working condition coefficient based on the load case and concrete class.

• I. E. Prokopovich [149] proposes adjusting strength calculations for prestressed elements by increasing Rsc (compressive strength) for high-strength reinforcement and modifying first-limit state calculations for over-reinforced bending and eccentrically compressed elements.

• V. M. Batashev and V. I. Fedorchuk [146] refine *Rc* and *Ec* values based on the level of compressive stress in the structure.

• D. V. Babenko recommends applying a 0.9 coefficient for permanent and long-term loads and 1.15 for short-term additional loads during operation.

In [126, 150], formulas are proposed to consider changes in prism strength (*Rc*) and initial modulus of elasticity (*Ec*) based on compression level:

$$R_c = R_c^0 + 0.26\ \sigma_{c,p} \tag{1.1}$$

$$E_c = E_c^0 + 230\ \sigma_{c,p} \tag{1.2}$$

Other works [127, 143, 151–154] suggest accounting for long-term load effects on beam load-bearing capacity by adjusting compressive strain limits to include creep deformations:

$$\frac{x}{x_1} = \frac{\varepsilon_{cu} + \varepsilon_{c(t)}}{\frac{R_i}{E_c} + \varepsilon'_{c(t)}}; \tag{1.3}$$

$$\frac{\sigma_s}{E_s\left(h_0 - x\right)} = \frac{\varepsilon_{cu} + \varepsilon_{c(t)}}{x}, \tag{1.4}$$

where

$\varepsilon_{c(t)}$ – creep coefficient;

$\varepsilon'_{c(t)}$ – additional strain at the boundary between elastic and plastic zones;

x – height of compressed zone;

x_1 | – of the compressed zone.

According to D. R. Mailian [127], failing to account for changes in compressed concrete properties can lead to errors in stress distribution in reinforcement and underestimating the actual load-bearing capacity by 20–25%. To correct this, he suggests using:

- a strength increase coefficient K_{Rc},
- a strain reduction coefficient $K_{\varepsilon c}$.

In the works of V. A. Zedgenidze and V. I. Polovets [153], as well as P. I. Vasiliev, Yu. I. Kononov, and Ya. N. Chirkov [152], the compression of hardened concrete is accounted for by introducing corresponding work condition coefficients into the calculations.

In strength calculations, V. Ya. Bachinsky and Yu. G. Ametov [151] assume that under prolonged loading, an internal force redistribution occurs between the concrete and reinforcement within the averaged section. This redistribution results from an increase in the height of the compressed zone and a reduction in the internal moment arm. At the same time, the contribution of the tensile concrete is neglected.

At the loading stage, a trapezoidal stress diagram in the concrete and a linear strain distribution law along the section height are assumed. The section's resistance is considered exhausted when the strain of the compressed fiber reaches its ultimate values. In calculations, a coefficient of concrete work conditions is introduced, determined based on research data [147].

Analyzing the aforementioned studies, it is important to note the existing contradictions regarding the effect of hardened concrete compression on its ultimate compressive strain. According to S. I. Lytvyak [143], the ultimate compressive strain of concrete increases, whereas D. R. Mailian [127] reports a decrease.

It can be assumed that under equal compression conditions, in hardened concretes with a higher cement paste content and greater dispersion of coarse aggregate particles, the ultimate strain may increase. Conversely, in cases where the aggregate forms a rigid framework within the concrete, this strain decreases, which can be explained by the structural characteristics of the concrete.

The above discussion pertained to structures in which concrete compression was applied after hardening. However, in reinforced concrete structures, pressurized concrete, which hardens under pressure, can also be used. The limited research on load-bearing

capacity in this area is based on the assumptions of existing standards [155] and is restricted to the adjustment of certain parameters.

For instance, in the work of A. A. Varlamov [156], an analysis of the stress-strain state characteristics of bar elements with a compressed concrete structure led to the conclusion that such structures can be calculated using existing standard methodologies. Based on the processing of experimental data, A. A. Varlamov adjusts the value of the stress diagram shape coefficient ω and the coefficient β, which characterizes the center of gravity of the stress diagram, in the standard calculation formulas.

A similar approach to assessing load-bearing capacity is found in the works of G. V. Murashkin [54] and I. E. Seskin [119]. A distinctive feature of their calculations is the consideration of decompression strains when determining the inherent deformations of concrete and the stress-strain state of the section.

According to the standards [155], calculations are performed based on the condition of ultimate equilibrium, where the stress state in the section is represented by a rectangular stress diagram in the compressed concrete zone and forces in the reinforcement, which depend on the height of the compressed zone. The ultimate equilibrium method is entirely justified for low-strength concretes and steels that exhibit a distinct yield plateau.

However, when using high-strength compressed concretes and high-strength reinforcing steels, there is a noticeable increase in the internal lever arm of forces, and experimental data may exceed calculated values by 20–25% or even more [157, 158]. The proposals of N. M. Mulin and Yu. P. Gushcha [155], aimed at reducing the discrepancy between experimental and theoretical data by introducing a dependence of the relative height of the compressed zone on the strength and deformation properties of concrete and reinforcement, imposed material property constraints on the ultimate equilibrium method, depriving it of universality.

As a result, to determine the load-bearing capacity of reinforced concrete elements with higher accuracy, calculation methods based on real stress-strain (σ-ε) diagrams of materials have been increasingly used in recent years. Notably, in international standards such as ECB-FIP (MC-90), stress-strain diagrams for concrete and

reinforcement with established ultimate stresses and strains are utilized in calculations [159].

Calculations of reinforced concrete structures using σ-ε\sigma – \varepsilonσ-ε diagrams obtained directly from material testing allow for the most accurate consideration of their properties, which is especially important for the still insufficiently studied compressed concretes. There are numerous proposals for the experimental determination of concrete's "σ-ε" diagram with a descending branch [54, 160, 161].

One successful solution was found at the Research Institute of Building Structures (NDIBK), where a special high-rigidity mechanical press is used to impose fixed deformations on a concrete specimen. The methodology for determining the σ-ε diagram and the description of the equipment are presented in the recommendations developed by V. Ya. Bachinsky, A. M. Bambura, S. S. Vatagin, and N. V. Zhuravleva [162].

Of particular interest in these recommendations is the methodology for determining the "σ-ε" diagram for non-uniformly compressed concrete. According to the guidelines, this involves testing rectangular cross-section beam specimens with specified dimensions, processing experimental data, and calculating the stresses corresponding to the observed deformations.

According to the research by S. S. Vatagin [163], the axial and non-uniform compression diagrams of concrete, obtained based on the "equivalent" section model, are identical. I. A. Uzun from OISI states that to transition from the axial compression diagram to the non-uniform compression diagram, an enhancement coefficient should be applied [164].

All of these findings pertain to conventional heavy concrete. However, there is a lack of comparative analysis data on axial and non-uniform compression for concrete compressed at the mix stage, which requires further study. Therefore, research is needed to justify the applicability of the axial compression diagram for calculating structures where non-uniform compression occurs in concrete that has been compressed at the mix stage.

To use the "σ-ε"diagram of concrete in the calculation of section load-bearing capacity, an analytical description of the diagram is

required. Numerous proposals exist for the functional representation of the "stress-strain" relationship of concrete, including those presented in the works of Ya.V. Stolyarov, G. K. Evgrafov, V. M. Baikov, L. I. Onishchik, R. O. Krasnovsky, I. E. Prokopovich, A. I. Zaikin, and N. I. Karpenko [165–175].

he description of the "σ-ε" diagram of concrete using a fifth-degree polynomial, based on research from NDIBK, ensures high accuracy, ease of use, and universality [176]. This polynomial can describe the compression diagram of concrete with strengths ranging from 10 MPa to 100 MPa with equal precision.

It can be assumed that, due to its universality, this mathematical expression can also be applied to compressed concrete.

This mathematical approach aligns with G. A. Murashkin's findings, confirming that stress-strain curves for pressed concrete resemble those of high-strength hardened concrete [154, 161, 163].

A. M. Bambura, V. Ya. Bachynskyi, N. V. Zhuravlova, and N. M. Pishkova developed "Methodical Recommendations for the Refined Calculation of Reinforced Concrete Elements Considering the Full Concrete Compression Diagram" [176]. These guidelines allow for determining the load-bearing capacity of elements with rectangular, T-shaped, and I-shaped cross-sections by finding the maximum on the "load-curvature" dependency curve.

In the calculations of the stress-strain state of the cross-section, the following assumptions are made:

1. The "equivalent" cross-section is considered as the calculation base, with deformations averaged over the length of the block between cracks.
2. The hypothesis of flat sections holds true for the assumed cross-section.
3. The relationship between stress and strain for concrete is expressed by a power polynomial, while for reinforcement, it follows a discrete-linear diagram.
4. The effect of progressive cracking is taken into account by multiplying by a corresponding coefficient.In the works of L. L. Lemish [177] and S. S. Vatagin [163], axial tension diagrams of concrete are considered to refine calculations. Based on experimental and theoretical data, S. S. Vatagin concludes that the behavior of

concrete in the tension zone has virtually no effect on the load-bearing capacity of reinforced concrete elements.

Therefore, when assessing the load-bearing capacity of reinforced concrete elements, it is sufficient to use a simplified rectangular stress distribution diagram for concrete tension in the cross-section, taking into account the coefficient ψbt in the stress-strain state equations. In most modern studies, numerical calculation methods using computers are preferred when solving integral equations of the stress-strain state (SSS). This approach is fully justified for practical calculations of the load-bearing capacity of reinforced concrete structures with complex cross-sectional contours.

However, for simple cross-sections that can be easily described analytically, such as rectangles, circles, or rings, an exact solution to the SSS integral equations, considering the accepted calculation assumptions, will be less cumbersome and can be fully or partially implemented within the capabilities of standard microprograms.

Moreover, an analytical solution is always more accurate than a numerical one, where significant error accumulation can occur due to approximation. It is important to note that while exact analytical solutions for the SSS integral equations are known for rectangular, T-shaped, and I-shaped cross-sections of reinforced concrete elements, such solutions are insufficient for circular and annular cross-sections. These cross-sections are particularly prevalent in various structures, such as columns, support shafts of buildings and structures, including bridge supports.

Based on the above, it can be concluded that research in the field of load-bearing capacity calculations for structures made from concrete compressed at the mixture stage is limited and requires further development. The determination of the load-bearing capacity of elongated structures with tensioned reinforcement and the transfer of pre-stressing force to freshly placed concrete requires investigation, as the production of such elements within the framework of existing technological solutions has proven challenging. The application of calculation methods using complete "σ-ε" diagrams for concrete in this class of structures is possible only after substantiating the identity or similarity of the axial and non-uniform compression diagrams for concrete pre-compressed at the mixture stage.

1.4. Conclusions and Research Objectives

The analysis of the aforementioned experimental and theoretical studies leads to the following conclusions:

1. The mechanical methods known in global construction practice for creating pre-stressed reinforced concrete structures involve transferring the pre-stressing force from the reinforcement to the concrete structure after it has hardened and reached the required strength.

2. Compression of hardened concrete has a relatively minor effect on its physical and mechanical properties. In cases of early loading of hardened concrete, the increase in compressive strength typically does not exceed 20%.

3. Pressing the concrete mixture and allowing it to harden under pressure can significantly enhance the compressive strength of concrete–by 1.5 to 2.3 times–and increase its tensile strength by up to 15–20%, while also altering the material's deformation characteristics.

4. The calculation of eccentrically compressed and flexural reinforced concrete elements, based on the use of experimental "σ-ε" diagrams for concrete and reinforcing steel, provides a more accurate picture of the stress-strain state of the element under load, allowing for a more precise assessment of its load-bearing capacity.

5. Based on the equivalent cross-section model and complete "σ-ε" diagrams of materials, analytical methods have been developed for calculating the load-bearing capacity of eccentrically compressed and flexural elements with rectangular, T-shaped, and I-shaped cross-sections. However, for circular and annular cross-sections, such analytical solutions require further development and refinement.

Research Objectives

1. To develop elongated reinforced concrete structures with enhanced load-bearing capacity, compressed by means of pre-stressing reinforcement on freshly placed concrete mixture. Propose a new method for their production, design principles for formwork and equipment that ensure the transfer of pre-stressing forces to the mixture, as well as measures for reliable quality control of compressed structures.

2. To develop an experimental methodology for studying the load-bearing capacity of eccentrically compressed and flexural reinforced

concrete elements manufactured by the method of pre-stressing reinforcement on freshly placed concrete mixture.

3. To experimentally determine the patterns of the influence of the preliminary compression level of the concrete mixture on the load-bearing capacity of reinforced concrete elements. Evaluate the possibility of using axial load diagrams of compressed concrete samples for calculating eccentrically compressed and flexural reinforced concrete elements produced by the new method.

4. Based on the "equivalent" cross-section model, develop analytical relationships for the stress-strain state and a methodology for determining the load-bearing capacity of eccentrically compressed and flexural reinforced concrete elements with circular, annular, and rectangular cross-sections, compressed using the "on the mixture" method. Assess the accuracy of calculations by comparing theoretical and experimental data.

5. Develop an algorithm for the practical calculation of reinforced concrete structures with circular, annular, and rectangular cross-sections pre-stressed on freshly placed concrete mixture. Verify the research results during the production of full-scale large-sized reinforced concrete structures.

CHAPTER 2
DURING-TENSIONING METHOD OF PRESTRESSING REINFORCED CONCRETE STRUCTURES

2.1. Methods of Prestressing Reinforced Concrete Structures

In modern construction, prestressed structures are traditionally manufactured either by tensioning the reinforcement against anchors before concreting or by tensioning the reinforcement after concreting onto the hardened concrete. The implementation of both methods of prestressing structures involves transferring the prestress forces of the reinforcement to the hardened concrete. This requires a certain amount of time for the concrete to achieve the necessary transfer strength and typically involves sequential operations of reinforcement tensioning and concrete compaction.

In such structures, it is challenging to significantly enhance strength, frost resistance, and water impermeability without substantial additional costs.

To develop high-strength and durable prestressed structures by making fuller use of the physical and mechanical properties of building materials, the author has proposed manufacturing structures with reinforcement tensioning and the transfer of prestress forces onto the freshly placed concrete mix [179, 186, 189, 212, 213–227]. The general scheme of prestressing methods in reinforced concrete structures, supplemented by the author's proposal, is presented in Fig. 2.1.

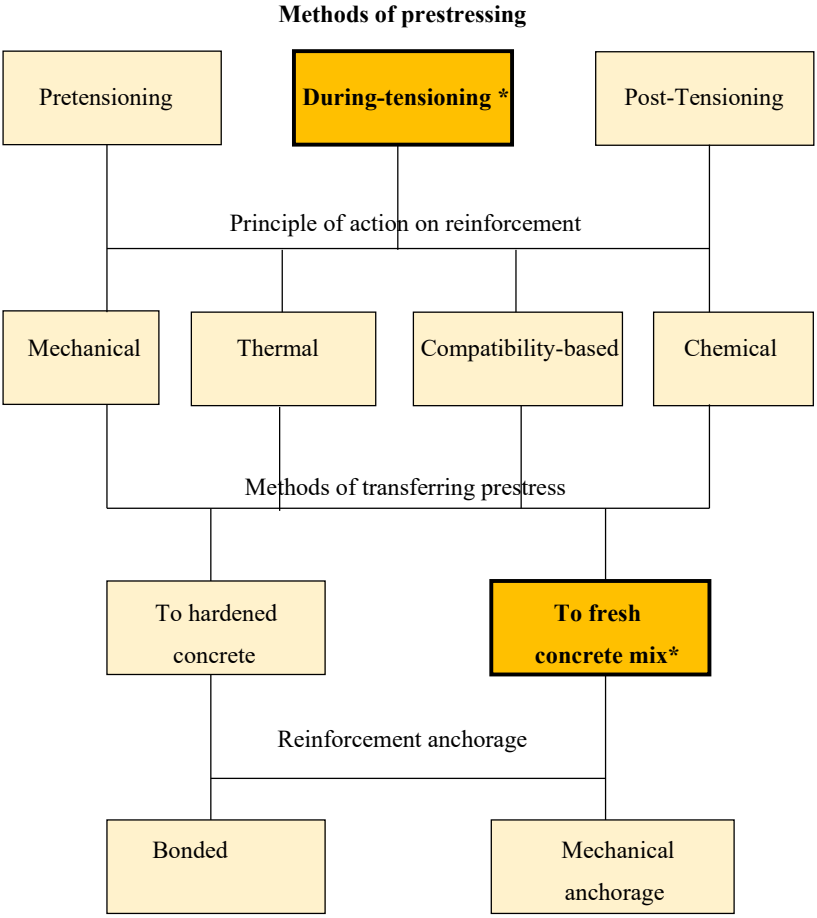

Figure 2.1. General classification of methods for inducing prestress in reinforced concrete structures

* Refers to freshly laid concrete mix being compressed.

2.2. Techniques for Manufacturing Reinforced Concrete Elements with During-tensioning on Freshly Laid Concrete Mix

In the technology of manufacturing prestressed reinforced concrete structures, tensioning the reinforcement onto the freshly placed concrete mix serves not only as a method for ensuring rigidity and crack resistance but also for increasing the load-bearing capacity of reinforced concrete elements. Within this approach, several specific methods have been developed for producing reinforced concrete elements, which involve either full or partial transfer of prestressing forces from the reinforcement to the compressed concrete mix.

Let us consider mechanical reinforcement tensioning methods, which are among the most reliable and precise in industrial production.

The production of reinforced concrete structures with reinforcement tensioning onto the compressed concrete mix involves placing the concrete mix using vibration, tensioning the reinforcement while simultaneously compressing the concrete mix, and subsequently curing the concrete in a compressed state. In this process, the concrete mix is compressed by the tensile force of the reinforcement, with full or partial transfer of this force to the mix before the concrete hardens (Author's Certificate No. 1548389).

During the transfer of prestressing forces from the reinforcement to the freshly placed concrete mix, the mix is compressed, expelling excess water and air beyond the formwork, compacting the aggregate, and improving surface contact (adhesion) with the reinforcement.

The compaction effect can be enhanced at the initial stages of compression through dynamic impact on the concrete mix, as well as by cyclically applying the load. In this process, the strength of the concrete mix components is utilized as a framework around which the reinforcement is tensioned.

Once the optimal density of the mix is achieved, the reinforcement tension force is increased to the required level. The concrete then hardens under the influence of the prestressing forces.

Thus, in a single operation and from a single drive, both the reinforcement tensioning and the concrete compaction through compression are performed simultaneously. The energy expended on reinforcement tensioning is utilized for compacting the concrete mix,

contributing to a reduction in the production cycle, an increase in concrete strength, and improved corrosion resistance of the structure.

The implementation of the proposed method of prestressing reinforced concrete elements is associated with the need for specialized formwork systems. An analysis of existing formwork design solutions, both in domestic practice and abroad, did not reveal an approach that ensures relatively uniform longitudinal compression of the concrete mix under the action of prestressing forces applied to the reinforcement [22, 31, 54, 105, 108, 136, 198–201, 204, 206, 207, 209, 211, 214–227]. This issue primarily arises due to the significant friction between the concrete mix and the inner surface of the formwork. When the end sections of a long structural element are compressed, the formwork absorbs a substantial portion of the prestressing force due to friction.

Under such conditions, the prestressing of reinforcement effectively corresponds to the conventional "pre-tensionsng" method, where the longitudinal rigid walls of the power formwork act as the abutments. Even with considerable friction reduction–achieved through the application of release agents, anti-friction coatings, or liners made of low-friction materials–the formwork still absorbs a significant portion of the longitudinal prestressing forces. As a result, the intended effect of prestressing "on the concrete mix" is largely negated, reverting to the traditional "abutment" method".

Therefore, for the effective implementation of this method, it is necessary to develop a fundamentally new formwork design that minimizes friction between the concrete mix and the formwork while ensuring a uniform stress distribution along the entire length of the element. Potential solutions may include the use of movable or flexible formwork walls, specialized vibration systems, or other innovative technical approaches.

Several traditional approaches have been tested to address this issue, including the introduction of specialized chemical admixtures into the concrete mix, the application of anti-friction coatings on the inner surface of the formwork, polishing of the formwork walls, the use of various liners made of materials such as PTFE (polytetrafluoroethylene), and the application of vibration and other dynamic effects.

Experimental studies have shown that these measures had some effect only on short laboratory specimens. However, they did not eliminate the transmission of longitudinal prestressing forces by the rigid formwork, especially in the production of long structural elements. Therefore, the challenge arose to develop a fundamentally new formwork system and equipment for the practical manufacturing of structures prestressed using the "on fresh concrete mix" method.

The author was the first to propose dividing the structural formwork into separate sections using deformation joints, with these sections interconnected by longitudinal guides (Author's Certificate No. 1548389). During longitudinal loading, the sections are able to move linearly and exert minimal resistance to compression. This type of formwork (Figures 2.2, 2.3, 2.4) practically does not absorb the longitudinal prestressing forces, thereby ensuring uniform transmission of prestressing compression to the fresh concrete mix along the entire length of the reinforced concrete element.

Since the longitudinal compressive force is almost entirely absorbed by the fresh concrete mix (due to the sectionalized formwork), and the transverse pressure on the formwork typically does not exceed 0.27–0.30 of the longitudinal pressure [111], it follows that the reinforcement is tensioned "on the concrete mix", with the prestressing force being directly transferred to the mix.

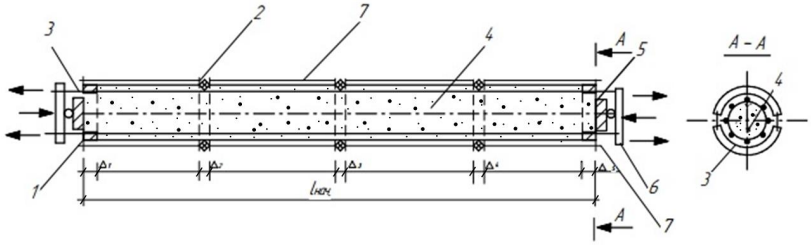

Figure 2.2. Longitudinally Movable Sectional Formwork for Prestressing Reinforcement on Concrete Mix

1 – formwork sections; 2 – transverse deformation joint; 3 – prestressed reinforcement; 4 – concrete mix; 5 – movable end; 6 – force traverse; 7 – longitudinal guides

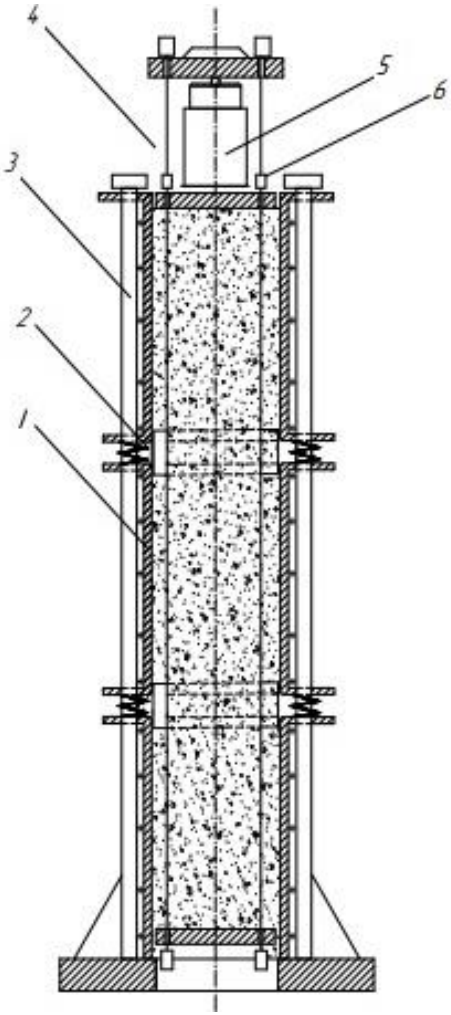

Figure 2.3. Longitudinally movable formwork for columns

1 – movable section; 2 – deformation joint; 3 – longitudinal guide; 4 – reinforcement bar; 5 – jack; 6 – fixator

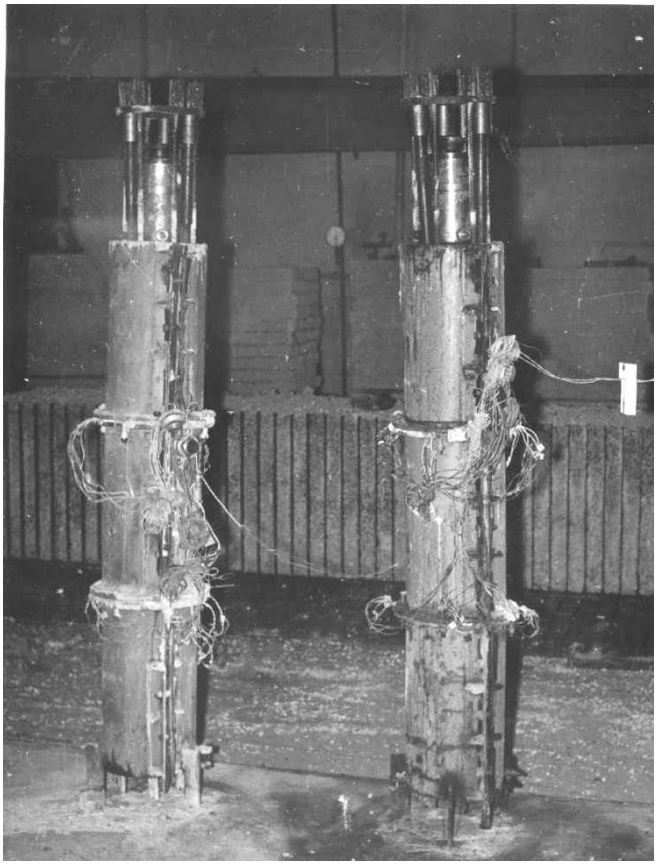

Figure 2.4. General view of the longitudinally movable formwork for columns

The working displacement of the formwork deformation joints is determined based on the condition of uniform compaction of the concrete mix along the entire element during the transfer of the prestressing force to the mix. This is achieved when the total possible displacements at the section joints, taking into account the movement of the formwork's movable ends, are equal to or exceed the displacement corresponding to the laboratory compaction of the concrete mix under the specified pressure.

To account for the condition of uniform compaction, it is convenient to use the specific compaction value:

$$\beta = \frac{\Delta V}{V}, \tag{2.1}$$

where ΔV is the change in the volume of the mix due to compression, and V is the initial volume of the mix.

For a constant cross-section of the formwork, the value of β is expressed as follows:

$$\beta = \frac{\Delta L}{L}, \tag{2.2}$$

where ΔL is the change in the initial length of the formwork L due to the compression of the concrete mix.

To determine the magnitude of the working displacement of the deformation joint, it is necessary to calculate the sum of the specific deformations of the concrete mix over the length of the section from the joint axis to the midpoint of the adjacent sections. The calculated length LLL in formula (2.3) is taken, according to the scheme shown in Fig. 2.5, as the sum of the distances from the midpoint of the adjacent sections to the axis of the deformation joint.

$$L = I_i + I_j \tag{2.3}$$

The minimum working displacement of the formwork deformation joint is determined by the formula:

$$\Delta L = \beta \cdot L, \tag{2.4}$$

where

- ΔL– minimum working displacement of the deformation joint;
- β – specific compaction of the concrete mix;
- L – design length according to the scheme (Fig. 2.5).

The value of β during compression is influenced by several factors, including the composition of the concrete mix, the quality of the formwork's shaping surfaces, friction between formwork elements and along the guiding tracks, and many other variables.

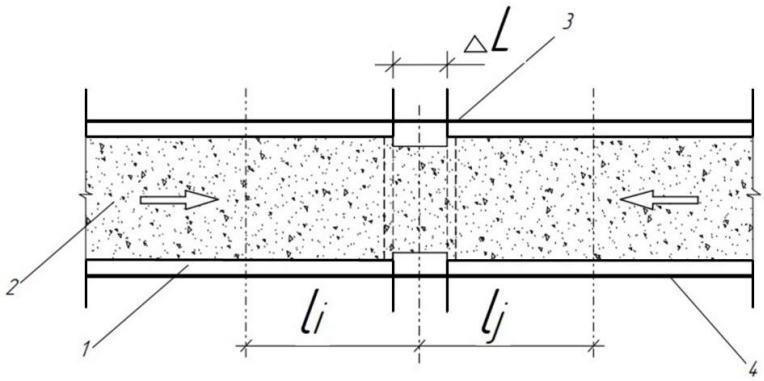

Figure 2.5. Scheme for determining the magnitude of the working displacement of the deformation joint:
1 – movable section; 2 – concrete mix; 3 – transverse deformation joint; 4 – longitudinal guides

In addition to the internal and external friction of the concrete mix, numerous other factors affect the compaction process, many of which are difficult to account for precisely.

Therefore, it is advisable to determine β using the experimental "β-p" dependence, obtained by compressing a sample of the concrete mix in a laboratory form with movable ends. When determining the practical working displacement of deformation joints, it is also necessary to consider the possibility of incomplete filling of the formwork with the concrete mix after placement.

The movable-sectional design of the formwork (Fig. 2.3) enables directed regulation of the density and strength of concrete within the element. This is achieved by specifying the appropriate displacements in the deformation joints of the formwork. Once the predetermined working displacement of the deformation joint is exhausted due to compression, adjacent formwork sections come into contact along their flanges, halting further compaction of the concrete mix in that section of the element.

This mechanism can be utilized to compensate for frictional forces during the production of long-span structures, ensuring uniform

density and strength along their length. The proposed production technology also allows for equipping each formwork section joint or a group of joints with individual actuators for controlled compaction of the concrete mix through compression.

To facilitate the longitudinal movement of sections in a long formwork, especially those located far from the movable ends, it is advisable to use spring, rubber, or other compression-transmitting devices between the sections. This approach helps achieve a more uniform or precisely controlled compaction of the concrete in the structure.

It should be noted that the excess water in highly flowable concrete mixtures, when expelled, leads to the formation of open channels and paths that reach the surface of the element. Therefore, for such concrete mixtures, it is necessary to apply high-frequency vibration after the complete cessation of water expulsion. This process helps to fill and seal the channels, paths, and pores with a cement-sand mortar. This method is effective for all implementations of the proposed pre-compression technique for concrete mixtures with excessive water content.

To improve the accuracy of structural fabrication, ensure the specified length, and prevent deformation of the reinforcement cage during the compression of the element, a specialized design for the end section of the formwork has been developed (Author's Certificate No. 1678618). Figure 2.6 presents the general view of one of the end sections of the formwork: (a) during reinforcement tensioning, (b) the same after its fixation.

Since the sleeve (4) is positioned within the formwork according to the specified dimensions of the product and is securely fixed, the required product length is maintained even if the piston (7) is recessed into its end. This design prevents deformation of the reinforcement cage (2) located beneath the sleeve (4) and significantly reduces the likelihood of jamming or clamping of the prestressed reinforcement (3).

If it is necessary to manufacture eccentrically precompressed reinforced concrete elements such as beams, columns, and slabs, in order to balance the eccentricity, in addition to compensators, the parallel tensioning of reinforcement for two or more elements can be used. Figures 2.7, 2.8, and 2.9 show the general view of a paired longitudinally movable formwork system during the simultaneous tensioning of reinforcement for two elements.

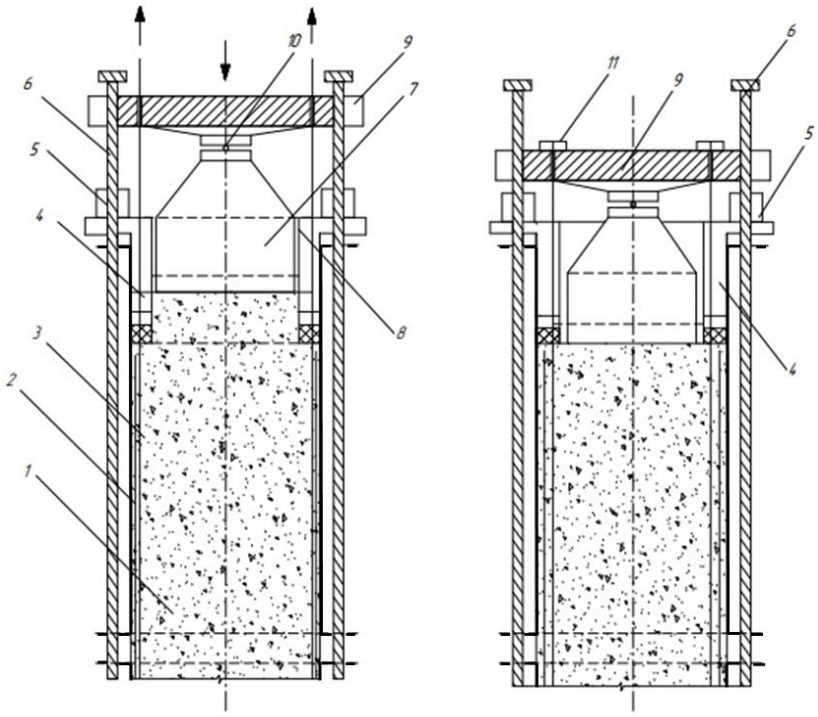

Figure 2.6. End section of the segmented formwork;
***a** – during reinforcement tensioning, **b** – after its fixation*
1 – concrete mix; 2 – reinforcement cage; 3 – prestressed reinforcement; 4 – sleeve; 5 – screw mechanism; 6 – guide; 7 – piston; 8 – retainer; 9 – power traverse; 10 – hinge; 11 – anchor

In mass production, the use of cassette technology is justified for manufacturing such precompressed reinforced concrete elements, particularly slabs. Cassette molds should typically have movable surfaces.

The transfer of prestressing force to the reinforcement can be carried out in stages both before and after the hardening of the

concrete mixture (Author's Certificate No. 1747632). The device for implementing this method is shown in Fig. 2.10.

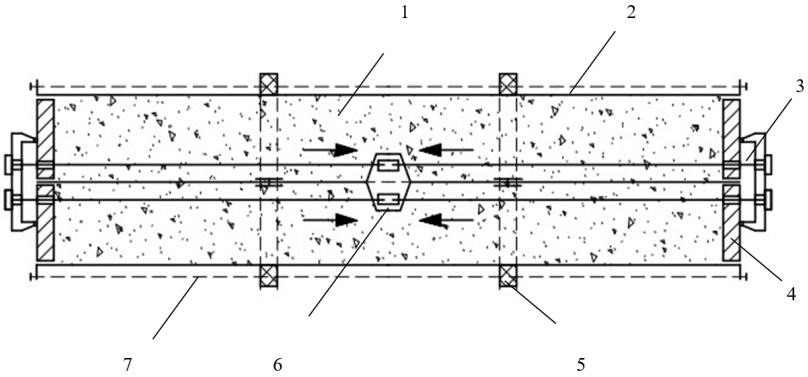

Figure 2.7. Paired Longitudinally Movable Formwork System During Reinforcement Tensioning on Freshly Placed Concrete Mix

1 – concrete mix; 2 – paired formwork sections; 3 – prestressed reinforcement; 4 – movable ends; 5 – deformation joint; 6 – joint anchor; 7 – section movement guides

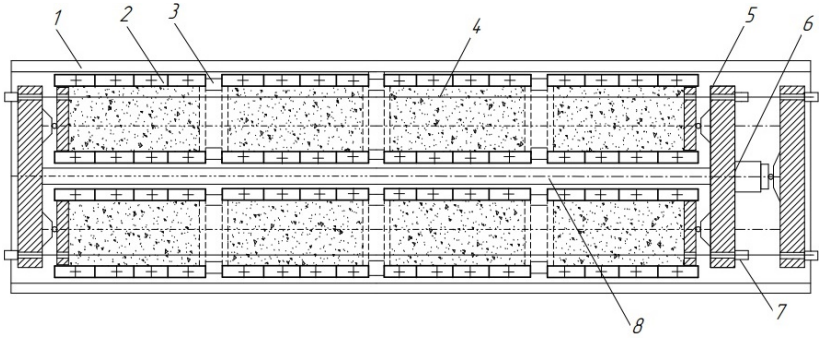

Figure 2.8. Longitudinally movable formwork for beams

1 – outer guide; 2 – movable section; 3 – deformation joint; 4 – prestressed reinforcement; 5 – traverse; 6 – jack; 7 – fastener; 8 – inner guide

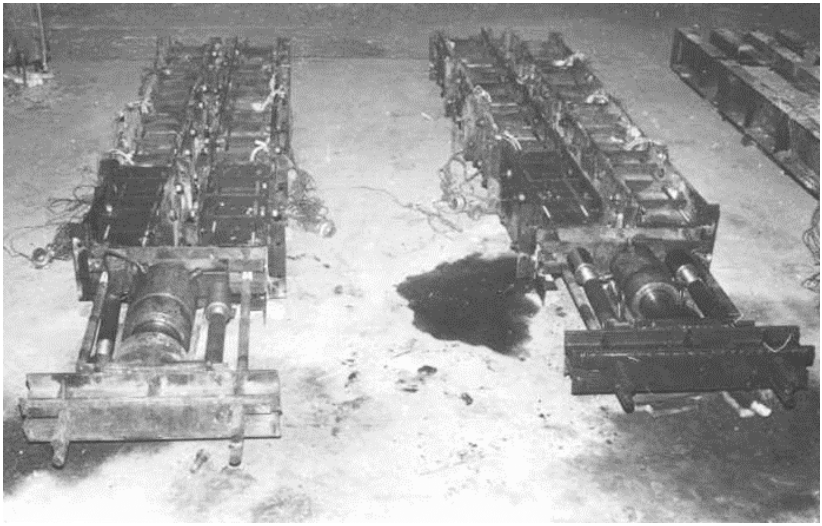

a

b

Figure 2.9. Longitudinally movable power formwork for beams. General view from the jack side:
a *and from the traverse side –* ***b***

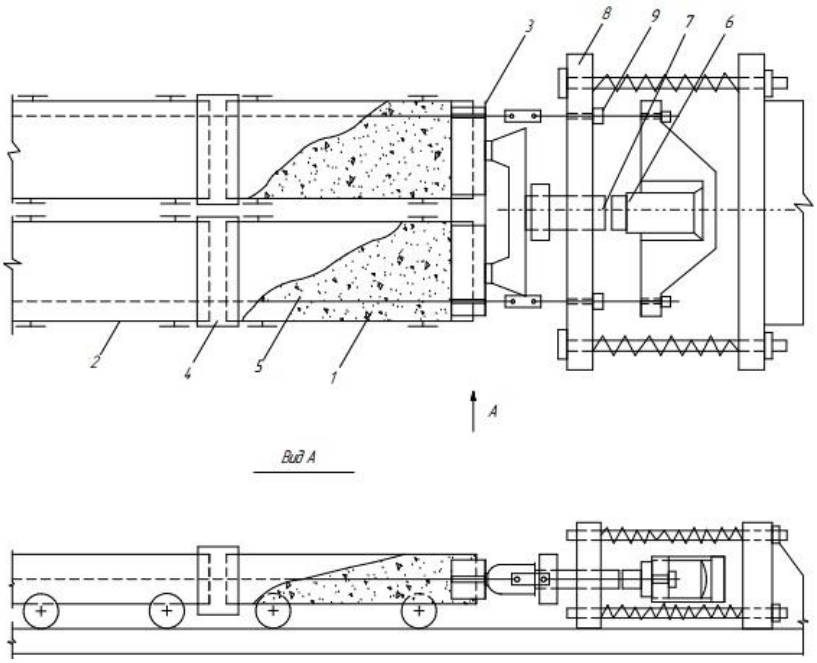

Fig. 2.10. Device for the Stepwise Transfer of Prestressing Forces to the Concrete Mixture:

1 – prestressed reinforcement; 2 – formwork sections; 3 – movable end; 4 – deformation joint; 5 – concrete mixture; 6 – hydraulic jack; 7 – screw; 8 – plate; 9 – nut

The increase in structural rigidity and crack resistance, while maintaining high strength, is achieved by transferring only part of the prestressing force to the freshly placed concrete mixture, followed by the full transfer of the prestressing force to the hardened structure. Additionally, the proposed method may provide for compressing the concrete mixture under the full tensile force of the reinforcement during the prestressing process.

To enhance the durability of the structure, a device is proposed that allows the compaction of the protective concrete layer through external volumetric precompression during reinforcement tensioning (Patent No. 175901). In Fig. 2.11a, the end view of the device is

shown during the compression of an annular cross-section element. In Fig. 2.11b, the cross-sectional view of the core is depicted during its separation from the finished structure.

As the reinforcement (11) is tensioned, the longitudinal ends of the outer shell (1) move towards each other, reducing the outer diameter of the forming space. This results in the compaction of the concrete mixture through external volumetric compression. To maintain the precompression force, a high-rigidity core (7) is used.

To release the core (7) from the finished compressed product, the drive shaft (8) with segments (9) is slowly rotated. The segments (9) press against the shaft (8), releasing the external compression from the core. Further rotation of the shaft (8) enables the separation of the sheet (10) from the inner contour of the reinforced concrete element. At each moment during the separation process, the detachment of the thin sheet (10) from the concrete surface occurs along a narrow strip of small area, minimizing force impacts during formwork removal.

The prestressing of a reinforced concrete element can be achieved through centrifugal forces with compaction of the concrete mixture– Fig. 2.12 (Patent No. 1330284).

For mass production of small-sized reinforced concrete elements with precisely defined geometric dimensions–such as railway sleepers (Fig. 2.13) – a manufacturing method (Patent No. 1799970) can be applied. This method ensures high strength and crack resistance of the structures by first transferring the prestressing force transversely to the reinforcement direction on the fresh concrete mixture. After the structure hardens, the reinforcement is released, and the same prestressing force is transferred longitudinally to the hardened concrete. The increased crack resistance effect is explained by the reduction of prestress losses during the setting and hardening of the concrete mixture.

The quality of the product can be improved by ensuring uniform compaction of the concrete mixture. This is achieved by reducing the size of the fixed mold-forming surfaces of the formwork and inducing compression of the mixture along the length of the product.

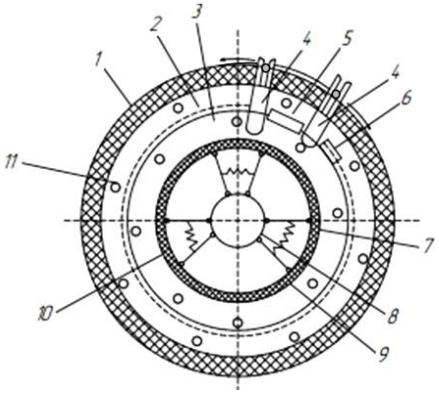

a

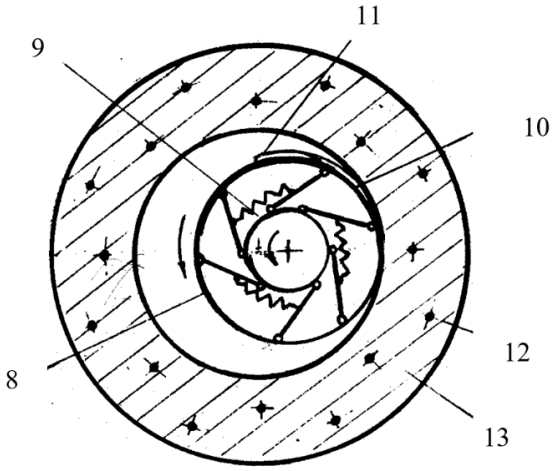

b

Figure 2.11. Diagram of the Manufacturing Process for a Ring-Section Element:

a *– end view of the device during external volumetric compression of concrete and prestressing of reinforcement;*

b *– cross-section of the finished element and the form core during its separation; 1 – outer casing; 2 – outer end ring; 3 – inner end ring; 4 – movable stops; 5 – hydraulic jack; 6 – ring rotation lock; 7 – rigid core; 8 – drive shaft; 9 – core segment; 10 – sheet inner casing fixed to one of the segments; 11 – prestressed reinforcement; 12 – concrete*

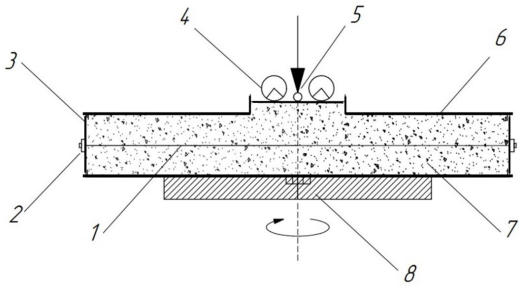

Figure 2.12. Diagram of Prestressing a Reinforced Concrete Element Using Centrifugal Forces:

1 – tensioned reinforcement; 2 – anchor; 3 – movable; 4 – vibropiston; 5 – hinge; 6 – formwork; 7 – concrete mix; 8 – rotating stand

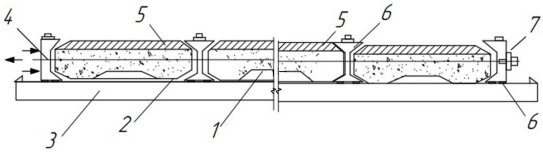

Figure 2.13. Diagram of a Device for Manufacturing Pre-Stressed Small Reinforced Concrete Elements:

1 – formwork molds; 2 – concrete mixture; 3 – guiding base; 4 – prestressed reinforcement; 5 – movable form shield; 6 – wedge clamps; 7 – retainer

Fig. 2.14 illustrates the mold developed by the author, which meets the specified requirements. The mold consists of an elastic movable casing (1), fixed in a stretched state on a spring frame (2), which is installed in a guiding sleeve (3). When the reinforcement (4) is tensioned, the concrete mixture (5) is compacted by compression. The movement of the spring frame in the compression direction is transmitted through the elastic casing, inducing uniform surface compaction of the concrete mixture. The gaps between the frame coils decrease, increasing the rigidity of the forming surface, which ensures a high-quality smooth product surface. The length of the mold shortens with slight transverse expansion, which contributes to the dense placement of coarse aggregate in the concrete.

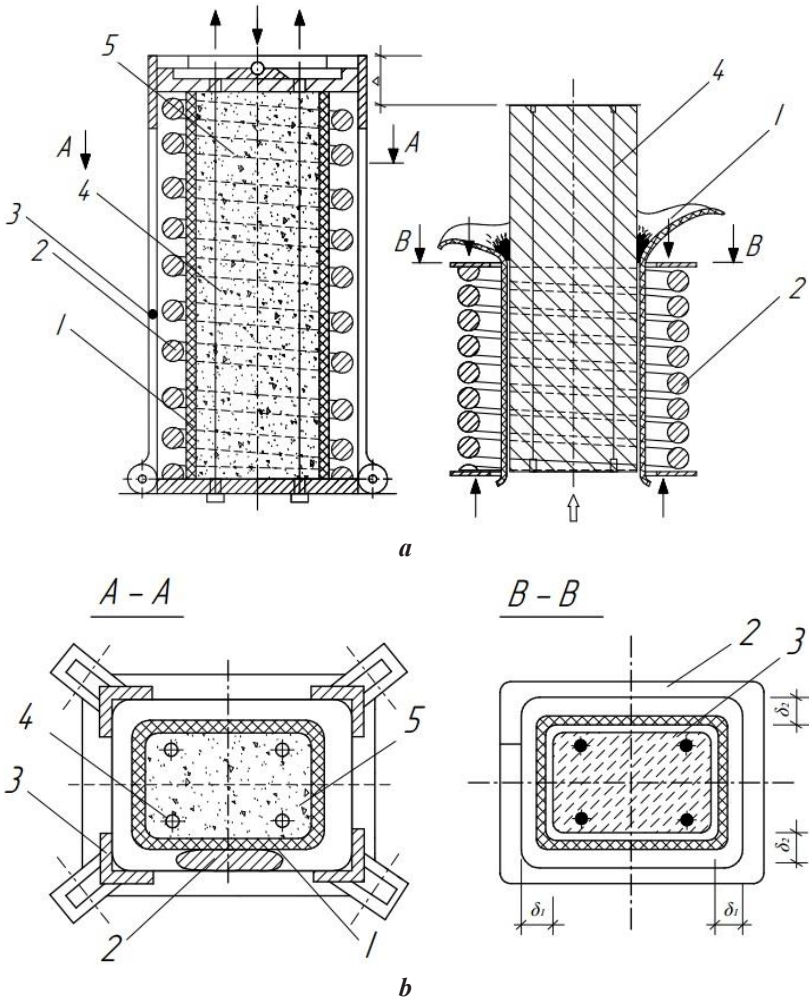

a

b

Figure 2.14. Longitudinally Movable Spring Mold:

a *– during reinforcement tensioning and concrete mixture compression;* ***b*** *– during demolding of the finished product: 1 – elastic shell; 2 – spring frame; 3 – guide casing; 4 – reinforcement; 5 – concrete mixture*

After the coarse aggregate is encased in the concrete mixture and the reinforcement reaches the designed stress, it is fixed in place. The further demolding of the finished product is carried out by separately compressing the spring frame (Fig. 2.14) and removing the elastic shell from the product.

A more versatile method for manufacturing prestressed reinforced concrete structures involves using formwork assembled from separate panels (Fig. 12). The key feature of this formwork is that the panels have a longitudinally movable surface. The mobility of the surface is ensured by the elasticity of the shell 1. The shell is secured in a stretched state on the rigid movable elements of the formwork. These elements are positioned with their axes 2 in longitudinal guides 3. Springs 4 are placed between the axes. All elements, except for the outermost ones, are designed as rollers 5. They make contact with the elastic shell along surface 3, providing it with the necessary rigidity.

To enable the placement of concrete mix into the formwork, the upper panel is designed as a grating, where instead of rollers, movable triangular cross-section elements 6 are used. During longitudinal compression, the rigid elements of the panels shift, promoting the compaction of the concrete mix. The space between them decreases, increasing the transverse rigidity of the form and ensuring the absorption of lateral expansion forces.

The presence of openings in the upper part of the formwork and fine perforations in the elastic shell facilitate the removal of excess water and air, preventing the formation of voids and pores. The movement of the form-shaping surfaces and the peristaltic action of the formwork contribute to closing open pores in the concrete.

Taking into account the above and the known methods and techniques for manufacturing prestressed reinforced concrete structures, the general scheme of their implementation is presented in Fig. 2.15.

The analysis of the considered technical solutions for manufacturing prestressed reinforced concrete structures by tensioning reinforcement on freshly placed concrete mix shows that the proposed technology significantly increases concrete strength, improves its joint performance with reinforcement, and enhances the durability of the structure by eliminating macro-defects and partially reducing micro-defects in the concrete structure.

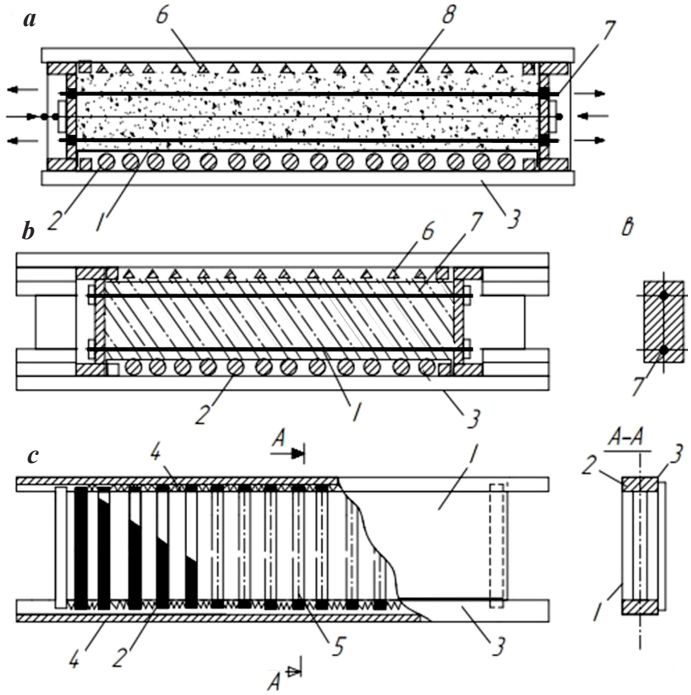

Figure 2.15. Longitudinally movable panel formwork and product:

a – preliminary compression; b – product in formwork; c – product cross-section; d – formwork panel: 1 – finely perforated elastic casing; 2 – roller axis; 3 – longitudinal guides; 4 – spring; 5 – roller; 6 – movable element of the upper panel; 7 – prestressed reinforcement; 8 – concrete mix

2.3. Technology for Producing Compressed Columns

The new technology was tested and refined under laboratory and production conditions during the manufacturing of both small and large-scale reinforced concrete elements with a volume of up to nine cubic meters. This allowed the research to cover the most commonly used construction volumes in practice.

The production of cylindrical support columns was carried out in accordance with the described technology, with the following specific features. The reinforcement cage, along with the rear movable end of the mold, was placed into the prepared lower half of the formwork (Figures 2.16, 2.17, 2.18). Initially, the rear end served as a jig during the fabrication of the reinforcement cage for the columns. The embedded component, designed as a flange at the end of the cage, facilitated the fixation of the reinforcement bars to the movable end. The rear end was positioned in the formwork according to the predetermined initial column length.

Next, the front end shield was installed and securely fastened to the lower half of the formwork using bolt connections. The protruding reinforcement bars of the cage were placed into the slots of the front end. These bars were then connected to the tensioning device using couplers and threaded rods. Any deviations in the actual length of the reinforcement bars were adjusted using threaded rods with nuts to ensure uniform tensioning of all bars.

After verifying the presence of through holes for the release of water and air in the upper half of the formwork, it was assembled onto the lower half and secured with clamping bolts

The initial position of the formwork sections before concreting was ensured by placing spacers in the joints between them, followed by securing the sections together with bolts. A special device for collecting concrete test samples was installed on the inspection window of the formwork.

After verifying the functionality of the pumping station and vibrators, the concrete mixture was fed into the formwork. The mixture was placed using vibrators to ensure proper compaction. Once the form was completely filled with concrete, the excess mixture was removed from the intake hoppers, and the hatches were sealed. The hatches were secured using a screw clamping mechanism.

Next, the process of pre-compression of the concrete mixture was initiated (Figs. 2.16, 2.17). For this, the spacers controlling the working movement of the deformation joints were removed from the formwork sections, and oil was pumped into the hydraulic jack cylinder. The compression force was gradually increased at a rate of 0.1 MPa per minute, with a hold time at each loading stage (no fewer

than ten) until the outflow of water from the designated formwork openings ceased.

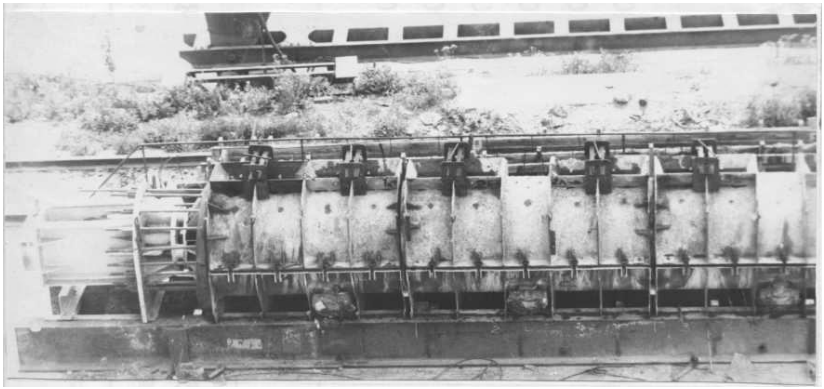

a

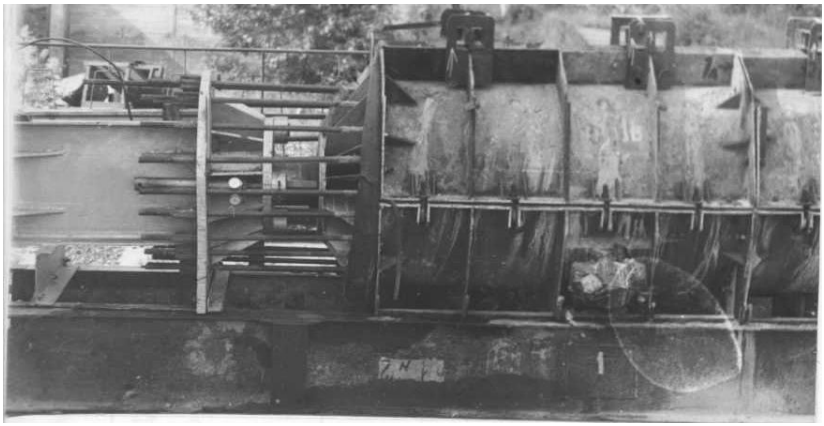

b

Figure 2.16. General view of the device for producing compressed bridge pier posts using the "on-mixture" method:
a *– top view of the longitudinally movable formwork;*
b *– tensioning unit*

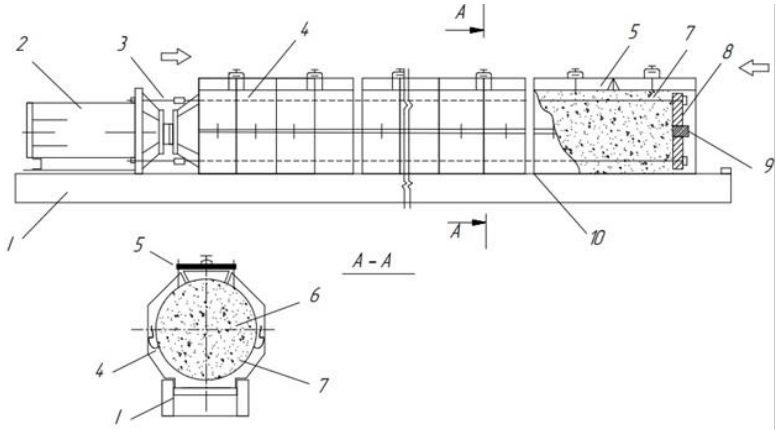

Figure 2.17. Compression scheme of a full-scale pier post in formwork using the "on-mixture" method

1 – frame; 2 – tensioning device; 3 – inventory rods; 4 – sectional formwork; 5 – hatch with screw fastener; 6 – concrete mixture; 7 – reinforcement bars; 8 – movable end; 9 – device for taking concrete samples; 10 – deformation joint

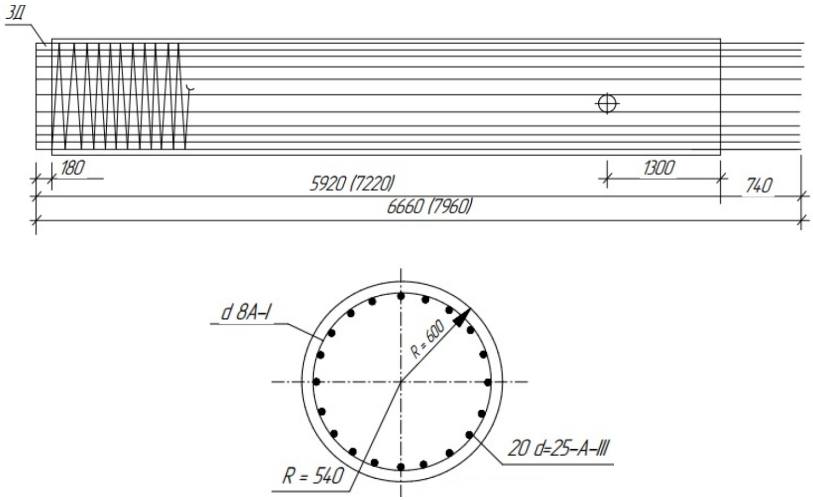

Figure 2.18. Reinforcement of full-scale bridge pier posts

The tension force of the reinforcement was monitored using the pressure gauge readings of the pumping station and mechanical strain gauges installed on the reinforcement bars. Simultaneously, the compaction of the concrete in the formwork was controlled by measuring the displacement of its sections and the movement of the rear movable end shield. The results are presented in Table 2.1.

Table 2.1

Results of Compression of Bridge Piers Using the "On Mix" Method

Concrete Mix Composition, kg/m³	Degree of Compression P, MPa	Pile Marking	Displacement, mm					$\beta = \frac{\Delta V}{V}$
			Sections in deformation joints			End face	Total	
			Δ_1	Δ_2	Δ_3			
C = 338 S = 565 G = 1272 V = 180	1.5	СБ – 5.92	93	58	–	26	177	0.029
		СБ – 7.92	94	58	51	10	235	0.031
		СБ – 7.92	93	79	52	17	241	0.032
		СБ – 7.92	92	79	50	10	231	0.031
		СБ – 7.92	91	80	53	15	239	0.032
		СБ – 7.92	92	58	–	30	180	0.029

During the compression of the concrete mixture, especially in the initial period, there was intense water expulsion. The water was expelled through all the designated special openings in the formwork, as well as through the rubber seals installed in the longitudinal joints of the sections. The amount of expelled water depended on its initial content in the concrete mixture, and at the final stage of compression, the water content was approximately the same in all the stands.

As manufacturing practice showed, the scale factor introduced significant corrections to the issue of water drainage from the formwork. While the amount of water expelled in the experimental laboratory samples of columns was relatively small and had little impact on the formwork pressure and the surface quality of the product, in the full-sized piers with a volume of more than six cubic meters, several liters of water were expelled. This water could locally wash away the cement paste from the surface of the concrete.

Therefore, to ensure peripheral water drainage and air expulsion, up to ten special holes per meter were made in the upper half of the formwork. These measures allowed for the achievement of a high-quality surface on the concrete of the full-sized pier and reduced the load on the formwork.

The process of compressing the pier was accompanied by the movement of the sections and the movable end shield of the formwork. The working stroke of the deformation joints did not exceed 100 mm. The compaction coefficient of the concrete mix, β, was in the range of 0.029–0.032 for the compressed piers (see Table 2.1). After reaching the design length of the pier, the compression was fixed using the screw spacers of the tension device (Fig. 2.16b), and then the external force exerted by the jack was removed.

The curing of the pier took place in the compressed state under natural conditions. After two days, the tensioned reinforcement was released, and the formwork was dismantled. During this process, the control samples of concrete were separated from the reinforced concrete pier. The finished pier was removed from the lower half of the formwork using a bridge crane, kept in humid conditions, and after quality inspection, it was sent to the construction site for installation.

The manufactured piers had a round solid cross-section with a diameter of 1.2 meters and lengths of 5.92 and 7.22 meters. The reinforcement of the piers was made in the form of a tied cage with 20 bars and transverse wire reinforcement. The longitudinal reinforcement used bars with a nominal diameter of 25 mm, class A-III (A400), which were placed in a circular arrangement with an equal step of 171 mm (Fig. 2.18). For transverse reinforcement, hot-rolled smooth bars with a diameter of 8 mm, class A240, were used. The spacing of the transverse reinforcement according to the design was 100 mm. To provide rigidity to the reinforcement cage, rings made of periodic profile reinforcement with a diameter of 16 mm were placed inside.

In the lower part of the pier, flat reinforcement meshes made of A240 class steel bars with a diameter of 10 mm were placed. In the upper part of the pier, the design provided for the extension of all longitudinal bars for their subsequent monolithic connection to the bridge support beam. The concrete cover layer was set at 40 mm.

The reinforcement layout and formwork dimensions of the pier are shown in Fig. 2.18. The concrete used for the bridge piers met the design strength class C35/40, frost resistance grade F200, and water impermeability grade W4.

The use of the new technology allowed for the timely delivery of a high-quality quantity of piers for the construction of the bridge crossing over the Dnipro River in Kamyanske. In this process, the grade of cement used in the piers was reduced from 600 to 400, and its consumption was decreased by a quarter. The additional costs of the technology were offset by the savings on cement and the reduction in the production cycle for manufacturing the reinforced concrete prestressed piers.

Among the promising structures that can be produced using the proposed technology are tram and railway ties, road slabs, heavily loaded columns for industrial and civil buildings, piles, curbstones for highways, masts, piers of bridge supports with a circular or cylindrical cross-section, and many other structures. The annual production volume of these could reach several million cubic meters in Ukraine alone.

CHAPTER 3
TEST RESULTS AND ANALYSIS

3.1. Strength and Deformability of Concrete and Reinforcement 3

Reinforced concrete elements with pre-stressed reinforcement on freshly placed concrete mix, according to the manufacturing technology, involve the transfer of pre-stressing forces to the unset concrete mix, which significantly affects the properties of the concrete. During the tensioning of the reinforcement, the initial stresses are perceived by the mixture of coarse and fine aggregates, cement binder, water, and trapped air. Under operational loads, the concrete works as a solid artificial stone material in the structure. The deformability of the concrete mix and the resulting stone material directly affects the loss of pre-stress in the reinforcement and the operational qualities of the finished structure. Therefore, in experimental studies, particular attention was given to the deformability of the concrete mix, especially during the phase transition to a solid state. The modeling of the behavior of the concrete mix under pre-compression was carried out in lever spring devices (Fig. 3.1).

The averaged data from the observations of the deformations of the concrete samples, compressed according to the "on the mix" method and the conventional samples with the same initial composition under a constant load P of 10 MPa, are shown in Fig. 3.2.

As follows from the observation results of the deformation of experimental prism samples, the expected losses of pre-stressing caused by the deformations of the concrete can be smaller for the structures manufactured using the "on the mix" method. In the experiments, the relative deformations of the compressed concrete were 2.4 times smaller compared to the initial ones. This is explained by the compaction of the fillers during the final stage of compression, leading to smaller shrinkage and creep deformations of the hardened compressed concrete.

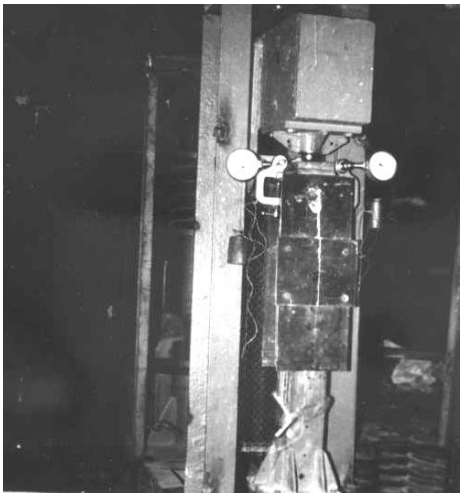

a

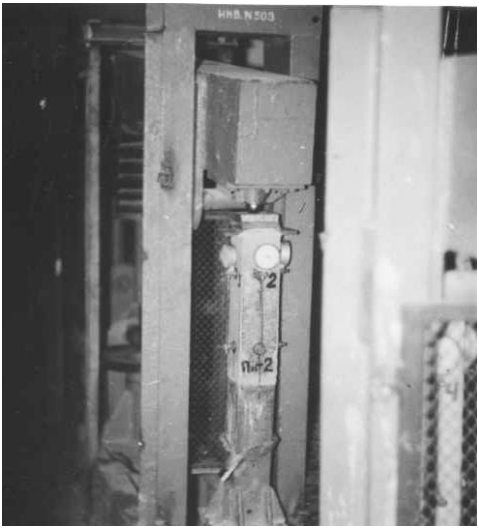

b

Figure 3.1 General appearance of the specimens compressed by the 'During-tensioning' method in a lever force device:
a *– specimen in the mold;* ***b*** *– specimen after removal from the mold without unloading*

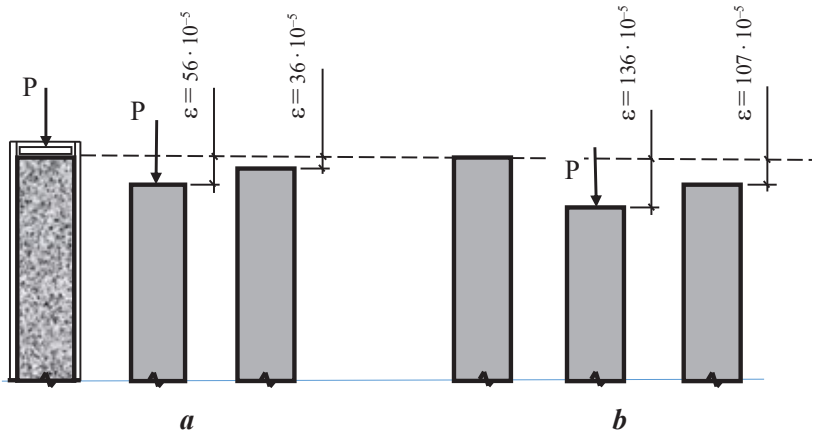

Figure 3.2. Deformation schemes of loaded prism specimens according to the method:
a *– During-tensioning;* ***b*** *– Pretensioning*

The intrinsic deformations of concrete caused by shrinkage and release in reinforced concrete elements are presented in Table 3.1. The monitoring of prestress losses in the reinforcement of specimen beams and columns was carried out from the moment the reinforcement was fixed until the start of their testing (300 days). As expected, the total values of such losses in reinforced concrete specimens, produced using the method of tensioning the reinforcement on fresh concrete mix, were lower than those in traditionally manufactured specimens. The results of observations of the reinforcement deformations in the test specimens are presented in Table 3.1. The values of the initial compression of the concrete mix ***P*** in the specimens corresponded to the initial value of the prestress in the reinforcement $\boldsymbol{\sigma_{sp}}$.

The characteristics of hardened concrete for each series were determined in accordance with DSTU B V.2.7-217 (corresponding to EN 12390-3 and EN 12390-13 for compressive strength and modulus of elasticity of hardened concrete), as well as by the ultrasonic pulse method based on DSTU B V.2.7-226 (corresponding to EN 12504-4: Testing concrete – Determination of ultrasonic pulse velocity).

Testing of cube specimens showed that uniaxially compressed concrete is an anisotropic material. The structure of the concrete formed under such compression better resists compression in the direction of the previous preloading. The strength ratio of concrete f_1 in the direction of pressing to the strength in the orthogonal plane f_2 during compression up to 10 MPa in the study reached 1.25. It should be noted that the proposed technology for manufacturing reinforced concrete elements involves the convergence of the directions of the initial concrete compaction by compression and the operational compressive forces. In the test specimens of columns and beams, prolonged compression of the concrete along the structure was performed, which, in direction, corresponded to the forces occurring in the compressed zone of the section of the structure under the test load. Accordingly, for the strength calculations of compressed structures, the characteristics of the concrete along the direction of the initial compression should be determined. Taking this into account, the concrete characteristics are presented in Table 3.2.

As a result of testing compressed and standard-sized ordinary prisms according to the methodology [162] in the volume presented in Table 3.2, **"σ_c-ε_c"** diagrams with a descending branch under axial compression were obtained. The prism specimens were tested directly before the testing of the main reinforced concrete specimens. The loading regime for the prism specimens was maintained close to the loading regime of the main specimens. The averaged **"σ_c-ε_c"** curves are shown in Figs. 3.3, 3.4, and 3.5. The main parameters of the diagrams and the values of the variation coefficients of the concrete characteristics, C_v, are presented in Table 3.3.

The table shows that the parameters of the 'load-deformation' relationship of concrete provided there are sufficiently accurate. The values of the variation coefficient of concrete characteristics in the studies do not exceed 9%. At the same time, for compressed concrete, they are lower – 8%. The test results for prestressed and normal concrete obtained using the methodologies of DSTU B V.2.7-217 (corresponding to EN 12390-3 and EN 12390-13) and the procedure [162] are in good agreement.

Table 3.1

Results of observations of deformations in the test specimens

Series Number	Concrete Mixture Compression (P),MPa	Free Intrinsic Deformations of Concrete ε_{sh} x10^{-5}	Reinforced Concrete Sample Code	Controlled Reinforcement Deformations $\varepsilon_{s,com} \times 10^{-5}$	Losses $\varepsilon_{s,loss} \times 10^{-5}$
1	2	3	4	5	6
I	4.0	32.9	БНС-1-1	320	61
			БНс-I-2	318	63
			КНс-I-I	131	32
			КНс-I-2	130	30
	2.0	38.3	БНс-I-3	160	26
			БНс-I-4	160	27
			КНс-I-3	66	24
			КНс-I-4	65	25
	0	47.5	Б0-I-5	–	–
			БО-I-6	–	–
			КО-I-5	–	–
			КО-I-6	–	–
II	5.0	31.2	БНс-II-I	117	57
			БНс-II-2	118	58
	2.5	37.5	БНс-II-3	59	25
			БНс-II-4	59	25
	0	48.2	БО-II-5	–	–
			БО-II-6	–	–
III	10.0	28.6	БНс-III-I	235	95
			БНс-III-2	236	95
	5.0	33.7	БНс-III-3	117	57
			БНс-III-4	117	56
			КНс-III-3	165	32
			КНс-III-4	166	33
	0	55.2	БО-III-5	–	–
			БО-III-6	–	–
			КО-III-I	–	–
			КО-III-2	–	–
1	2	3	4	5	6
	0	55.2	БНу-III-7	236	114
			БНу-III-8	236	112
			БНу-III-9	118	64
			БНу-III-10	117	66

Table 3.2

Strength and Deformability Characteristics of Compressed and Ordinary Concrete

Series	Compression Value P, MPa	f_{15}, MPa C_v^{R15}, %	f_{10}, MPa C_v^{R10}, %	f_c, MPa C_v^{Rc}, %	f_{ct}, MPa C_v^{Rct}, %	$E_c \times 10^{-3}$, MPa C_v^{Ec}, %
I	0	40.2 4.3	43.2 5.2	38.8 6.2	2.97 6.1	32.4 2.3
	2.0	–	72.1 6.4	58.3 5.1	3.42 7.3	37.1 3.8
	4.0	–	85.3 3.7	66.8 4.3	3.79 5.3	42.2 1.8
II	0	42.3 8.2	46.1 8.3	39.2 7.5	2.91 6.9	32.8 6.0
	2.5	–	78.5 5.1	63.3 6.1	3.52 6.6	36.2 4.2
	5.0	–	93.5 4.7	73.0 5.7	3.90 5.8	41.0 3.5
III	0	41.2 6.1	44.3 7.4	38.7 6.6	3.05 6.3	32.7 5.2
	5.0	–	98.2 4.4	74.6 4.9	4.02 5.3	44.0 2.4
	10.0	–	108.6 3.1	84.0 4.4	4.21 4.5	47.3 1.6

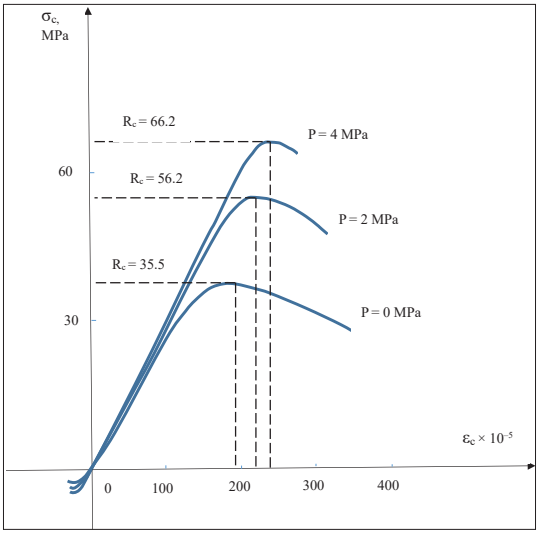

Figure 3.3. Experimental "σ-ε" dependencies for compressed and ordinary concrete of the first series

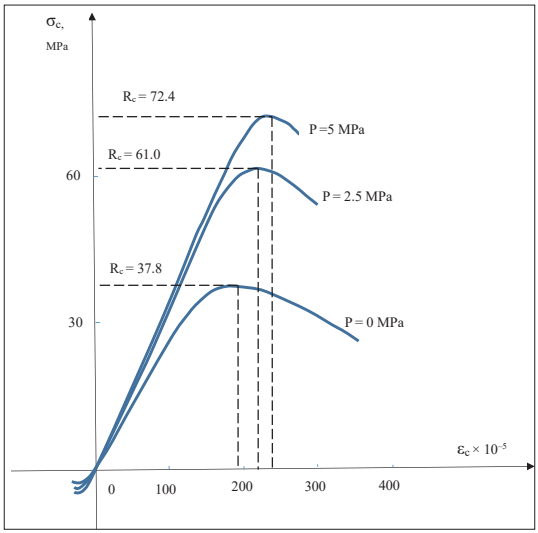

Figure 3.4. Experimental "σ-ε" dependencies for compressed and ordinary concrete of the second series

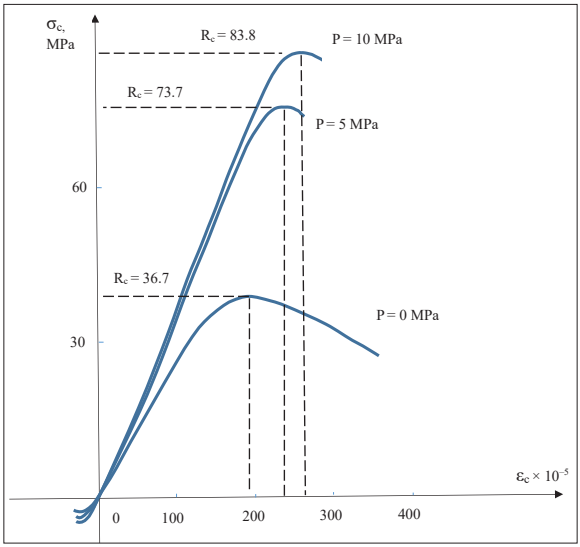

Figure 3.5. Experimental "σ-ε" dependencies for compressed and ordinary concrete of the third series

Table 3.3

Characteristics of the Complete Axial Compression Diagram of Concrete

Series	Compression Value P, MPa	$E_c \times 10^3$, MPa C_v^{Ec}, %	R_c, MPa C_v^{Rc}, %	$\varepsilon_{cR} \times 10^{-5}$ $C_v^{\varepsilon cR}$, %	σ_{cu}, MPa $C_v^{\sigma cu}$, %	ε_{cu}, MPa $C_v^{\varepsilon cu}$, %
1	2	3	4	5	6	7
I	0	32.4	35.5	186	24.8	352
		4.2	5.4	6.6	8.1	8.3
	2.0	37.2	56.2	224	43.5	315
		3.8	4.9	5.0	7.1	6.8
	4.0	42.2	66.2	247	59.9	305
		3.1	3.8	4.1	5.9	6.1
II	0	32.8	37.8	199	26.5	360
		6.1	7.9	7.8	9.5	9.9
	2.5	36.2	61.0	240	56.2	320
		4.9	6.2	6.5	7.2	7.4

Continuation of Table 3.3

1	2	3	4	5	6	7
III	5.0	41.0 4.2	72.4 5.1	262 5.3	66.7 6.2	311 604
	0	32.7 3.8	36.7 4.7	188 5.2	25.7 7.3	356 7.8
	5.0	44.0 4.0	73.7 4.5	260 4.8	68.9 6.4	306 6.2
	10.0	47.3 3.2	83.8 3.9	272 4.0	81.7 5.8	286 6.0

For the adopted concrete mix, the results of the tests established a tendency for the reduction of tensile deformations εct as the compression of the concrete mixture increased. According to the experimental data, this reduction in deformability compared to ordinary uncompressed concrete was 18-22% at a compression of 5 MPa and 26–30% at a compression of 10 MPa. This can be explained by structural changes in the concrete, with the presence of internal tensile stresses in the matrix after the release of the concrete. The aforementioned occurs against the background of an increase in concrete tensile strength as a result of compression.

The strength and deformability characteristics of reinforcing steel were determined in accordance with DSTU EN ISO 6892-1 (corresponding to EN ISO 6892-1: Tensile testing of metallic materials) and are presented in Table 3.4.

Table 3.4

Characteristics of Reinforcing Steel

Nominal Diameter, mm	**Reinforcing Steel Class**	**Yield Strength $\sigma_{s,0.2}$, MPa**	**Ultimate Strength σ_{su}, MPa**	**Elastic Modulus $E_s \times 10^{-5}$, MPa**	**Relative Elongation δ, %**
6	A-I (A240)	378	466 .	2.10	26.4
8	A-I (A240)	395	471	2.10	27.2
14	A-v (A800)	892	1143	1.98	7.8
25	A-Iv (A600)	668	965	1.91	8.8

The tensile diagrams of the reinforcement are shown in Fig. 3.6. As a result of the surface treatment of the reinforcement bars for attaching strain gauges, the working cross-section of the bars decreased, and according to the field measurements, it was 1.26 cm² for 14 mm diameter bars and 4.44 cm² for 25 mm diameter bars.

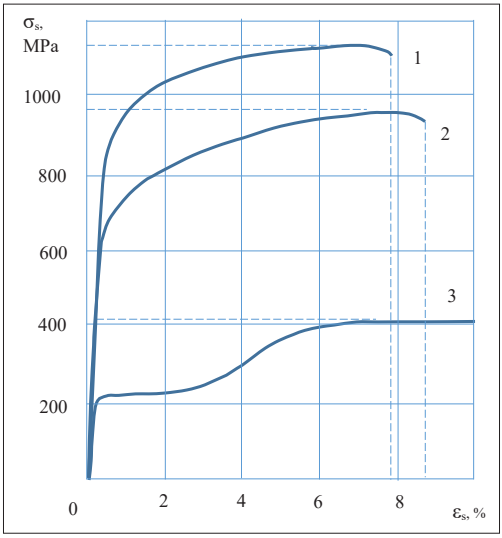

Figure 3.6. Experimental tensile diagram of reinforcing steel:
1 – class A-II (A800); 2 – class A-III (A600); 3 – class A-I (A240)

The effect of concrete strengthening due to prolonged compression of the specimens from each series is illustrated by the 'strengthening coefficient – compression value' dependencies in Fig. 3.7. Here, the strengthening coefficient ***Kc*** is taken as the ratio of the prism strength of compressed concrete f_c^* to the strength of ordinary concrete R_c^0 of the same initial mix. From this dependency, it follows that the most intense increase in concrete strength occurs when the mixture is compressed to a pressure of 5–6 MPa.

Higher levels of compression of the concrete mixture result in a less noticeable strength increase, but in this case, for structures prestressed using the 'on mix' method, the determining factor may be the requirements for crack resistance.

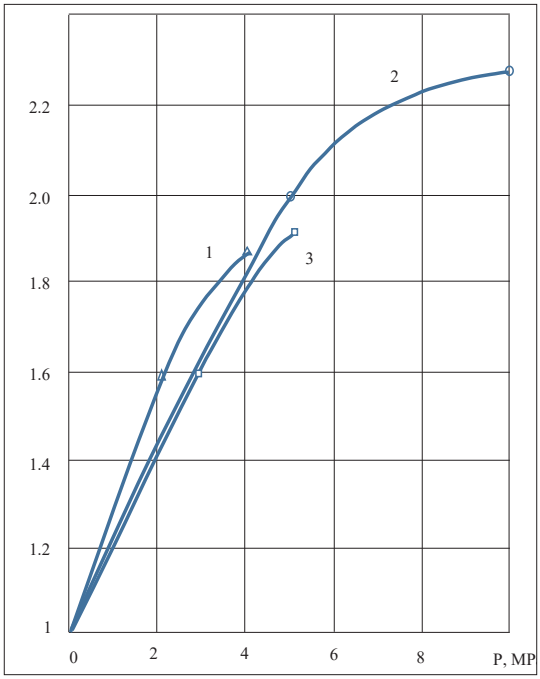

Figure 3.7. Dependence of the concrete strengthening coefficient *Kc* on the magnitude of pre-compression P:
1 – for specimens of the first series; 2 – for specimens of the third series; 3 – for specimens of the second series

Overall, the increase in strength and the change in the deformability characteristics of concrete as a result of its compression under dynamic action at the initial stages of loading can be explained by the elimination of mixing defects, the densification of aggregates, the expulsion of excess water and air from the mixture, the thinning of the adsorptive films on the cement grains, the suppression of destructive hardening processes, and, consequently, the reduction in pore sizes with a general decrease in porosity [180], a slight increase in the degree of cement hydration, improvement in adhesion, and other primarily structural changes. As for the relationship between concrete properties and the formation of special chemical compounds

under pressures up to 10 MPa under natural temperature and humidity conditions, according to our data and information from works [43; 53, 66–70; 86; 130; 132; 152], it is insignificant.

The anisotropic properties of compressed concrete, established through experimental studies, are effectively used in the developed reinforced concrete specimens. Longitudinal compression allows for the most efficient use of the strength properties of concrete in the compressed zone of the beam or column cross-section. Structural changes and the increased density of compressed concrete are confirmed by the results of ultrasonic investigations and the data on the dependencies of the differential deformation coefficient of concrete on the load (Fig. 3.8).

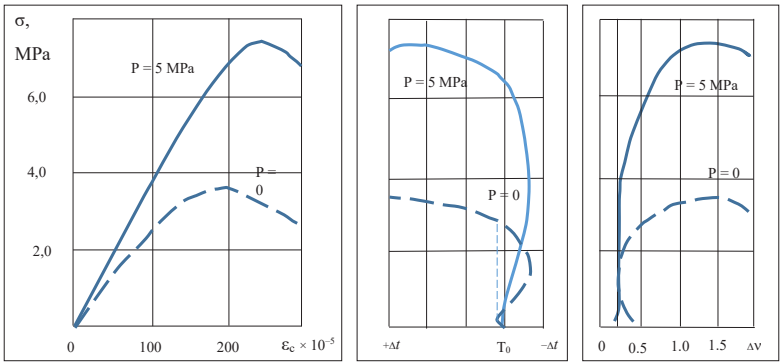

Figure 3.8. Results of testing concrete prisms:
— compressed, ---- ordinary
***a** – deformation curve; **b** – state diagram based on ultrasonic data;*
***c** – curve of the change in the differential coefficient of lateral deformation*

The experimental results of the study of the physicomechanical properties of compressed concrete before and after hardening indicate the possibility of pre-stressing reinforcement on fresh concrete mix and the retention of pre-stress forces in the reinforcement in the finished structure. In this case, the transfer of pre-stress forces to the uncured concrete mix contributes to an increase in concrete strength by up to 2.3 times, as well as an increase in the initial modulus of elasticity E_c of relative deformations ε_{cR} to 40–45%.

3.2. Test Results of Reinforced Concrete Beams

According to the experimental plan, beams with pre-stressed reinforcement on the concrete mix, on supports, and ordinary reinforced concrete beams were fabricated and tested. In total, 22 beams were tested. The overall testing scheme for reinforced concrete beams is shown in Fig. 3.9.

To prevent the formation and propagation of radial cracks along the anchorage zone of the stressed reinforcement and for technological reasons of compression, a new anchoring element was invented by the author and applied (author's certificate 17284271). The anchoring element was made of a thin ($\delta = 1$ mm) steel sheet in the form of a truncated cone with cuts for filling the cavity with concrete mix (Fig. 3.10). The reliability assessment of the applied anchoring element was carried out by measuring the displacement of the reinforcement bar in the concrete at the ends of the beams during testing (Fig. 3.9). The obtained data allow us to state that such displacements do not exceed the allowable limits according to DSTU B V.2.6-7, i.e., $\delta \leq 0.1$ mm.

The main test results, as well as the actual data on the geometric dimensions of the specimens, the arrangement of reinforcement in the cross-section, the level of its pre-stress, the percentage of reinforcement, and the magnitude of the initial compressive force on the concrete mix are presented in Table 3.5. The data in the table take into account the reduction in the working cross-section of the reinforcement due to surface treatment for bonding strain gauges. The same table also includes data on the cracking moment M_{crc}, the maximum moment M_{max} and the curvature $\varkappa_{max}$.

For all the beams, it was possible to record the maximum bending moment during the tests. The destructive moment was obtained for most of the tested beams.

The values of the maximum bending moments for the twin beams made using the 'on the mix' method are within 2–5%, while for traditionally made beams, the differences reach up to 7%. The statistical variation in the values of M_{max} for the twin beams is primarily caused by the different magnitude of the internal force couple arm due to deviations in the actual position of the reinforcement in the

cross-section, as well as differences in the properties of the concrete. The slightly improved homogeneity of the results for the compressed concrete in beams with pre-stressed reinforcement on the concrete mix has led to a reduction in the variation coefficient $C_v^{M\max}$.

Table 3.5

Results of Testing Pre-stressed and Ordinary Reinforced Concrete Beams

Beam Code	Actual Cross-sectional Dimensions	$\frac{h_o}{h}$	$\mu = A_s/bh \times 100$, %	Stress in Reinforcement σ_{sp}, MPa	Compression value P, MPa	M_{cre}, kN·m	$\varkappa_{\max} \times 10^5$, cm^{-1}	$M_{\max}$, kN m
БНс-I-I	99 × 198	0.80	0.64	512.8	4.0	10.62	103.7	20.08
БНс-I-2	101 × 198	0.82	0.63	504.9	4.0	10.94	102.6	19.25
БНс-I-3	100 × 197	0.81	0.64	196.0	2.0	4.41	89.4	19.07
БНс-Т-4	100 × 199	0.80	0.63	198.0	2.0	4.60	90.7	18.29
БО -1-5	101 × 200	0.79	0.62	–	0	3.66	84.8	17.77
БО -1-6	100 × 200	0.80	0.63	–	0	3.41	84.7	17.03
БНс-II-1	99 × 199	0.79	2.25	114.6	5.0	9.06	60.3	47.92
БНс -II-2	100 × 198	0.81	2.24	114.6	5.0	9.03	59.1	47.27
ЕНс-II-3	99 × 198	0.80	2.26	64.9	2.5	7.14	57.8	45.56
БНс-II-4	100 × 199	0.79	О 0^0	64.9	2.5	7.08	58.1	43.92
БО-II-5	102 × 200	0.79	2.18	–	0	2.68	52.1	37.22
БО-II-6	101 × 199	0.82	2.21	–	0	2.49	49.2	36.49
БНс-III-1	100 × 198	0.80	2.24	267.4	10.0	14.74	65.4	48.39
БНс-III-2	101 × 199	0.79	2.21	269.3	10.0	14.86	65.6	49.35
БНс-III-3	101 × 198	0.81	2.22	114.6	5.0	9.18	59.3	47.60
БНс-III-4	100 × 198	0.80	2.24	116.5	5.0	9.22	60.4	47.72
БО-III-5	102 × 199	0.82	2.19	–	0	2.48	47.1	36.21
БО-III-6	102 × 201	0.78	2.17	–	0	2.59	51.2	36.73
БНу-III-7	100 × 200	0.81	2.18	233.0	0	12.66	50.2	38.88
БНу-III-8	102 × 198	0.80	2.20	236.8	0	12.31	49.9	38.20
БНу-III-9	102 × 198	0.82	2.20	103.1	0	7.98	50.5	39.06
БНу-III-IO	101 × 200	0.79	2.22	97.4	0	7.61	49.4	36.50

During the tests, deformations were measured with indicators at four levels along the height of the beam, which allowed for an assessment of the validity of the plane section hypothesis for structures with pre-stressed reinforcement on the concrete mix. The analysis of the experimental data confirmed a linear distribution of deformations along the height of the beam cross-section until the moment reached the value of $\boldsymbol{M}_{\mathbf{max}}$.

The deformation measurements of the compressed edge of the beams, using mechanical action devices based on 300 mm and strain gauges, showed that the data from the strain gauges, with deformations up to 200×10^{-5}, were within the measurement error range. As the deformations increased, the strain gauge data became "delayed," and at the moment of failure, they tended to zero. The failure of the experimental beam samples occurred when the concrete reached the critical deformations εcu of the compressed fibers, and it was characterized by the spalling of the concrete in the compressed zone (Fig. 3.11). In samples made with pre-stressed reinforcement on the concrete mix, the failure had a brittle character and was accompanied by a sound effect. The compressed zone section would immediately detach from the body of the beam, fly off, and subsequently, the concrete would spall from the tensioned edge, exposing the reinforcement (Fig. 3.11 c). The brittle failure effect intensified with the increase of the pre-compression force in the over-reinforced beams.

According to the experimental data for each beam, the "bending moment – curvature" curves are shown in Fig. 3.12–3.16. As can be seen from the graphs, for the twin specimens, the "**M-$\boldsymbol{\varkappa}$**" dependencies are quite similar.

Hus, the proposed anchoring element provided reliable fixation of the reinforcement in the concrete of the experimental beams.

The results of the tests show that the load-bearing capacity of the beams pre-compressed using the "on mixture" method depends on the magnitude of the initial pre-stress, the content, and the placement of the reinforcement in the cross-section.

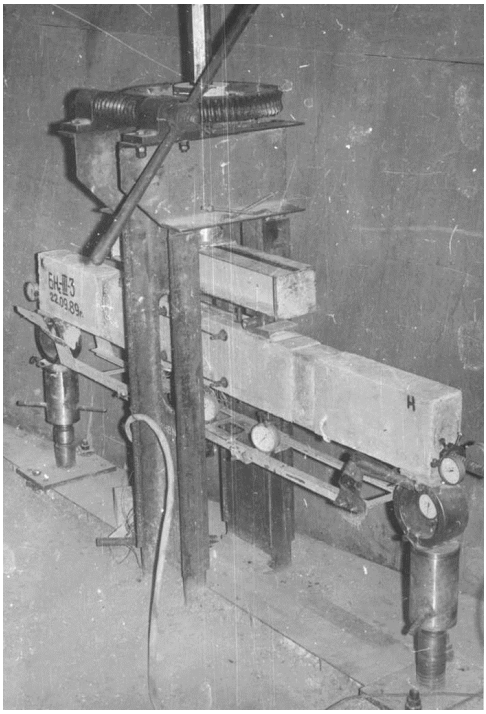

Figure 3.9 General view of the beam testing

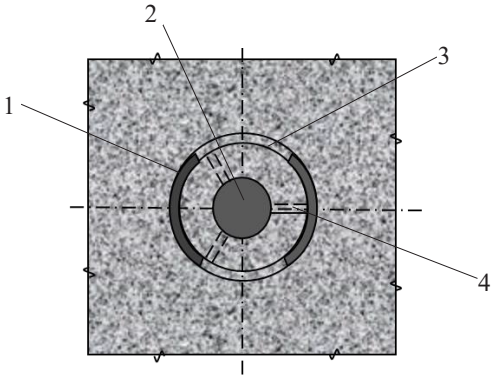

Figure 3.10. Construction of the anchoring element:
1 – steel sheet; 2 – reinforcing bar; 3 – slits;4 – plate springs

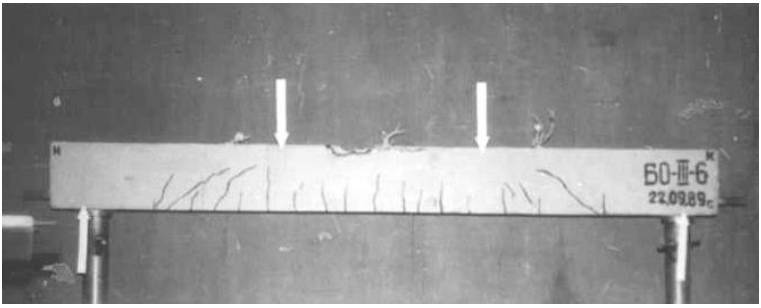

a

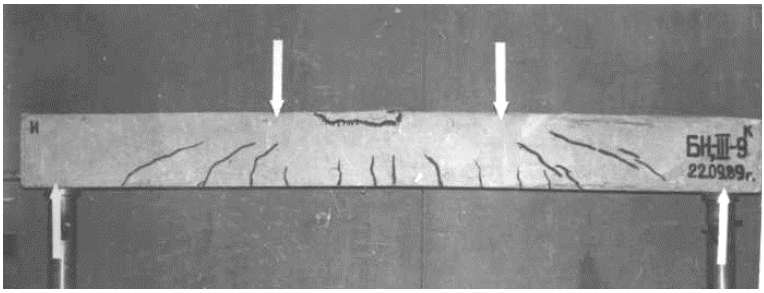

b

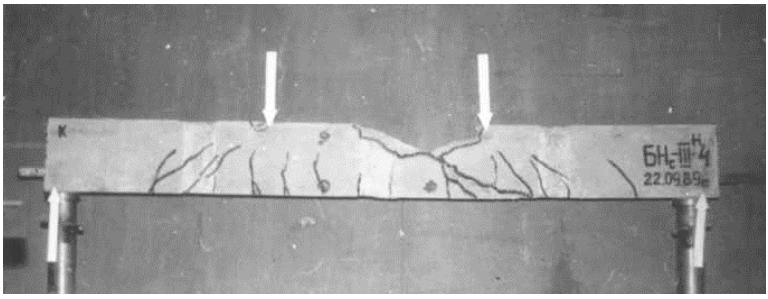

c

Figure 3.11. Characteristics of the failure of experimental beams:
a – conventional reinforced concrete beam; b – pre-stressed concrete beam traditionally; c – during-tensioned concrete beam using the proposed "on mixture" method

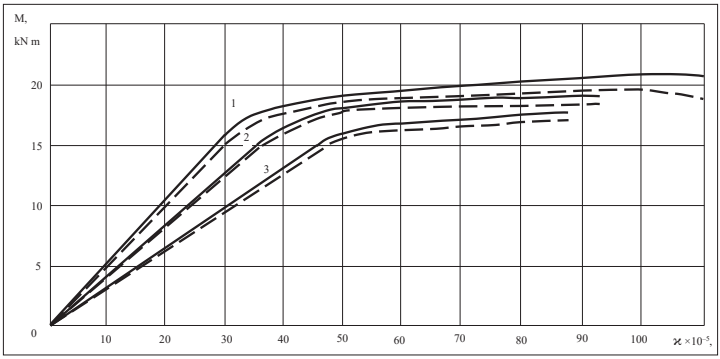

Figure 3.12. The dependence "M-$\varkappa$" for beams of the first series:
1 – during-tensioned concrete beam using the proposed "on mixture" method at P = 4 MPa: — – БН$_c$-I-1, ---- – БН$_c$-I-2;
2 – during-tensioned concrete beam at P=2 MPa: — – БН$_c$-I-3, ---- – БН$_c$-I-4;
3 – conventional reinforced concrete beams (P = 0): — – БО-I-5, ---- – БО-I-6

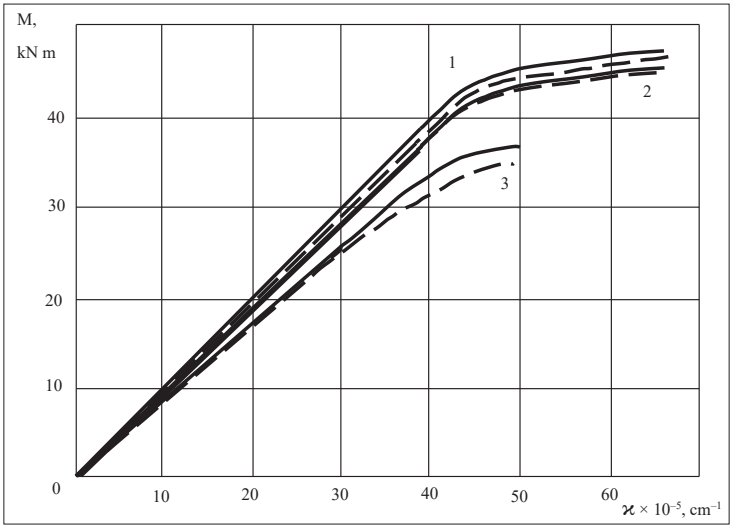

Figure 3.14. Dependence of "M-$\varkappa$" for pre-compressed beams by the "on mixture" method – 1, 2, and ordinary – 3 beams of the third series:
1 – at concrete mixture compression pressure P = I0 MPa:
— – БНс-III-2, ---- – БНс-III-I;
2 – the same, at P = 5 MPa: — – БНс-III-4, ---- – БН$_c$-III-3;
3 – ordinary reinforced concrete beams (P = 0): — – БО-III-6, ---- – БО-III-5

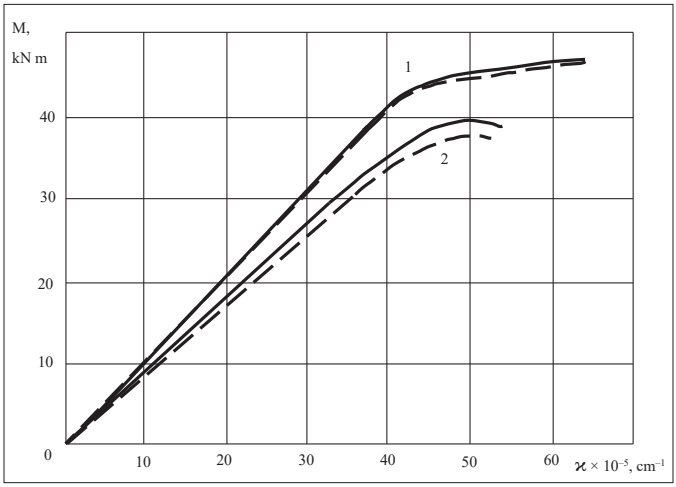

Figure 3.15. Dependence of "M-ϰ" for beams of the third series:
1 – by the "on mixture" method at P = 5 MPa: — – БНс-III-4, ---- – БНс-III-3;
2~ traditionally pre-stressed; — – БНу-III-9; ---- – БНу-III-10

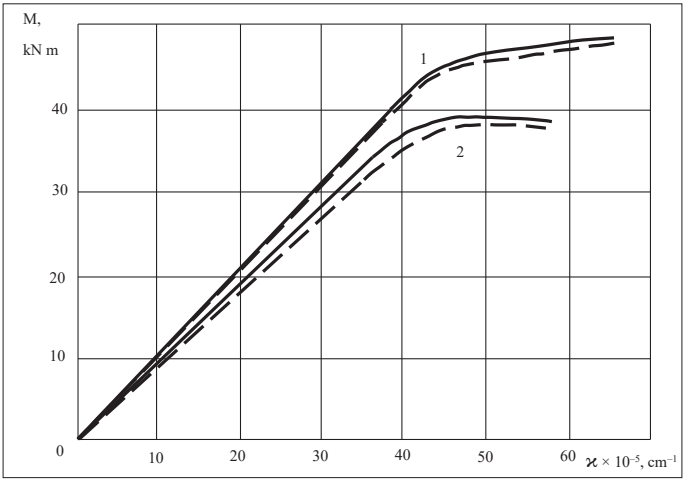

Figure 3.16. Dependence of "M-ϰ" for pre-compressed beams of the third series:
1 – by the "on mixture" method at P=I0 MPa: — – БНс-III-2, ---- – БНс-III-I ;
2 – traditionally pre-stressed: — – БНу-IB-7, ---- – БНу-III-8

In the beams of the first series, with a reinforcement content of 0.65% in the cross-section, the effect of pre-compression had only a minor impact on their load-bearing capacity. For example, at a compression pressure of 4.0 MPa, the average increase in the load-bearing capacity of the beams did not exceed 13%. This can be explained by the fact that with low reinforcement percentages, the increase in concrete strength has little effect on the load-bearing capacity of the elements due to the very small height of the compressed concrete zone in the cross-section.

The load-bearing capacity of the second series of beams, with a higher reinforcement content in the cross-section (from 2.18% to 2.25%), significantly depended on the magnitude of the pre-compression. For the beams of this series, the average value of the maximum bending moment $\mathbf{M}_{max}$ was: 36.85 kNm, 44.74 kNm, and 47.60 kNm, respectively, for the pre-compression pressures of 0, 2.5, and 5.0 MPa. The maximum value of the load-bearing capacity increase coefficient for the beams pre-compressed using the "on mixture" method in the second series was 1.29.

According to the results of the third series of beam tests, the following values of the maximum bending momen $\boldsymbol{M}_{max}$: were obtained: 36.47 kNm for a conventional reinforced concrete beam (with $\boldsymbol{P} = 0$ MPa); 47.66 kNm for a compressed beam with a pressure of 5 MPa, and 48.87 kNm for a compressed beam with a pressure of 10 MPa. The increase in load-bearing capacity due to the transfer of pre-stress force to the freshly laid concrete mixture in this series reached 34%.

In beams traditionally pre-stressed using the "support method", with the same initial stresses in the reinforcement $\boldsymbol{\sigma}_{sp}$ of 450 MPa and 225.2 MPa, as in the compressed samples, the averaged values were 38.54 kNm and 37.78 kNm, respectively. Therefore, the change in the magnitude of the pre-stressing in the reinforcement practically did not affect (within 2%) the load-bearing capacity of the traditional beams.

Based on the test results presented in Table 3.5, it follows that the nature of the relationship between the cracking moment $\mathbf{M}_{crc}$ and the pre-compression force is similar for both methods of pre-stressing. At the same time, the strength of the over-reinforced beams with tensioned reinforcement on the freshly laid concrete mixture was 25% higher than that of the traditional beams.

3.3. Test Results of Reinforced Concrete Columns

Within the experiment, both ordinary columns and those with pre-stressed reinforcement on the unset concrete mixture were fabricated and tested. A total of ten columns were tested under eccentric loading. Six of them were pre-compressed using the "on mixture" method. The overall testing scheme for the columns is shown in Fig. 3.17.

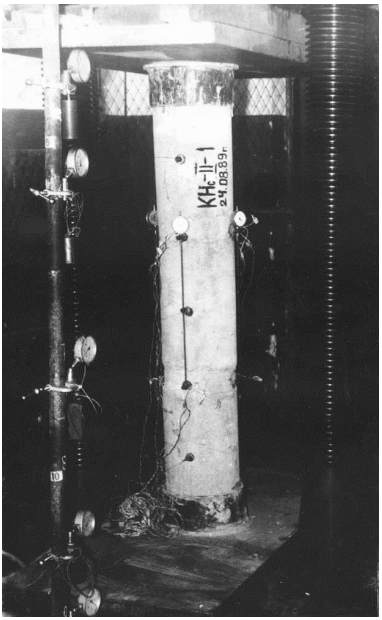

Figure 3.17. General view of the testing of compressed columns

The actual geometric dimensions of the test columns, reinforcement percentage, the value of the initial compression of the concrete mixture, the eccentricity of load application, as well as the test results, are provided in Table 3.6.

The first series of columns – KHc-I-I, KHc-I-2, KHc-I-3, KHc-I-4, KO-I-5, and KO-I-6 – were tested with an eccentricity of load application equal to 10 mm, corresponding to a random eccentricity magnitude.

Table 3.6

Results of experiments on conventionally reinforced concrete columns compressed by the 'on mixture' method

Identification for the columns	Actual diameter D, cm	Cross-sectional area A, cm^2	Longitudinal reinforcement content $\mu = A_s/bh \times 100$, %	Established stresses σ_{sp}, MPa	Amount of compression P, MPa	Eccentricity e_o, cm	Experimental value		
							Maximum load N_{max}^{ex}, kN	Curvature max $\varkappa_{max} \times 10^5$, cm^{-1}	$\varepsilon_{cu} \times 10^{-5}$
KHc-I-1	25.2	498.5	1.52	196.0	4.0	1.0	3597.2	8.5	313
KHc-I-2	25.0	530.5	1.42	188.0	4.0	1.0	3600.8	8.3	298
KHc-I-3	25.2	498.5	1.52	83.2	2.0	1.0	3076.4	8.0	–
KHc-I-4	25.7	518.5	1.45	79.2	2.0	1.0	3084.6	7.9	329
KO-1-5	25.2	498.5	1.52	–	0	1.0	1999.6	9.2	–
KO-1-6	25.0	490.6	1.54	–	0	0.9	2109.5	10.1	362
KO-III-5	25.0	490.6	1.54	–	0	4.6	1249.6	17.8	366
KO-III-6	25.2	498.5	1.52	–	0	4.7	1229.1	17.8	347
KHc-III-3	25.8	522.5	1.45	263.3	5.0	4.6	2051.1	15.9	312
KHc-III-4	26.2	538.8	1.40	263.3	5.0	4.7	2038.1	16.0	303

The results of measurements of longitudinal deformations and deflections of the first series columns showed that their stressed state during loading was quite close to the central one. At the same time, the load-bearing capacity and stiffness of columns with the same concrete mix composition varied significantly. The maximum increase in the load-bearing capacity of these columns due to the compression of the concrete mixture reached 75%. Based on the deformation measurements of the columns under load, the "**Ne-$\varkappa$**" diagrams were constructed and are shown in Figures 3.18–3.20.

The columns of the third series were tested with an eccentricity of load application corresponding to the operational value intended for natural supports before being implemented into production. For the test columns, the eccentricity of the applied test load was 46–47 mm. The "load-curvature" dependencies for the columns compressed at a pressure of 5.0 MPa and the conventional columns are shown in Figure 3.18.

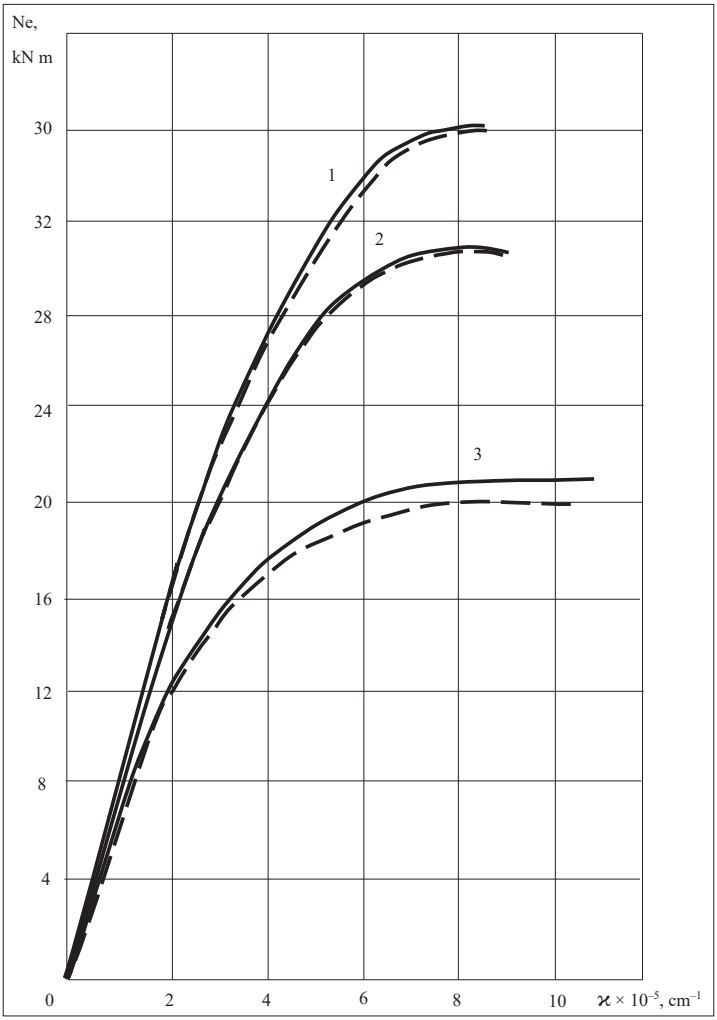

Figure 3.18 – The dependence of "load – curvature" for compressed columns of the first series using the "mixture method":

1, 2 and ordinary reinforced concrete columns –
3 with a load eccentricity of up to 1.0 cm
1 – at P=4 MPa: — – KH_c-I-2, ---- – KH_c-I-1;
2 – at P=2 MPa: — –KH_c-I-4, ---- – KH_c-I-3;
3 – for traditionally columns (P=0): — – KO_c-I-6, ---- – KO_c-I-5;

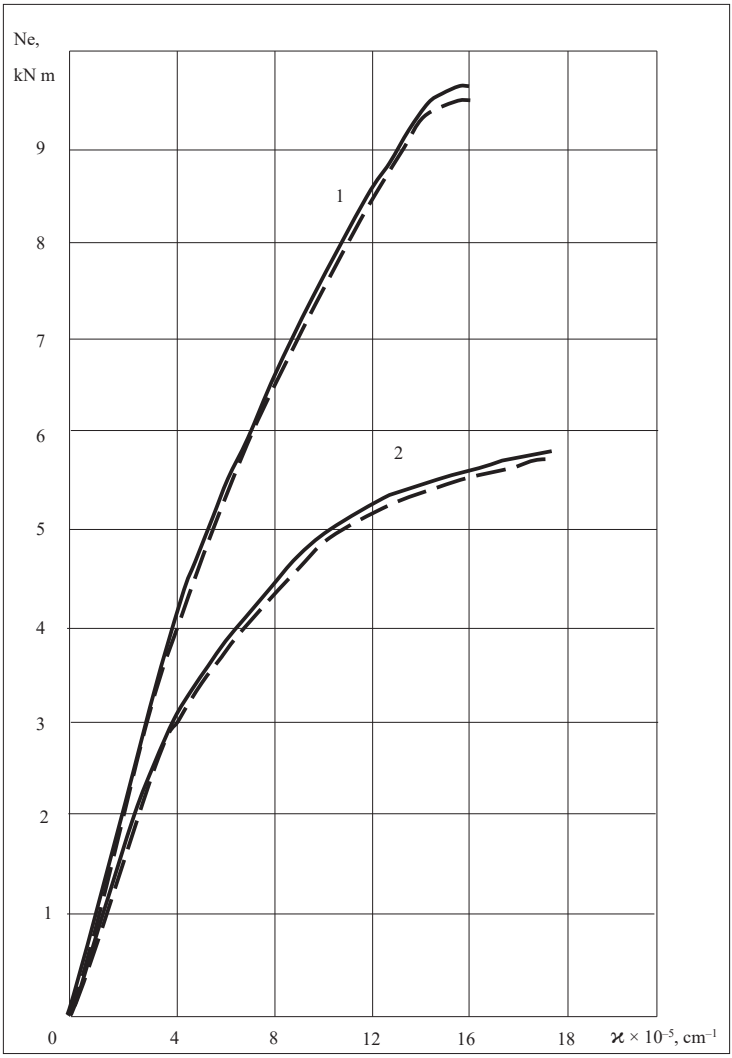

Figure 3.19 – The dependence of "load – curvature" for compressed columns of the third series using the "mixture method" – 1 and ordinary reinforced concrete columns – 2 with an increased load eccentricity of up to 4.7 cm

1 – at P=5 MPa: — – KH_c-III-3, ----- – KH_c-III-4;
2 – for traditionally columns (P = 0): — – KO_c-III-1, ----- – KO_c-III-2

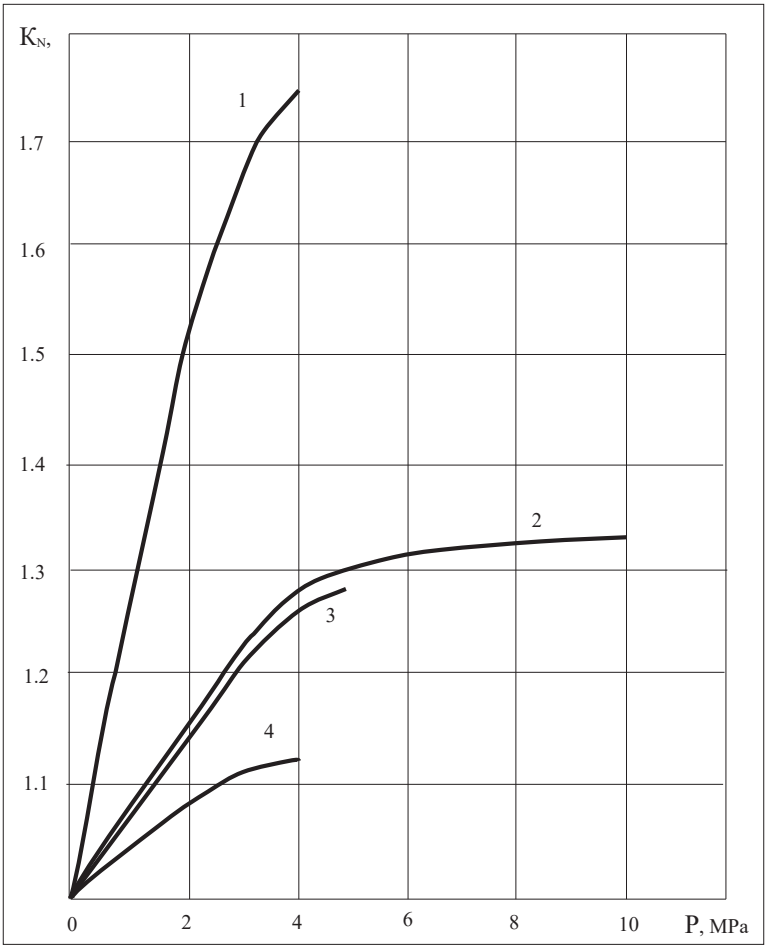

Figure 3.20. The dependence of the capacity increase factor K_N on the pre-compression of the concrete mixture P

1 – for columns of the first series; 2 – for beams of the third series; 3 – for beams of the second series; 4 – for beams of the first series

The increase in the bearing capacity of the compressed columns for the applied compression force and the eccentricity of the applied test load was on average 65%.

The failure of the column specimens predominantly occurred during the holding phase under constant load, which allowed for the accurate recording of the maximum load value. All specimens from the first series failed in the middle part of the columns. The failure of the conventional specimens was more plastic compared to the compressed ones.

All eccentrically compressed columns from the third series failed due to the spalling of concrete from the side of the most compressed fiber. No rupture of the transverse spiral reinforcement wire was observed during the experiments.

The measured deformations of the columns during the tests, using mechanical devices and strain gauges, were consistent within 200×10^{-5} relative units. The differences in these measurements did not exceed 10%.

The dependence of the capacity increase factor $\boldsymbol{K_N}$ for the test samples on the pre-compression force $\boldsymbol{p}$ of the concrete mixture is shown in Figure 3.16. The capacity increase factor was defined as the ratio of the load-bearing capacity of the compressed sample to that of the standard (non-compressed) sample.

The results from the experimental data indicate that the most effective use of pre-compression force for increasing the strength in reinforced concrete elements occurs when there is minimal eccentricity in the application of the external load.

CHAPTER 4
METHOD FOR CALCULATING THE LOAD-BEARING CAPACITY OF REINFORCED CONCRETE STRUCTURES

4.1. Strength of Compressed Concrete with a Matrix-Frame Structure

An effective method for increasing the strength of prestressed concrete structures can be considered the compression of the concrete mix and its hardening under external pressure. As shown above, it is advisable to use the pre-stressing force of the reinforcement for compressing the concrete mix. The technology for such compression has already been largely developed and was used in industrial production. However, the problem of calculating the strength of compressed concrete, taking into account the specifics of the technology, requires further clarification and elaboration.

Existing theories for calculating the strength of long-term compressed and regular concrete [111, 198, 199, 108; 33, 200, 201, 48, 155, 202, 203, 207, 31, 54, 208, 209] predominantly consider it as a composite material with a matrix structure, where the coarse aggregate particles do not contact each other. However, according to the author's research, to maintain the pre-stressing force on the mix, it is necessary to use concretes with a contacting framework arrangement of coarse aggregate particles in the structures. In this case, a significant portion of the pre-compression force is transmitted contact-wise through thin solution films from one aggregate particle to another.

In light of the above, a calculation apparatus for the strength of pre-compressed concrete with a framework structure and dense placement of aggregate particles has been proposed [213]. The calculation apparatus for practical use is based on a two-component model of concrete: cement-sand mortar and coarse, strong aggregate.

For deriving the mathematical expressions for calculating the strength of compressed concrete, the following assumptions were considered:

The pre-compression force of the concrete is perceived by the cement-sand mortar and coarse aggregate according to the magnitude of their deformation moduli. In this case, the deformation modulus of the compressed mortar is smaller than the corresponding modulus for the coarse aggregate.

The difference in stress between the coarse aggregate and the mortar, when subjected to external loading on the concrete, is transferred from one aggregate particle to another, concentrated at the contact points.

The failure of the concrete with the adopted framework structure occurs due to the cracking of the coarse aggregate particles under the action of internal tensile stresses.

The destructive load depends on the crushability of the coarse aggregate in the mixture as an integral characteristic of its strength.

The pre-stressing force of the reinforcement is predominantly perceived by the framework of coarse aggregate particles (considering long-term processes such as contraction, shrinkage, and creep in the mortar).

The adhesive and mechanical bond between the coarse aggregate and the cement-sand mortar is accounted for by the tensile strength of the compressed mortar and the values of shape, texture, and microtexture coefficients of the aggregate particles.

For the adopted two-component concrete model, the loading scheme of the coarse aggregate particles under the action of external forces on the concrete is shown in Figure 4.1. At the contact points of the coarse aggregate, concentrated forces **N** act on the particle, while along the contact surface between the aggregate and the cement-sand mortar, a distributed load $\boldsymbol{q}$. is applied. The effect of these loads on the coarse aggregate particle is considered as three-dimensional.

Considering the fact that the coarse aggregate particles have different shapes, surfaces, and sizes, and their arrangement in the concrete is similar to that of a packed mixture of coarse aggregate, the author proposes evaluating the strength of the concrete based on the crushability of the coarse aggregate mixture under compression in a standard cylinder.

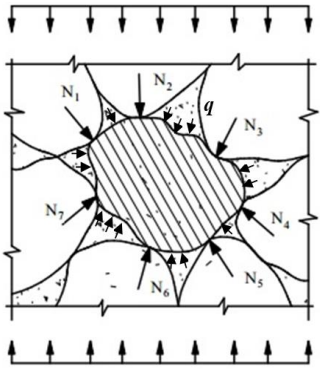

Figure 4.1. Loading Scheme of a Coarse Aggregate Particle

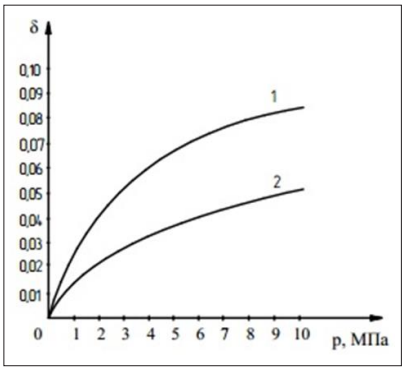

Figure 4.2. Compressibility of Cement-Sand Mortar-1 and Concrete Mix-2

The effect of pre-compression and dynamic action on the concrete mix results in the densification and additional loading of the framework formed by the coarse aggregate particles. While the material properties of the coarse aggregate (granite) remain unchanged in this process, the characteristics of the cement-sand mortar significantly depend on the degree of compression. The increase in tensile strength and the initial deformation modulus of the cement-sand mortar can be characterized by logarithmic dependencies in relation to the magnitude of the external pressure [207].

It is quite clear that under pre-compression of the concrete mix, only a portion of the pressure is transmitted to the cement-sand mortar. The magnitude of the pressure depends on the deformation of the concrete mix during compaction. Based on the comparison of experimental **"δ-*p*"** diagrams for the concrete mix and cement-sand mortar, and considering the proportion of the mortar in the concrete mix, the pressure acting on the cement-sand mortar can always be determined. Figure 4.2 shows the characteristic **"δ-*p*"** dependencies for the concrete mix and cement-sand mortar.

Given all the information above and based on well-known assumptions, the formula for the strength of pre-compressed concrete with a matrix-framework structure is derived as follows:

$$f_c = \left(K_n \frac{q}{K_{\partial p.}} + K_1 \cdot K_2 \cdot K_3 \cdot K_{bt} \cdot f_{p-ну\,ct} - c\sigma_N \right) \times \times \left(\frac{1}{1 - K_E \cdot n} - K_V r \right), \quad (4.1)$$

where

K_n – is the proportionality coefficient, equal to 0.2–0.36;

q – is the standard load for determining the crushability of the coarse aggregate particles, equal to 11.32 MPa;

$K_{\partial p.}$ – is the crushability coefficient of the coarse aggregate particles, arranged in the way they are in the concrete (i.e., in bulk, vibrated, compacted with dynamic effects and loading);

K_1 – is the shape coefficient of the coarse aggregate particles, which can range from 1.27 to 1.55;

K_2 – is the surface texture coefficient of the aggregate (1.18–1.40);

K_3 – is the microtexture coefficient of the aggregate (1–1.41).

The values of the coefficients K_1, K_2, K_3 can be determined using the methodology outlined in the work [12, 202]. For a typical coarse aggregate made of granite gravel, the product $K_1 \times K_2 \times K_3$ can be approximately taken as 2.5.

The increase in the tensile strength of ordinary mortar $f_{p\text{-}ну\,ct}$ due to compression is accounted for by the coefficient K_{cr}. It can be determined using the logarithmic dependence:

$$K_{cr.} = 1 + \alpha_1 ln 9.8p, \quad (4.2)$$

where

$\alpha_1 = 0.18$ for the given concrete composition,

p – represents the applied external pressure.

In formula (4.2), σ_N – represents the pre-compression stress transmitted to the concrete mix, while the coefficient C accounts for the portion of this stress that compresses the coarse aggregate particles. For a framework concrete structure, considering long-term processes in the concrete (such as creep and shrinkage), the value of the coefficient C is approximately equal to one.

The given ratio $r = \frac{V_{p-ну}}{V_c}$ characterizes the volumetric fraction of the mortar in the concrete. The compaction coefficient of the cement-sand mortar K_v, depending on the applied pressure $\boldsymbol{p}$ for the concrete shown in Figure 4.2, is determined by the formula:

$$K_V = 1 - 0.027\, p^{0.46}, \tag{4.3}$$

where

$$p = 0.279\, \sigma_N^{1.11}$$

The coefficient of increase in the initial modulus of deformation of the cement-sand mortar K_E due to compression is calculated using the following logarithmic dependence:

$$K_E = 1 + \alpha_2 \ln 9.8p, \tag{4.4}$$

where

$\alpha_2 = 0.1$ for the given concrete composition,

p – represents the applied external pressure.

The ratio of the initial deformation moduli of the cement-sand mortar (matrix) $E_{p-ну}$ and the original coarse aggregate material $E_з$ is denoted in formula (4.1) as n, meaning:

$$n = \frac{E_{p-ну}}{E_з}.$$

According to the given formula (3), it is also possible to determine the strength of concrete in cases where the pre-compression force σ_N is later removed and no longer contributes to the loading of the coarse aggregate framework. To account for this condition, the term $c \cdot \sigma_N$ in the formula should be set to zero.

In the case of ordinary non-compressed concrete with a framework arrangement of coarse aggregate particles, the parameters $\boldsymbol{K_{ст}}$, $\boldsymbol{\sigma_N}$, $\boldsymbol{K_E}$ and $\boldsymbol{K_v}$ in formula (4.1) are equal to one. As a result, the strength formula for such concrete takes on a simplified form:

$$f_c = \left(K_n \frac{q}{K_{\partial p.}} + K_1 \cdot K_2 \cdot K_3 \cdot f_{p-ну\,ст} - c\sigma_N \right) \cdot \left(\frac{1}{1-n} - r \right) \tag{4.5}$$

Formulas (4.1) and (4.5) are intended for calculating the prismatic strength of concrete with a matrix-framework structure. However, they do not account for the well-known confinement effect caused by the press plates when testing cube samples.

Since we now have all the necessary expressions for calculating the strength of both ordinary and pre-compressed concrete with a matrix-framework structure, the theoretical strength values can be determined for the concrete composition listed in

Table 4.1

Concrete Mix Composition	Values of the Coefficients			Compression Stress σ_N, MPa
	K_{bt}	K_E	K_v	
Cement – 450 kg Sand – 454 kg Coarse aggregate – 1305 kg Water – 183 kg	1.36	1.2	0.976	2.5
	1.5	1.28	0.969	5
	1.64	1.36	0.951	10

According to the results of preliminary tests of the initial materials for concrete, the crushability coefficient of coarse granite aggregate K_{dp} for ordinary concrete is 0.14, and for concrete compressed with dynamic impact:

- under 2.5 MPa pressure – 0.098,
- under 5 MPa pressure – 0.089,
- under 10 MPa pressure – 0.083.

The product of the shape, relief, and micro-relief coefficients $\boldsymbol{K_1 \times K_2 \times K_3}$ for the applied granite crushed stone is 2.48.

The initial modulus of deformation of granite $\boldsymbol{E_3}$ is $5/1 \cdot 10^4$ MPa.

The tensile strength of ordinary cement-sand mortar as a component of concrete $\boldsymbol{f_{p\text{-}ny\ ct}}$ is 1.87 MPa, and its initial modulus of deformation $\boldsymbol{E_{p\text{-}ny}} = 1/810^4$ MPa.

The relative volume fraction of mortar in concrete r is 0/46.

Let's calculate the ratio of the initial deformation moduli of the mortar $E_{р\text{-}ну}$ and the coarse aggregate E_3:

$$n = \frac{1.8}{5.1} = 0.35$$

Let's determine the strength of conventional concrete with a matrix-framework structure using formula (4.5):

$$f_c = \left(0.36\frac{11.32}{0.14} + 2.48 \cdot 1.87\right)\left(\frac{1}{1-0.35} - 0.46\right) = 36.4\ МПа$$

To determine the strength of compressed concrete using formula (4.1), it is necessary to first calculate a number of parameters that depend on the magnitude of the load σ_N. he results of previous calculations using expressions (4.2), (4.3), and (4.4) are summarized in Table 4.1. According to the table, the values of the strength enhancement coefficient $\boldsymbol{K_{ct}}$ and the initial deformation modulus $\boldsymbol{K_E}$ of the cement-sand mortar increase with the increase in pre-compression σ_N, especially intensively up to a pressure of 5 MPa. At the same time, the value of coefficient $\boldsymbol{K_V}$, which characterizes the compaction of the mortar under the influence of the pre-load, decreases accordingly.

Now, we have all the necessary grounds to determine the strength of the compressed matrix-frame structured concrete using formula (4.1). In the case where the pre-compression of 2.5 MPa is gradually removed from the concrete after the mixture compaction:

$$f_c^* = \left(0.36\frac{11.32}{0.14} + 2.48 \cdot 1.36 \cdot 1.87\right) \times$$

$$\times\left(\frac{1}{1-1.2 \cdot 0.35} - 0.976 \cdot 0.46\right) = 61.1\ \text{MPa}.$$

In the case of maintaining the pre-compression force of the mixture in the hardened concrete at a level of 2.5 MPa:

$$f_c^{*'} = \left(0.36\frac{11.32}{0.098} + 2.48 \cdot 1.36 \cdot 1.87 - 2.5\right) \times$$

$$\times\left(\frac{1}{1-1.2 \cdot 0.35} - 0.976 \cdot 0.46\right) = 57.9\ \text{MPa}.$$

Similarly, we will perform strength calculations for compressed concrete under pressures of 5 MPa and 10 MPa.

Under compression σ_N = 5 MPa:

$$f_c^* = \left(0.36\frac{11.32}{0.089} + 2.48 \cdot 1.5 \cdot 1.87\right) \times$$

$$\times \left(\frac{1}{1 - 1.28 \cdot 0.35} - 0.969 \cdot 0.46\right) = 72 \text{ MPa};$$

$$f_c^{*'} = \left(0.36\frac{11.32}{0.089} + 2.48 \cdot 1.5 \cdot 1.87 - 5\right) \times$$

$$\times \left(\frac{1}{1 - 1.28 \cdot 0.35} - 0.969 \cdot 0.46\right) = 65.2 \text{ MPa}.$$

Under compression σ_N = 10 MPa:

$$f_c^* = \left(0.36\frac{11.32}{0.083} + 2.48 \cdot 1.64 \cdot 1.87\right) \times$$

$$\times \left(\frac{1}{1 - 1.36 \cdot 0.35} - 0.951 \cdot 0.46\right) = 83.4 \text{ MPa}.$$

$$f_c^{*'} = \left(0.36\frac{11.32}{0.083} + 2.48 \cdot 1.64 \cdot 1.87 - 10\right) \times$$

$$\times \left(\frac{1}{1 - 1.28 \cdot 0.35} - 0.951 \cdot 0.46\right) = 68.7 \text{ MPa}$$

For the previously discussed cases of concrete mix compaction by compression, a dynamic impact was applied to the mix, leading to the rearrangement of coarse aggregate grains, an increase in the number and total area of grain contacts. This, as is well known, contributes to the reduction of stresses in the aggregate grains, which in turn enhances the load-bearing capacity of the framework and increases the concrete strength.

For the case of concrete mix compaction by compression without dynamic action and rearrangement of coarse aggregate grains, the crushing coefficient $K_{\partial p}$ in the strength formula (4.41) should be considered as a constant value.

Figure 4.3 presents graphs showing the dependence of the strength enhancement coefficient of concrete on the magnitude of pre-compression and the mode of its application.

$$K^* = \frac{f_c^*}{f_c}.$$

The comparison of the calculated dependencies with experimental data indicates their consistency.

Summarizing the above, it can be noted that the proposed strength formula for pre-compressed matrix-frame structured concrete provides results satisfactory for practical use. It allows for the consideration of the transfer of pre-compression forces to the concrete mix, both in cases where the force is retained and when it is released. Additionally, accounting for the strength of the coarse aggregate framework through its crushability enables the theoretical model of material behavior to be brought closer to reality, yielding more accurate calculation results.

It is evident that the physico-mechanical properties of the rock material, the shape, size, and roughness of the aggregate particles, as well as their packing density in concrete, play a significant role in determining its strength. Test results indicate that the crushability of coarse aggregate varies nearly twofold depending on its compaction. Therefore, the application of dynamic impact during the placement and pre-compression of the concrete mix is highly effective.

Regarding the shape of the coarse aggregate grains, preference should be given to cubic-shaped crushed stone, as it has higher crushing resistance. The use of gravel with a smooth surface slightly reduces its adhesion to the cement-sand mortar, which negatively affects the strength of the concrete. Additionally, the ratio of the deformation moduli of the coarse aggregate material and the mortar plays a significant role. The closer this ratio is to one, the more evenly the internal forces are distributed between the concrete components, resulting in higher overall strength. As is well known, this effect is further enhanced by the compression of the cement-sand mortar in the concrete.

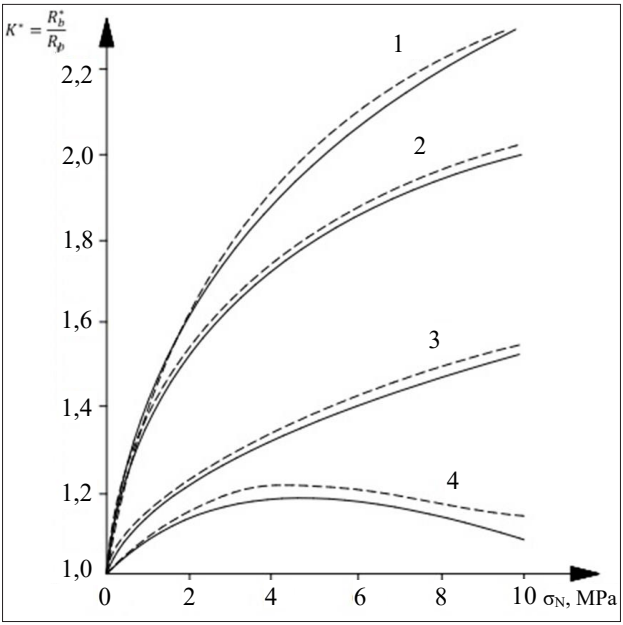

Figure 4.3. Dependence of the Strength Enhancement Coefficient of Compressed Concrete on the Magnitude and Mode of Application of the Preload

---------- – experimental; _____ – theoretical; 1 – compression under dynamic impact with subsequent load removal; 2 – the same, with preload force retention; 3 – compression without dynamic impact with subsequent load removal; 4 – the same, with preload force retention

The actual increase in the strength of concrete with a matrix-framework structure due to its compression under dynamic impact on the mixture reaches 1.5 to 2 times at a pressure of up to 10 MPa. Such high-strength concrete can be effectively used to ensure the high load-bearing capacity of prestressed reinforced concrete elements.

4.2. Analysis of Stress-State Equations for Concrete and a New Additional Criterion

The mathematical interpretation of the concrete stress-strain diagram plays a crucial role in the calculations of reinforced concrete structures [175]. Among numerous proposals for the analytical representation of the "stress-strain" diagram of concrete, one of the most accurate mathematical descriptions is a function based on a power polynomial [172–176]. As noted by most researchers [176] and based on the author's own experience [178], this dependency describes the behavior of concrete under external loading with high accuracy.

However, to date, there is no sufficiently substantiated explanation for this. The author proposes to consider the stress in concrete as the sum of three components (Fig. 4.4a):

$$\sigma_s = \sigma_{el} + \sigma_{pl} + \sigma_{crc}, \tag{4.6}$$

where

σ_{el} – represents elastic stresses;

σ_{pl} – represents plastic stresses;

σ_{crc} – accounts for crack inhibition and friction processes.

Elastic stresses are determined by the following expression:

$$\sigma_{el} = \frac{f_c}{\varepsilon_{c1}} a_1 \varepsilon . \tag{4.7}$$

Plastic stresses and stresses that account for crack growth inhibition processes and friction are characterized by the following expression:

$$\sigma_{pl} = f_c \left(a_2 \left(\frac{\varepsilon}{\varepsilon_{c1}} \right)^2 + a_3 \left(\frac{\varepsilon}{\varepsilon_{c1}} \right)^3 \right). \tag{4.8}$$

The stresses caused by crack formation are described by the following relationship:

$$\sigma_{crc} = f_c \left(a_4 \left(\frac{\varepsilon}{\varepsilon_{c1}} \right)^4 + a_5 \left(\frac{\varepsilon}{\varepsilon_{c1}} \right)^5 \right). \tag{4.9}$$

Accordingly, the deformation modulus of concrete (Fig. 4.4 b) also consists of three components:

$$E = E_{el} + E_{pl} + E_{crc}, \tag{4.10}$$

which are determined by the expressions:

$$E_{el} = \frac{f_c}{\varepsilon_{c1}} a_1$$

$$E_{pl} = f_c \left(2a_2 \frac{\varepsilon}{\varepsilon_{c1}^2} + 3a_3 \frac{\varepsilon^2}{\varepsilon_{c1}^3} \right)$$

and

$$E_{crc} = f_c \left(4a_4 \frac{\varepsilon^3}{\varepsilon_{c1}^4} + 5a_5 \frac{\varepsilon^4}{\varepsilon_{c1}^5} \right), \tag{4.11}$$

or

$$E_{el} = E_{sh} a_1, \tag{4.12}$$

and

$$E_{pl} = E_{sh} \left(2a_2 \frac{\varepsilon}{\varepsilon_{c1}} + 3a_3 \left(\frac{\varepsilon}{\varepsilon_{c1}} \right)^2 \right), \tag{4.13}$$

$$E_{crc} = E_{sh} \left(4a_4 \left(\frac{\varepsilon}{\varepsilon_{c1}} \right)^3 + 5a_5 \left(\frac{\varepsilon}{\varepsilon_{c1}} \right)^4 \right), \tag{4.14}$$

where

E_{sh} – ultimate secant modulus $E_{sh} = \frac{f_c}{\varepsilon_{c1}}$

f_c – prism strength of concrete,

a_i – coefficients of the power polynomial,

ε – given relative deformations,

ε_{c1} – relative deformations corresponding to the prism strength of concrete.

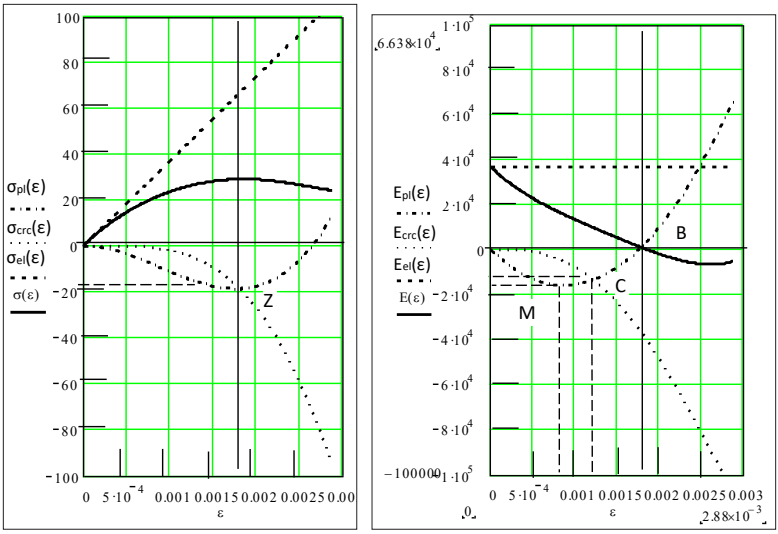

a ***b***

Figure 4.4. Diagrams:
a *– "Stress-Strain"* ***b*** *– "Modulus-Deformation" for Concrete Class C 32/40*

The general expression for determining the relationship between stresses and deformations in concrete can be represented as a power polynomial [4, 5]:

$$\sigma = f_c \sum_{i=1}^{5} a_i \left(\frac{\varepsilon}{\varepsilon_{c1}} \right)^i , \tag{4.15}$$

imilarly, for the deformation modulus, we obtain:

$$E = E_{sh} \sum_{i=1}^{5} i a_i \left(\frac{\varepsilon}{\varepsilon_{c1}} \right)^{i-1} . \tag{4.16}$$

The product of the secant modulus of elasticity ***Ec*** and the polynomial coefficient $\mathbf{a_1}$ represents the instantaneous modulus of elasticity:

$$E = kE_c a_1 , \tag{4.17}$$

where ***k*** is a coefficient that accounts for the ratio between the instantaneous modulus of elasticity and the standard initial modulus

of elasticity, caused by differences in loading rates. For most practical calculations, ***k*** can be assumed as **1**.

From this, the first polynomial coefficient in the first approximation can be easily determined:

$$a_1 = \frac{E}{E_c}. \tag{4.18}$$

As is well known, plastic deformations consist of creep deformations, ε_p, and deformations caused by crack formation, ε_{crc}.

$$\varepsilon_{pl} = \varepsilon_n + \varepsilon_{crc}. \tag{4.19}$$

The former are governed by the gel component of the concrete microstructure and other related factors, whereas the latter are associated with the disruption of internal bonds within the concrete structure.

Accordingly, the stresses can also be divided into two similar components:

$$\sigma = \sigma_{el} + \sigma_{pl}. \tag{4.20}$$

Elastic stresses are determined by expression (3), since:

$$\sigma_{el} = \sigma_1. \tag{4.21}$$

The plastic component:

$$\sigma_{pl} = E_c \sum_{i=2}^{5} a_i \frac{\varepsilon^i}{\varepsilon_{c1}^{i-1}},$$

requires a more detailed analysis.

As an example, let us consider concrete of class C 32/40. Figure 4.5 shows the complete “stress-strain” diagram, while Figure 4.6 separately presents the dependencies of elastic and plastic deformations.

At the moment of loading, close to reaching the prism strength of concrete, significant cracking occurs, leading to substantial material degradation. Due to bond disruptions, the stress state of the material becomes extremely heterogeneous. Plastic deformations caused by creep are exhausted. In some parts of the material volume, stresses decrease, and unloading processes, as well as reverse plastic aftereffects, occur. The process of crack growth inhibition intensifies.

Internal friction significantly increases, creating additional resistance within the concrete.

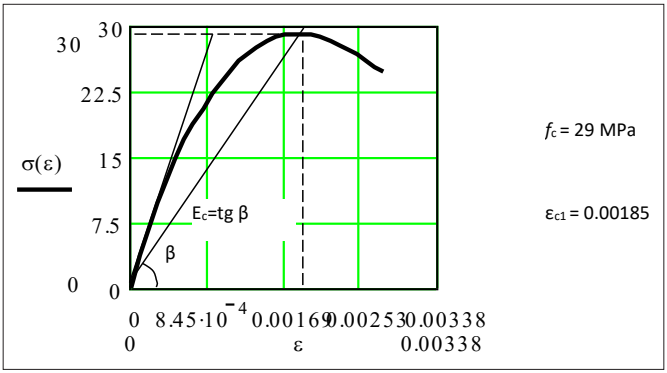

Figure 4.5. Stress Diagram for Concrete Class C 32/40

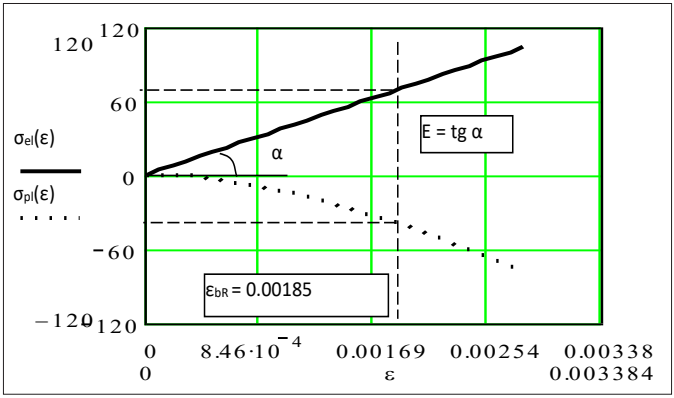

Figure 4.6. Stress-Strai" Diagrams of the Elastic $\sigma_{el}(\varepsilon)$ and Plastic($\sigma_{pl}(\varepsilon)$ Components

The resistance curve $\boldsymbol{\sigma_{pl} = f(\varepsilon)}$, according to formula (4.21), reaches its minimum and then gradually increases (see Fig. 4.4). At the same time, the crack formation process accelerates (see $\boldsymbol{\sigma_{crc} = f(\varepsilon)}$ in Fig. 4.4). The moment when these function graphs intersect corresponds to the ultimate strength of concrete $\boldsymbol{f_c'}$.

The intersection point of these function graphs – ***Z*** – is characterized by the condition:

$$\sigma_{pl} = \sigma_{crc} = \sigma_z . \tag{4.22}$$

The magnitude of the relative deformations will be $-\ \boldsymbol{\varepsilon} = \boldsymbol{\varepsilon}_{c1}$ with an accuracy of up to five percent for concrete classes ranging from C 12/15 to C 40/50.

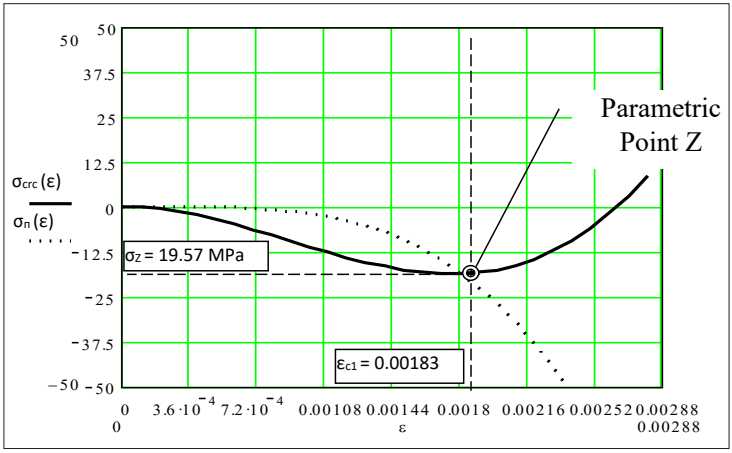

Figure 4.7. Stress–Strain Diagrams of the Plastic Components $\boldsymbol{\sigma}_{crc}$ (ε) and $\boldsymbol{\sigma}_{\text{п}}$ (ε), and the Position of the Parametric Point ZP

Let us determine these stresses. At the given relative deformations – $\boldsymbol{\varepsilon}_{c1}$, the total stresses are known. They correspond to the prism strength of concrete $\boldsymbol{f}_c$. The stresses from the elastic deformations of concrete $\boldsymbol{\sigma}_{el}$ are known from formula (4.7).

$$\sigma_{el} = E\varepsilon_{c1} . \tag{4.23}$$

At relative deformations – $\boldsymbol{\varepsilon}_{c1}$, taking into account formulas (1) and (6), we obtain:

$$R_b = E\varepsilon_{c1} + 2\sigma_z . \tag{4.24}$$

From this:

$$\sigma_z = \frac{E\varepsilon_{c1} - f_c}{2} , \tag{4.25}$$

or:

$$\sigma_z = \frac{\sigma_{el} - R_c}{2}. \tag{4.26}$$

For example, for concrete of class C 32/40, the stresses at the parametric point ***Z*** (see Fig. 4.7) are – 18.31 MPa. For medium concrete classes, the stresses are presented in Table 4.2.

Table 4.2

Parametric Stresses

Concrete Class	f_c, MPa	σ_{z1}, MPa
C 30/35	25.5	−15.89
C 32/40	29.0	−18.31
C 35/45	32.0	−19.68
C 40/50	36	−21.46

Equation (4.26) made it possible to obtain an additional condition for determining the coefficients of the power polynomial of the "stress-strain" diagram of concrete, namely:

$$a_2 + a_3 = a_4 + a_5. \tag{4.27}$$

If we take into account that the sum of all coefficients equals one, then expression (13) can be written as:

$$\begin{aligned} a_2 + a_3 &= \frac{1 - a_1}{2}; \\ a_4 + a_5 &= \frac{1 - a_1}{2}, \end{aligned} \tag{4.28}$$

where $\boldsymbol{a_1}$ is a known value related to the modulus of elasticity and depends on the loading rate [176].

The intersection point ***C*** on the graph (Fig. 4.7) of the plastic deformation modulus and the crack formation deformation modulus characterizes the onset of processes in concrete that will lead to the ultimate state and failure of the concrete. In other words, it predicts concrete failure under certain influences over a given period.

This point is physically related to the upper limit of microcrack formation in concrete [175]. Knowing the deformations corresponding to this point for a specific concrete–typically within $\boldsymbol{\varepsilon_c} = 0.0012 \pm 0.0001$ – and the stress relationships,

$$\beta_c = \frac{\sigma_c}{f_c}, \tag{4.29}$$

the first coefficient of the polynomial can be determined as follows:

$$a_1 = \frac{5\left[2\beta_c - 3\left(\frac{\varepsilon_c}{\varepsilon_{c1}}\right)^2 + 2\left(\frac{\varepsilon_c}{\varepsilon_{c1}}\right)^3 - 5\left(\frac{\varepsilon_c}{\varepsilon_{c1}}\right)^4 - 4\left(\frac{\varepsilon_c}{\varepsilon_{c1}}\right)^5\right]}{\frac{\varepsilon_c}{\varepsilon_{c1}}\left[10 - 15\left(\frac{\varepsilon_c}{\varepsilon_{c1}}\right) + 10\left(\frac{\varepsilon_c}{\varepsilon_{c1}}\right)^2 - 15\left(\frac{\varepsilon_c}{\varepsilon_{c1}}\right)^3 + 12\left(\frac{\varepsilon_c}{\varepsilon_{c1}}\right)^4\right]}. \tag{4.30}$$

Let us formulate additional conditions that allow determining the polynomial coefficients. The deformation modulus of concrete at its maximum strength is equal to zero, i.e., $\boldsymbol{E_{c1} = 0}$, or:

$$E_{el} = -(E_{pl} + E_{crc}). \tag{4.31}$$

For concretes of class C 30/35 and higher, the plastic deformation modulus at this point is close to zero. Let us assume $\boldsymbol{E_{pl} = 0}$. Then:

$$E_{el} = -E_{crc}. \tag{4.32}$$

Let us consider the condition for the minimum of the plastic deformation modulus function (see point ***M*** in Fig. 4.4 b):

$$\frac{dE_{pl}}{d\varepsilon} = 0. \tag{4.33}$$

From which, after transformations, we obtain:

$$a_2 + 3a_3\frac{\varepsilon_m}{\varepsilon_{c1}} = 0. \tag{4.34}$$

The combined solution of the above equations made it possible to determine the deformations at which the minimum of the plastic deformation modulus function is reached. For concretes with a compressive strength class higher than C 30/35, this deformation is:

$$\varepsilon_m = \frac{\varepsilon_{c1}}{2}. \tag{4.35}$$

For the specified concrete classes, among various solutions, the following methodology for determining the coefficients of the power polynomial appears to be the most concise.

For the first coefficient, which characterizes the elastic work of concrete, the following condition must be satisfied:

$$a_1 \geq \frac{E_0 \varepsilon_{c1}}{f_c}. \tag{4.36}$$

The plastic work of concrete is characterized by a pair of coefficients.

The second coefficient is determined by the following dependency:

$$a_2 = \frac{3}{2}(1 - a_1). \tag{4.37}$$

The third coefficient is found using the following ratio:

$$a_3 = -\frac{3}{2} a_2. \tag{4.38}$$

The fourth coefficient is calculated using the following expression:

$$a_4 = \frac{5 - 3a_1}{2}. \tag{4.39}$$

And the fifth coefficient is determined by the expression:

$$a_5 = \frac{-a_1 - 4a_4}{5}. \tag{4.40}$$

The calculation results of the coefficients are presented in Table 4.3.

Table 4.3

Presents the calculated polynomial coefficients for different concrete classes

Concrete Class	a_1	a_2	a_3	a_4	a_5
C 30/35	2.246	−1.869	1.246	−0.869	0.246
C 32/40	2.263	−1.894	1.263	−0.894	0.263
C 35/45	2.230	−1.845	1.230	−0.845	0.230
C 40/50	2.192	−1.788	1.192	−0.788	0.192

As follows from the table, in the considered range of values, the coefficients formally differ by a magnitude that is a multiple of one:

$$a_3 = a_1 - 1, \tag{4.41}$$

$$a_5 = a_1 - 2, \tag{4.42}$$

and

$$a_4 = a_2 + 1, \tag{4.44}$$

which makes it easy to verify the calculations.

The results of the calculations of heavy concrete parameters are presented in Table 4.4.

Table 4.4

Values of the Parameters of the Concrete Compression Diagram

Concrete Class	f_c	$\sigma_{max\,t}$	E_{c1} $\times 10^5$	$\varepsilon_{max\,t}$ $\times 10^5$	ε_{cu} $\times 10^5$	ε_{ctu} $\times 10^5$	β_u	$\beta_{u\,t}$
C 30/35	25.5	25.5	183	183	313	313	0.78	0.77
C 32/40	29.0	29.0	185	185	288	288	0.83	0.85
C 35/45	32.0	32.0	188	188	263	263	0.88	0.87
C 40/50	36	36	190	190	237	237	0.93	0.91

The calculated parameters of the concrete compression diagram in Table 4.4 are denoted by the index ***t***.

The ratio of the stress at the conditional failure limit [175], which is reached when the concrete specimen splits into separate blocks or parts, to its prism strength is denoted in the table by the symbol β_u.

$$\beta_u = \frac{\sigma_{bu}}{f_c}. \quad (4.45)$$

As follows from Table 2, for the first three parameters, all calculated data exactly match those given in study [175], while the fourth parameter – the zone of unstable concrete behavior–differs by less than 2.15%.

Plastic and pseudo-plastic processes are described by the second and third terms together, as well as the fourth and fifth terms together, in the power polynomial. The first two are determined by the gel component of the concrete structure, crack growth inhibition, friction, and other factors, while the latter are associated with the disruption of bonds within the concrete structure.

In this context, the identified parametric point ***Z*** can serve as an additional criterion for concrete strength. The existence of this parametric point can be considered an established fact.

Thus, based on the three-component stress model, an interpretation of the stress-strain state of concrete under compression is provided, explaining the physical and mechanical processes described by the well-known fifth-order power polynomial. A parametric point has been obtained that defines the compressive strength limit of concrete. It does not depend on elastic deformations and is entirely determined by plastic and pseudo-plastic processes in concrete.

4.3. Stress-State Equations for Reinforcing Steel

For reinforced concrete structures, the stress state of the reinforcement steel largely determines their strength and deformability under external loading. Therefore, to model the stress-strain state of a reinforced concrete structure at all stages of its performance, up to failure, it is necessary to have general state equations for the reinforcement steel that fully cover all stages of steel loading.

here are several challenges in developing such equations. The nature of the stress-strain ("σ-ε") relationship exhibits a relatively sharp transition from a linear to a nonlinear curve when the diagram crosses certain limits. Approximating these dependencies using

elementary functions leads to significant discrepancies. Introducing high-order polynomial dependencies–beyond the fifth order–reduces absolute deviations but fails to accurately represent the actual behavior of reinforcement steel. Graphically, this approximation appears as a wave oscillating around the experimental points. As the polynomial order increases, the number of maxima and minima in the approximation curve also increases.

At the same time, reliable computational dependencies for the discrete description of the "σ-ε" diagrams of reinforcement steel are well known [48, 155, 162, 176]. Figure 4.8 presents the computational **"σ_S-ε_S"** relationship for mild reinforcement steel, while Figures 4.9 and 4.10 illustrate the same for hard steel. Each linear segment of the computational **"σ_S-ε_S"** diagram is well described by an expression in the form of the product of relative deformations and the corresponding modulus of deformation of the reinforcement steel. By combining individual solutions into a single continuous dependency through the introduction of a special function in the form of several coefficients, it is possible to derive a general equation for the stress state of reinforcement steel across all stages of loading.

To achieve this, utilizing the properties of an irrational mathematical function with an odd degree, we derive expressions for the aforementioned coefficients:

$$K_{0,\,i} = S_i + 0.5;$$
$$K_{1,\,i} = 0.5 - S_i$$

where

$$S_i = 0.5\ (\varepsilon_s - \alpha_i)^{1/n}.$$

Here, n is an odd positive integer, and its magnitude determines the accuracy of the proposed function. For most practical calculations, as will be shown below, a value of $\boldsymbol{n} = 9999$ fully satisfies the required accuracy.

As follows from Figures 4.8, 4.9, and 4.10, the values of coefficients $\boldsymbol{K_0}$ and $\boldsymbol{K_1}$; are opposite and change sharply from zero to one and vice versa. The boundary of this abrupt change is the value a_i. Considering this, by appropriately multiplying the linear dependencies for "σ_s-ε_s" by the coefficients $\boldsymbol{K_0}$ and $\boldsymbol{K_i}$, it becomes possible to unify

discrete solutions into a comprehensive dependency. This is achieved by preserving the magnitude of one linear functional dependency when multiplied by a coefficient close to one while reducing others to zero by multiplying them by a coefficient close to zero.

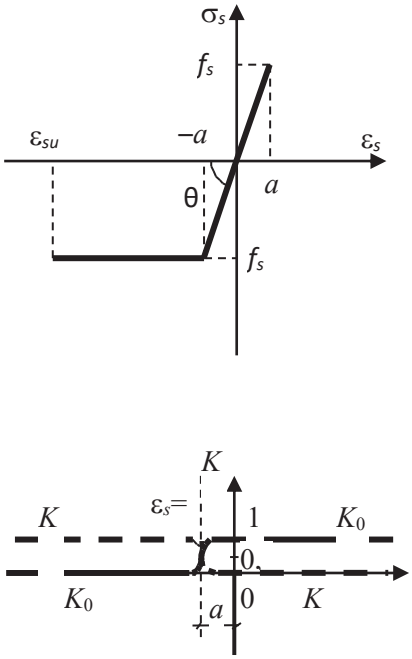

Figure 4.8. Computational "σ_S-ε_S" diagram and the corresponding "K_1-ε_s" dependency for mild reinforcement steel

Based on the above, we derive the general equations for the stress state of reinforcing steel. For mild reinforcing steel, which exhibits a physical yield plateau (Figure 4.9), the "σ_s-ε_s" diagram is discretely described by two linear dependencies:

$$\sigma_s = E_{s1} \cdot \varepsilon_s, \tag{4.46}$$

and

$$\sigma_s = f_s. \tag{4.47}$$

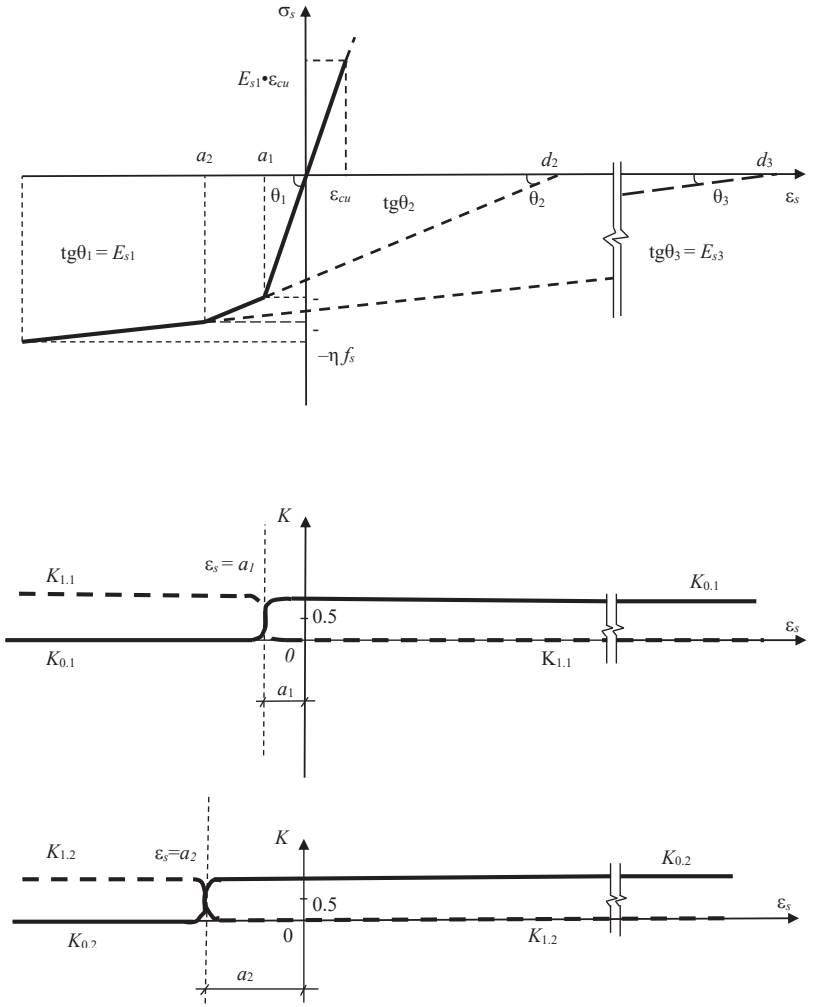

Fig. 4.9

Figure 4.9 presents the calculated diagram of "σ_S-ε_S" and the corresponding dependencies "$Ki_{,1}$-ε_s" and "$Ki_{,2}$-ε_s" for high-strength reinforcing steel

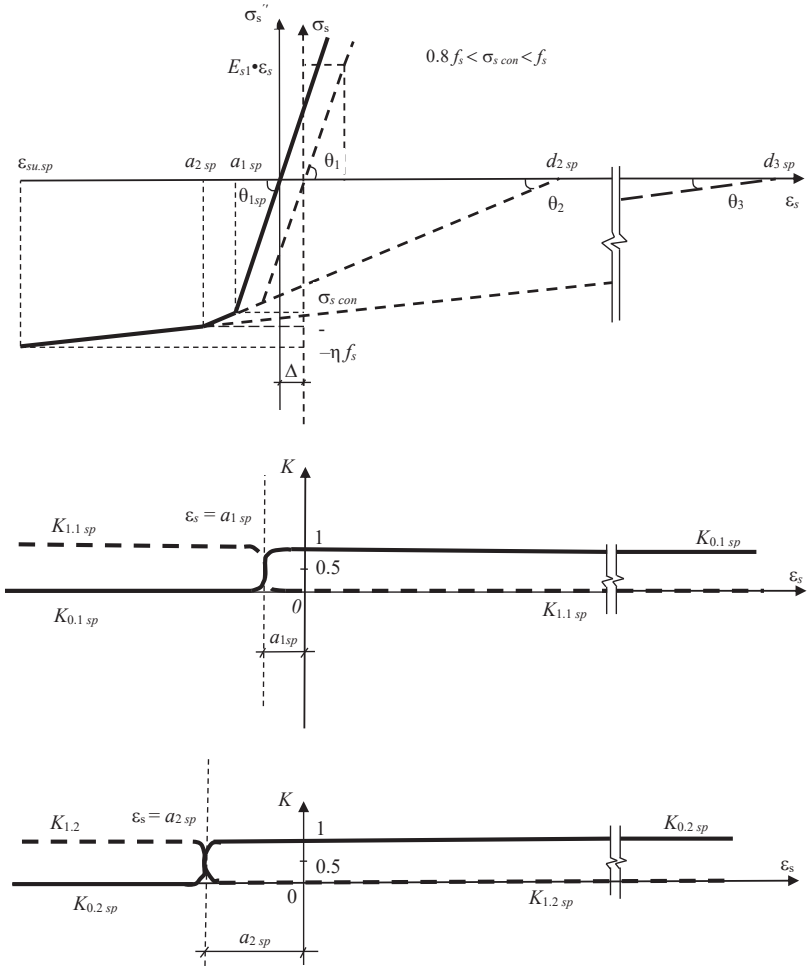

Fig. 4.10

Figure 4.10 presents the calculated diagram of "σ_S-ε_S" and the corresponding dependencies «$Ki_{,1\,sp}$-ε_s" and «$Ki_{,2\,sp}$-ε_s" for pre-stretched high-strength reinforcing steel

The boundary between the first dependency (4.46) and the second (4.47) is the deformation value equal to α, where

$$\alpha = \frac{f_S}{E_{S1}}. \tag{4.48}$$

We combine the separate known expressions (10) and (11) into a single general equation by multiplying them by the coefficients $\boldsymbol{K_0}$ and $\boldsymbol{K_1}$, respectively:

$$\varepsilon_s = K_0 E_{s1} \varepsilon_s + K_1 f_s. \tag{4.49}$$

To verify the effectiveness and determine the accuracy of the proposed stress state equation for mild steel, we will perform calculations for reinforcement of class A240. For the specified reinforcement steel, we assume: $\boldsymbol{f_s}$ = 225 MPa, $\boldsymbol{E_s}$ = 21 · 10⁴ MPa.

Let's determine the boundary value using expression (4.48).

$$\alpha = \frac{-225}{21 \cdot 10^4} = -0,00107.$$

For $\boldsymbol{\varepsilon_s}$ = 0.0005

$$S = (0.0005 + 0.00107)^{\frac{1}{9999}} = 0.99935;$$

$$K_0 = 0.5 \cdot 0.99935 + 0.5 = 0.99968;$$

$$K_1 = 0.5 - 0.5 \cdot 0.99935 = 0.00032.$$

The stress value in the steel according to the state equation (4.49) is:

$$\sigma_S = 0.99968 \cdot 21 \cdot 10^4 \cdot 0.0005 + 0.00032 \cdot 225 = 105.0\,\text{MPa}$$

For $\varepsilon_S = a = -0.00107$:

$$S = (-0.00107 + 0.00107)^{\frac{1}{9999}} = 0;$$

$$K_0 = 0.5 \cdot 0 + 0.5 = 0.5;$$

$$K_1 = 0.5 + 0.5 \cdot 0 = 0.5;$$

The stress in the reinforcement steel is:

$$\sigma_S = 0.5 \cdot 21 \cdot 10^4 \cdot (-0.00107) + 0.5 \cdot (-225) = -224.9\,\text{MPa} \cdot$$

These and other characteristic values of the **"σ_s-ε_s"** diagram for mild reinforcement steel of class A240 are presented in Table 4.5. The performed calculations indicate sufficient accuracy (deviations do not exceed 0.6%) of the stress values σ_s, determined using formula (4.79) for reinforcement steel that exhibits a physical yield plateau.

Table 4.5

ε_s	σ_s, MPa		$\Delta\sigma_s$, MPa
	calculated using equation (4.9)	exact value	
0.0005	105.0	105.0	0
−0.0005	−105.0	−105.0	0
−0.000107	−224.9	−225.0	0.1
−0.05	−226.5	−225.0	1.5

The calculation formula for determining the stresses based on the given deformations of high-strength reinforcement steel with a nominal yield limit is as follows:

$$\sigma_S = K_{0;2}(K_{0;1}\cdot\varepsilon_S\cdot E_{S;1} + K_{1;1}(\varepsilon_S - d_2)E_{S;2}) + K_{1;2}(\varepsilon_S - d_3)E_{S;3}. \quad (4.50)$$

The values of the four coefficients K_{ij} re determined considering the limits $\boldsymbol{a_1}$ and $\boldsymbol{a_2}$ (see Figs. 4.5 and 4.6).

$$\alpha_1 = \frac{0.8 f_S}{E_{S1}}, \quad (4.51)$$

and

$$\alpha_2 = \frac{f_S}{E_{S1}} = -0.002. \quad (4.52)$$

The deformation modules of the reinforcement steel can be determined using the expressions:

$$E_{S2} = tg\theta_2 = \frac{1}{\frac{1}{E_{S1}} + \frac{0.01}{f_S}}, \quad (4.53)$$

and

$$E_{S3} = tg\theta_3 = \frac{f_S\cdot(\eta - 1)}{E_{Su} - \frac{f_s}{E_{S1}} - 0.02}. \quad (4.54)$$

In this case, the values of the nominal initial deformations for the first segment of the **"σ_S-ε_S"** diagram are zero, while for the second and third segments, they are respectively:

$$d_2 = 0.8 f_S \left(\frac{1}{E_{S3}} - \frac{1}{E_{S1}} \right), \tag{4.55}$$

and

$$d_3 = f_S \left(\frac{1}{E_{S3}} - \frac{1}{E_{S1}} \right) - 0.002 . \tag{4.56}$$

The given expressions (10–16) describe the behavior of both conventional and prestressed high-strength reinforcement steel within the range of $+0.8\boldsymbol{f_s}$ to $-0.8\boldsymbol{f_s}$.

If the specified limits of the initial steel stress are exceeded, namely:

$$0.8 f_s < \sigma_s < f_s$$

partial irreversible deformations occur. This can be accounted for by shifting the coordinate axes by the magnitude of the plastic deformations (see Fig. 4.6).

$$\Delta = \left(\sigma_{S,con} - 0.8 f_S \right) \left(\frac{1}{E_{S3}} - \frac{1}{E_{S1}} \right). \tag{4.57}$$

Such initial tensile stress in the reinforcement steel expands the range of possible elastic deformations (see Fig. 4.6).

$$\alpha_{1,sp} = \frac{\sigma_{S\,con}}{E_{S1}} . \tag{4.58}$$

This occurs due to the reduction of the elastic-plastic regions of the steel **"σ_s-ε_s"** diagram:

$$\alpha_{2,sp} = \alpha_2 - \Delta; \tag{4.59}$$

and

$$\varepsilon_{su,sp} = \varepsilon_{su} - \Delta. \tag{4.60}$$

Accordingly, the nominal initial deformations of the steel increase in absolute value:

$$d_{2,sp} = d_2 + \Delta; \tag{4.61}$$

and

$$d_{3,sp} = d_3 + \Delta; \tag{4.62}$$

The given dependencies are sufficient to determine the stress state of the reinforcement steel at any stage of its loading.

For the given deformations ε_s we will determine the actual stress σ_s for high-strength reinforcement steel of class A800, which had a controlled initial stress of $\boldsymbol{\sigma_{s\,con}} = 610$ MPa. For the specified reinforcement steel: $\boldsymbol{f_s} = 680$ MPa, $\boldsymbol{E_{s1}} = 19 \cdot 10^4$ MPa and $\boldsymbol{\eta} = 1.15$.

Since the value of the prestressing reinforcement steel stress lies within the range $\boldsymbol{0.8f_s < \sigma_{s\,con} < f_s}$, we apply the state equation (4.50) with additional formulas (4.17–4.22). The "σ_s-ε_s" diagram for this case is shown in Fig. 4.10. Let's determine the steel deformation modules:

$$E_{S2} = \frac{1}{\dfrac{1}{19 \cdot 10^4} + \dfrac{0.01}{680}} = 50077 \text{ MPa};$$

and

$$E_{S3} = \frac{680 \cdot (1.15 - 1)}{0.02 - \dfrac{680}{19 \cdot 10^4} - 0.02} = 7073 \text{ MPa}.$$

The magnitude of the coordinate axis shift due to the plastic deformations of the reinforcement is:

$$\Delta = \left(-610 - 0.8 \cdot 680\right)\left(\frac{1}{50077} + \frac{1}{19 \cdot 10^4}\right) = -0.00097.$$

Let us determine the boundaries of the linear segments of the "σ_s-ε_s" diagram.

$$\alpha_{1,sp} = \frac{-610}{19 \cdot 10^4} = -0.0032;$$

$$\alpha_{2,sp} = \frac{-680}{19 \cdot 10^4} - 0,002 + 0,00097 = -0.00461.$$

At the same time, the possible tensile deformations of the reinforcement steel are limited by the value:

$$\varepsilon_{su,sp} = -0.02 + 0.00097 = -0.01903;$$

The nominal initial strains are determined using expressions (4.55; 4.56) and (4.61; 4.62).

$$d_{2,sp} = 0.8 \cdot 680 \cdot \left(\frac{1}{50077} - \frac{1}{19 \cdot 10^4} \right) + 0.00097 = 0.00897;$$

$$d_{3,sp} = 680 \cdot \left(\frac{1}{7073} - \frac{1}{19 \cdot 10^4} \right) + 0.00097 = 0.09153.$$

To determine the strain $\varepsilon_s = -0/0005$

$$S_1 = 0.5 \cdot (-0.0005 + 0.00321)^{\frac{1}{9999}} = 0.49970;$$

$$K_{0,1sp} = 0.49970 + 0.5 = 0.99970;$$

$$K_{1,1sp} = 0.5 - 0.49970 = 0.00030;$$

$$S_2 = 0.5 \cdot (-0.0005 + 0.0461)^{\frac{1}{9999}} = 0.49972;$$

$$K_{0,2sp} = 0.49972 + 0.5 = 0.99972;$$

$$K_{1,2sp} = 0.5 - 0.49972 = 0.00027.$$

The stress in the reinforcement is determined using equation (4.50):

$$\sigma_s = 0.9997 \cdot (-0.9997(-0.0005)19 \cdot 10^4 + 0.0003 \times$$
$$\times (-0.0005 - 0.00897) \cdot 50077 + 0.00027 \times$$
$$\times (0.0005 - 0.09153) \cdot 7073 = -95.3 \text{ MPa}$$

The stress values at characteristic points of the **"σ_s-ε_s"** diagram for A800 – class reinforcing steel are given in Table 4.6.

The deviations of the calculated stress values σ_s of the reinforcing steel, obtained using equation (4.50), from the given values are insignificant.

Table 4.6

ε_s	$K_{0;\,1\,sp}$	$K_{1;\,1\,sp}$	$K_{0;\,2\,sp}$	$K_{1;\,2\,sp}$	σ_s, MPa	
					calculated using equation (4.50)	**exact value**
0.0005	0.99972	0.00028	0.99974	0.00026	94.7	95.0
–0.0005	–0.99970	0.00030	0.99972	0.00027	–95.3	–95.0
–0.00321	0.5	0.5	0.99967	0.00033	–609.9	–610.0
–0.00461	0.00033	0.99967	0.5	0.5	–680.0	–680.0
–0.01903	0.00021	0.99979	0.00021	0.99979	–782.1	–782.0

The derived equations describing the stress state of mild and high-strength reinforcing steels as continuous functions enable the modeling of their behavior at all loading stages of conventional and pre-stressed reinforced concrete structures up to failure.

The proposed approach, which integrates discrete solutions into a single generalized and continuous function, can also be applied to solving various other design calculation problems.

4.4. Stress-Strain State of Reinforced Concrete Elements with Solid Circular and Annular Cross-Sections

In construction practice, reinforced concrete elements with circular and annular cross-sections are quite common. These include columns, support posts, piles, masts, pipes, and many other structural components. For a more precise analysis of the stress-strain state of reinforced concrete elements, as previously demonstrated [176, 162, 48, 205], it is advisable to use a nonlinear **"σ-ε"** diagram for concrete.

Let us consider the analytical solution of the stress-strain state equations for normal sections of reinforced concrete elements within the assumptions of the "equivalent" cross-section.

To derive the equations of the stress-strain state of the normal cross-section of reinforced concrete elements, we assume the following provisions:

The design cross-section is considered the one where deformations are equal to the average along the length of the block between cracks (if cracks are present).

The average deformations of concrete and reinforcement are distributed across the cross-section according to a linear law.

The relationship between concrete stresses and deformations (see Fig. 4.11) is described by a polynomial of degree:

$$\sigma_c = \sum_{K=1}^{5} \alpha_K \varepsilon_i^{\,K} . \tag{4.63}$$

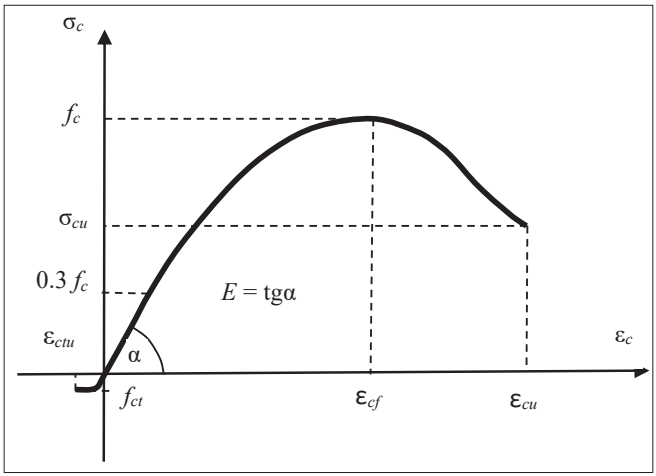

Figure 4.11. Design "σ-ε" diagram for concrete

The relationship between stresses and deformations of reinforcement steel is assumed in the form of the "σ_s-ε_s" diagram, whose parameters are obtained from experimental data or the recommendations of the previous section.

He reduction of force carried by the tensile concrete zone due to cracking can be accounted for using a coefficient:

$$\psi_{ct} = \sqrt{\frac{\varepsilon_{ct}}{\varepsilon_2}} . \tag{4.64}$$

where ε_2 – is the relative deformation of the extreme fiber in tension.

Based on the above assumptions, the stress-strain state equations for any cross-section take the following form:

$$N = \int_A \sigma_c dA + \sum \sigma_{si} A_{si}; \tag{4.65}$$

$$M = \int_A \sigma_c h dA + \sum \sigma_{si} A_{si} h_{si}; \tag{4.66}$$

where

$\boldsymbol{\sigma_c}$ – normal stresses on the elementary plane dA, located at a distance h from the outermost compressed fiber,

$\boldsymbol{\sigma_{si}}$, $\boldsymbol{A_{si}}$, $\boldsymbol{h_{si}}$ – normal stresses, area, and distance to the outermost compressed fiber of the cross-section for the i-th reinforcement bar.

In equations (4.65) and (4.66), the defined integral characterizes the work of the compressed concrete. For an element with a ring-shaped cross-section, it can be geometrically represented as a complete or open cylinder, whose height is described by a power polynomial.

In this case, the bending moment carried by the compressed concrete is determined as the product of the resultant force, applied at the geometric center of the given body, and the distance h from the force to the outermost compressed fiber in the cross-section (see Fig. 4.12).

Considering the above, the stress-strain state equations for reinforced concrete elements with a ring-shaped cross-section can be expressed as:

$$N = 2\,[\,\sum a_K \Big(\int_0^{h_b} \sqrt{2Rh - h^2}\,\left(\varepsilon_1 - \chi h\right)^K dh -$$

$$-\int_{R-r}^{h_b - R + r} \sqrt{2r(h - R + r) - (h - R + r)^2}\,(\varepsilon_1 - \chi h)^k\, dh\Big) - \psi_{bt} R_{bt} \times$$

$$\times \Big(\int_{h_b}^{2R} \sqrt{2Rh - h^2}\, dh - \int_{h_b - R + r}^{R + r} \sqrt{2r(h - R + r) - (h - R + r)^2}\, dh\Big)\Big] +$$

$$+ \sum \sigma_{si} A_{si}; \tag{4.67}$$

$$M = 2\Big[\,\sum a_K \Big(\int_0^{h_b} \sqrt{2Rh - h^2}\,\left(\varepsilon_1 - \chi h\right)^K dh -$$

$$-\int_{R-r}^{h_b - R + r} \sqrt{2r(h - R + r) - (h - R + r)^2}\,(\varepsilon_1 - \chi h)^k\, dh\Big) - \psi_{bt} R_{bt} \times$$

$$\times\left(\int_{h_b}^{2R}\sqrt{2Rh-h^2}\,dh-\int_{h_b-R+r}^{R+r}\sqrt{2r(h-R+r)-(h-R+r)^2}\,dh\right)+,$$
$$+\sum\sigma_{si}A_{si}h_{si}, \qquad (4.68)$$

where

$2\sqrt{2Rh-h^2}$ – chord length of a circle with radius R,

$2\sqrt{2r(h-R+r)-(h-R+r)^2}$ – the same for radius r;

$\varepsilon_1-\chi h$ – the relative strain corresponding to each accepted value of h within the range from zero to $2\boldsymbol{R}$; here $\boldsymbol{\chi}$ is the curvature.

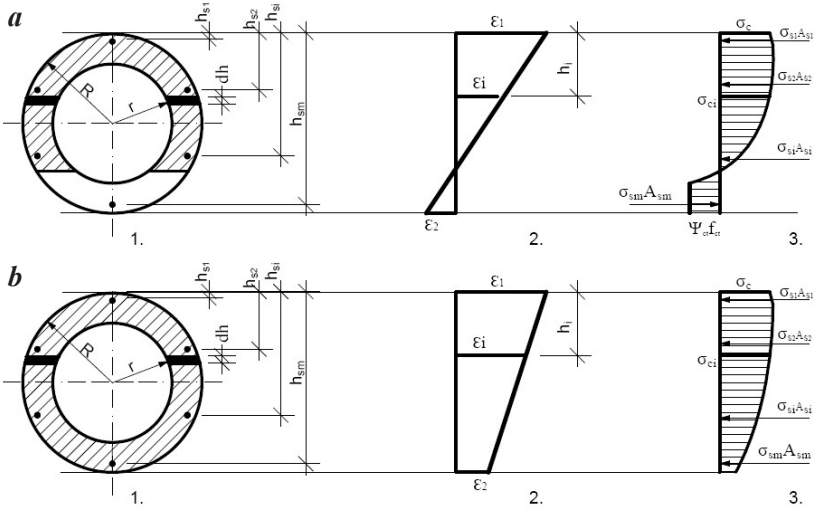

Figure 4.12. Stress-strain state of a ring-shaped cross-section:
***a** – for the first equilibrium form; **b** – for the second equilibrium form; 1 – cross-section; 2 – strain distribution diagram; 3 – stress distribution diagram*

The given equations (4.67) and (4.68) describe both the first and second equilibrium forms of reinforced concrete structures with ring-shaped and circular cross-sections. The difference between them is accounted for by substituting the appropriate integration limits.

If we denote the integrals as:

$$I_K=\int h^K\sqrt{2Rh-h^2}\,dh,$$

and

$$J_K = \int h^K \sqrt{2r(h-R+r)-(h-R+r)^2}\,dh,$$

then equations (4.35) and (4.36) take the form:

$$N = 2\left[\sum N_K - N_{bt}\right] + \sum \sigma_{si} A_{si}; \tag{4.69}$$

$$M = 2\left[\sum M_K - M_{bt}\right] + \sum \sigma_{si} A_{si} h_{si}, \tag{4.70}$$

where

$$N_1 = a_1\left[\varepsilon_1 (I_0 - J_0) - \chi (I_1 - J_1)\right];$$

$$N_2 = a_2\left[\varepsilon_1^{\,2} (I_0 - J_0) - 2\chi\varepsilon_1^{\,2} (I_1 - J_1) + \chi^2 (I_2 - J_2)\right];$$

$$N_3 = a_3\left[\varepsilon_1^{\,3} (I_0 - J_0) - 3\chi\varepsilon_1^{\,2} (I_1 - J_1) + 3\chi\varepsilon_1 (I_2 - J_2) - \chi^3 (I_3 - J_3)\right];$$

$$N_4 = a_4\left[\varepsilon_1^{\,4} (I_0 - J_0) - 4\chi\varepsilon_1^{\,3} (I_1 - J_1) + \right.$$
$$\left. + 6\chi^2\varepsilon_1 (I_2 - J_2) - 4\chi^3\varepsilon_1 (I_3 - J_3) + \chi^4 (I_4 - J_4)\right];$$

$$N_5 = a_5\left[\varepsilon_1^{\,5} (I_0 - J_0) - 5\chi\varepsilon_1^{\,4} (I_1 - J_1) + \right.$$
$$+ 10\chi^2\varepsilon_1^{\,3} (I_2 - J_2) - 10\chi^3\varepsilon_1^{\,2} (I_3 - J_3) +$$
$$\left. + 5\chi^4\varepsilon_1 (I_4 - J_4) - \chi^5 (I_5 - J_5)\right];$$

$$N_{bt} = \psi_{bt} R_{bt} \left(I_0^{bt} - J_0^{bt}\right);$$

$$M_1 = a_1\left[\varepsilon_1 (I_1 - J_1) - \chi (I_2 - J_2)\right];$$

$$M_2 = a_2\left[\varepsilon_1^{\,2} (I_1 - J_1) - 2\chi\varepsilon_1^{\,2} (I_2 - J_2) + \chi^2 (I_3 - J_3)\right];$$

$$M_3 = a_3\left[\varepsilon_1^{\,3} (I_1 - J_1) - 3\chi\varepsilon_1^{\,2} (I_2 - J_2) + \right.$$
$$\left. + 3\chi\varepsilon_1 (I_3 - J_3) - \chi^3 (I_4 - J_4)\right];$$

$$M_4 = a_4\left[\varepsilon_1^{\,4} (I_1 - J_1) - 4\chi\varepsilon_1^{\,3} (I_2 - J_2) + \right.$$
$$+ 6\chi^2\varepsilon_1 (I_3 - J_3) - 4\chi^3\varepsilon_1 (I_4 - J_4) +$$
$$\left. + \chi^4 (I_5 - J_5)\right];$$

$$M_5 = a_5\left[\varepsilon_1^{\,5}\left(I_1 - J_1\right) - 5\chi\varepsilon_1^{\,4}\left(I_2 - J_2\right) + \right.$$
$$+10\chi^2\varepsilon_1^{\,3}\left(I_3 - J_3\right) - 10\chi^3\varepsilon_1^{\,2}\left(I_4 - J_4\right) +$$
$$\left. +5\chi^4\varepsilon_1\left(I_5 - J_5\right) - \chi^5\left(I_6 - J_6\right)\right];$$

$$M_{bt} = \psi_{bt} R_{bt}\left(I_1^{bt} - J_2^{bt}\right).$$

Here $J_1 = L_1 + (R-r)\,L_0$;

$$J_2 = L_2 + 2\,(R-r)\,L_1 + (R-r)^2 L_0;$$

$$J_3 = L_3 + 3(R-r)\,L_2 + 3\,(R-r)^2\,L_1 + (R-r)^3 L_0;$$

$$J_4 = L_4 + 4\,(R-r)\,L_3 + 6(R-r)^2\,L_3 + 4\,(R-r)\,L_2 + (R-r)^4\,L_0;$$

$$J_5 = L_5 + 5\,(R-r)\,L_4 + 10\,(R-r)^2\,L_3 + $$
$$+ 10\,(R-r)^3\,L_2 + 5\,(R-r)^4\,L_1 + (R-r)^5\,L_0;$$

$$J_6 = L_6 + 6\,(R-r)\,L_5 + 15\,(R-r)^2\,L_4 + 20\,(R-r)^2\,L_3 + 15\,(R-r)^4 L_2 + $$
$$+ 6\,(R-r)^5\,L_1 + (R-r)^6\,L_0.$$

For $K = 0$, the equations take the form:

$$I_0 = 0{,}5\left[(h-R)\sqrt{2Rh - h^2} + R^2 \arcsin\frac{h-2R+r}{h}\right], \quad (4.71)$$

and

$$J_0 = 0{,}5\left[\begin{array}{l}(h-2R+r)\sqrt{2r(h-R+r) - (h-R+r)^2} + \\ +r^2 \arcsin\dfrac{h-2R+r}{h}\end{array}\right]. \quad (4.72)$$

For $K = 1, 2, \ldots 5, \ldots$, the analytical solution of the integrals I_k and L_k is obtained based on the recurrence formula for the integral of the differential binomial:

$$I_k = -2\,(2R)^{K+2}(I'_{K-1} - I'_K), \quad (4.73)$$

where

$$I'_K = \frac{h^{K+1}\sqrt{2(R-h)h}}{2(K+2)\cdot(2R)^{K+2}} + \frac{2K+3}{2K+4} I'_{K-1}; \quad (4.74)$$

$$I'_0 = -\frac{3}{16}\left(\frac{h-R}{R^2}\sqrt{2Rh-h^2} + R^2 \arcsin\frac{h-R}{R}\right) + \frac{h\sqrt{(2R-h)h}}{4R^2}. \quad (4.75)$$

Accordingly:

$$L_K + -2(2r)^{K+2}\left(L'_{K-1} - L'_K\right), \quad (4.76)$$

where

$$L'_K = \frac{(h-R+r)^{K+1}\sqrt{Rh-h^2-R^2}}{2(K+2)\cdot(2r)^{K+2}} + \frac{2K+3}{2K+4}L'_{K-1}; \quad (4.77)$$

$$L'_0 = -\frac{3}{16}\left(\frac{h-R}{r^2}\sqrt{2r(h-R+r)-(h-R+r)^2} + \arcsin\frac{h-r}{r}\right) + \frac{(h-R+r)\sqrt{Rh-h^2-R^2}}{4r^2}. \quad (4.78)$$

Thus, all the required formulations have been established for the analysis of the equations describing the stress–strain state of reinforced concrete elements with annular and circular cross-sections. It should be emphasized that the values of the coefficients $\boldsymbol{a_k}$ in the formulas are taken based on the approximation of the experimental full stress-strain diagram **"σ-ε"** of concrete or according to the recommendations in [176].

In the formulas, it is necessary to account for the integration limits. For the compressed zone of the ring-shaped cross-section, the value of $\boldsymbol{h}$ varies: from **0** to $2\boldsymbol{R}$ for the outer circle and from $\boldsymbol{R-r}$ – to $\boldsymbol{R+r}$ – for the inner circle. If a tensile zone is present in the cross-section, $\boldsymbol{h}$ varies: from 0 to $\boldsymbol{h_c}$ for the outer circle, and from $\boldsymbol{R-r}$ – to $\boldsymbol{h_c-R+r}$ – for the inner circle (see Fig. 4.12).

By substituting the corresponding integration limits into expressions (4.75) and (4.78) for the compressed zone of the cross-section, we obtain:

$$I'_0 = -\frac{3}{16}\left(\frac{h_c-R}{R^2}\sqrt{2Rh_c-h_c} + R^2 \arcsin\frac{h_c-R}{R}\right) + \frac{h_c\sqrt{(2R-h_c)h_c}}{4R^2} - \frac{3}{32}\pi; \quad (4.79)$$

$$L_0^{'} = -\frac{3}{16}\left(\begin{array}{l} \dfrac{h_c - 2R + r}{r^2}\sqrt{2r(h_c - 2(R+r)) - (h_c - 2(R+r))^2} + \\ + r^2 \arcsin\dfrac{h_c - 2R - r}{r} \end{array} \right) +$$

$$+ \frac{(h_c - 2R - r)}{4r^2}\sqrt{R(h_c - R + r) - (h_c - R + r)^2 - R^2} - \frac{3}{32}\pi \,. \quad (4.80)$$

Finally, the values of the integral expressions are calculated according to formulas (4.73), (4.74), (4.76) and (4.77).

The values of $\boldsymbol{I^{bt}}$ and $\boldsymbol{J^{bt}}$ for the tensile zone of concrete in the cross-section are as follows:

$$I_0^{\,bt} = 0,5\left[\frac{\pi R^2}{2} - (h_c - R)\sqrt{2Rh_c - h_c^{\,2}} - R^2 \arcsin\frac{h_c - R}{R} \right], \quad (4.81)$$

$$I_1^{\,bt} = 0,5\left[\begin{array}{l} \dfrac{\pi R^3}{2} + R^3 \arcsin\dfrac{R - h_c}{R} - \dfrac{2}{3}(2Rh_c - h_c^{\,2}) \times \\ \times\sqrt{2Rh_c - h_c^{\,2}} - R(r - h_c)\sqrt{2Rh_c - h_c^{\,2}} \end{array} \right], \quad (4.82)$$

$$J_0^{\,bt} = 0,5\Big[r\sqrt{2r(R+r) - (R+r)^2} - r^2\left(\arcsin\frac{h_c - 2R + r}{R} - \arcsin\frac{r}{R} \right) -$$

$$-(h_c - 2R + r)\sqrt{2r(h_c - R + r) - (h_c - R + r)^2}\Big], \quad (4.83)$$

$$J_1^{\,bt} = 0,5\Big[r^3\left(\arcsin\frac{R - h_c}{r} + \arcsin\frac{R}{r} \right) + \frac{2}{3}\cdot$$

$$\cdot\Big((2r(h_c - 2R + r) - (h_c - 2R + r)^2 \cdot \sqrt{2r(h_c - R + r) - (h_c - R + r)^2} -$$

$$-(2r(R+r) - (R+r)^2)\sqrt{2r(R+r) - (R+r)}\Big) +$$

$$+ r\Big(R\sqrt{2r(R+r) - (R+r)^2} +$$

$$+ (R - h_c)\sqrt{2r(h_c - R + r) - (h_c - R + r)^2}\Big)\Big]. \quad (4.84)$$

By substituting the obtained values of $\boldsymbol{I_K}$ and $\boldsymbol{J_K}$ into equations (4.69) and (4.70), we obtain the corresponding values of the normal force and bending moment in the ring-shaped or circular cross-section of the structure, based on the known deformations ε_1 and curvature χ. This cross-section may have cracks in the tensile zone of the concrete.

In the case where the circular cross-section of the reinforced concrete structure has no tensile zone, after performing mathematical transformations, we obtain the exact solution of the stress-strain state equations (4.69) and (4.70):

$$N = \pi R^2 \Big[a_1(\varepsilon_1 - \chi R) + a_2\left(\varepsilon_1^{\,2} - 2\chi\varepsilon_1 R + \frac{5}{4}\chi^2 R^2 \right) +$$

$$+ a_3\left(\varepsilon_1^{\,3} - 3\chi\varepsilon_1^{\,2} R + \frac{15}{4}\chi^2\varepsilon_1 R^2 - \frac{7}{4}\chi^3 R^3 \right) +$$

$$+ a_4\left(\varepsilon_1^{\,4} - 4\varepsilon_1^{\,3} R + \frac{15}{2}\chi^2\varepsilon_1^{\,2} R^2 - 7\chi^3\varepsilon_1 R^3 + \frac{21}{8}\chi^4 R^4 \right) +$$

$$+ a_5\left(\begin{array}{l} \varepsilon_1^{\,5} - 5\chi\varepsilon_1^{\,4} R + \frac{25}{2}\chi^2\varepsilon_1^{\,3} R^2 - \frac{35}{2}\chi^3\varepsilon_1^{\,2} R^3 \\ + \frac{105}{8}\chi^4\varepsilon_1 R^4 - \frac{33}{8}\chi^5 R^5 \end{array} \right) \Big] + \sum_{i=1}^{m} \sigma_{si} A_{si}; \quad (4.85)$$

$$M = \pi R^3 \Big[a_1\left(\varepsilon_1 - \frac{5}{4}\chi R\right) + a_2\left(\chi_1^{\,2} - \frac{5}{2}\chi\varepsilon_1 R + \frac{7}{4}\chi^2 R^2 \right) +$$

$$+ a_3\left(\varepsilon_1^{\,3} - \frac{15}{4}\chi\varepsilon_1^{\,2} R + \frac{21}{4}\chi^2\varepsilon_1 R^2 - \frac{21}{8}\chi^3 R^3 \right) +$$

$$+ a_4\left(\varepsilon_1^{\,4} - 5\chi\varepsilon_1^{\,3} R + \frac{21}{2}\chi^2\varepsilon_1^{\,2} R^5 - \frac{21}{2}\chi^3\varepsilon_1 R^3 + \frac{33}{8}\chi^4 R^4 \right) +$$

$$+ a_5\left(\begin{array}{l} \varepsilon_1^{\,5} - \frac{25}{4}\chi\varepsilon_1^{\,4} R + \frac{35}{2}\chi^2\varepsilon_1^{\,3} R^5 - \frac{105}{4}\chi^3\varepsilon_1^{\,2} R^3 \\ + \frac{165}{8}\chi^4\varepsilon_1 R^4 - \frac{429}{64}\chi^5 R^5 \end{array} \right) \Big] + \sum_{i=1}^{m} \sigma_{si} A_{si} h_{si}; \quad (4.86)$$

The stress values in the reinforcing steel σ_{si} can be determined using equations (4.46–4.62). At the same time, the deformations ε_s are found based on the fiber deformations of the concrete:

$$\sigma_{si} = \varepsilon_1 - \chi h_{si},$$

were

$$\chi = \frac{\varepsilon_1 + \varepsilon_2}{2R}. \qquad (4.87)$$

Thus, the obtained analytical dependencies for determining the stress-strain state of reinforced concrete elements with circular and ring cross-sections in the possible range of variation of the properties of concrete and reinforcement for any loading stage of the structure.

The calculation of the bearing capacity of normal sections of compressed and ordinary reinforced concrete structures involves finding the relationship between the load and deformations. The maximum point on the "load-curvature" curve corresponds to the bearing capacity of the reinforced concrete structures.

To determine the bearing capacity of a column with circular or ring cross-sections, one can use the equations of the stress-strain state provided in the section. The solution of the two equilibrium equations of the section with three unknowns, such as the normal force N and the deformations at the extreme fibers of the section ε_1, can be achieved through iteration and verification. For this, fixed values of ε_1 are assumed, and the value of ε_2 is selected that satisfies the condition $N \cdot e = M$ with the given accuracy. When determining the boundary conditions, it is assumed that the strength of the section is considered exhausted when the deformations of the concrete or reinforcement reach their limit values, specifically $\boldsymbol{\varepsilon_c = \varepsilon_{cu}}$ or $\boldsymbol{\varepsilon_s = \varepsilon_{su}}$.

The load-curvature diagrams for compressed and ordinary piers of a bridge transition with a circular cross-section are shown in Fig. 4.13.

The diagrams show that, in the case with $\boldsymbol{\mu} = 0.68\%$, the reduction in cement consumption due to lowering its grade from 600 to 400 and pre-compressing the concrete mix with a pressure of 1.5 MPa amounts to 25 percent, or 112 kg per cubic meter of concrete. For one bridge pier with a length of 7.22 m and a volume of 8.2 m³, this represents just under one ton of cement. In the variants with cement consumption of 450 kg/m³ of grade 600, the calculated steel savings for longitudinal

reinforcement bars when using steel class A-IIIv (A400) reach 23 percent, and over 38 percent when using steel class A800.

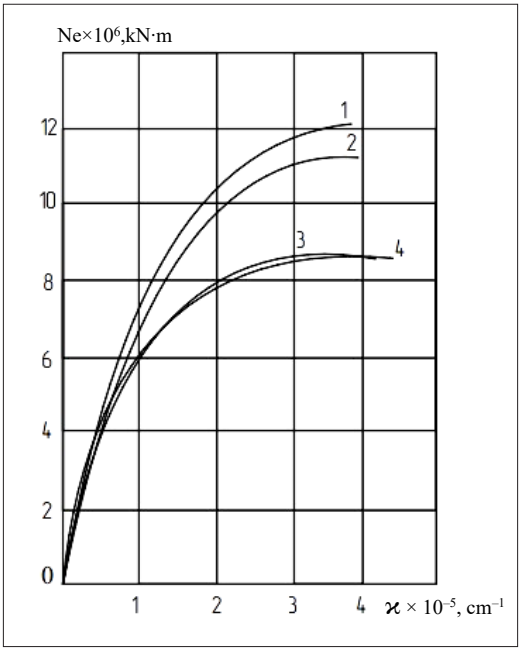

Figure 4.13. Calculated dependencies "Ne-χ" for full-scale bridge pier supports:

a *– compressed using the "mixing" method:*
1 – at p = 3.5 MPa, C=450 kg/ m³, M 600, and μ=0.54%
with class A800 steel; 2 – at p = 2 MPa, C=450 kg/ m³, M 600 and
μ=0.68% with class A-III$_в$steel.; 3 – at p = 1.5 MPa, C =338 kg/ m³, M 400
and μ=0.88% with class A-III$_в$ steel;
b *– ordinary reinforced concrete as per the project:*
4 – at C=450 kg/ m³, M 600 and μ=0.88%

The analysis of the results for the calculation of the bearing capacity of production piers with a circular cross-section using electronic computing machines showed the potential for significant reductions in the consumption of reinforcement steel and cement when compressing freshly placed concrete mix using the new method.

Taking into account the capabilities and production conditions of Bridge Construction Unit 73 ("MOSTOBUD" of Ukraine), a variant of the compressed pier with = 0.88% and p = 1.5 MPa was adopted and successfully implemented in construction practice.

4.5. Quality Control of Compressed Reinforced Concrete Structures

One of the most important issues when implementing the new technology for manufacturing compressed reinforced concrete piers (see Figs. 4.14, 4.17) was ensuring reliable and accurate control of the concrete quality.

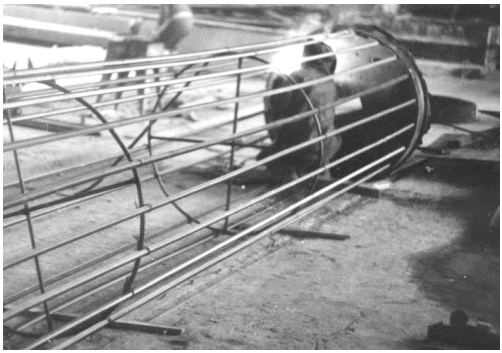

Figure 4.14. Manufacturing of the reinforcement cage

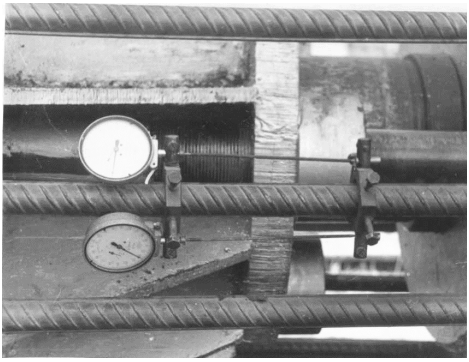

Figure 4.15. Control of reinforcement elongation

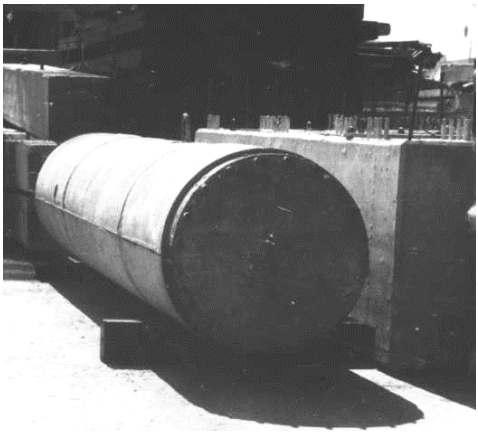

Figure 4.16. Compressed bridge pier

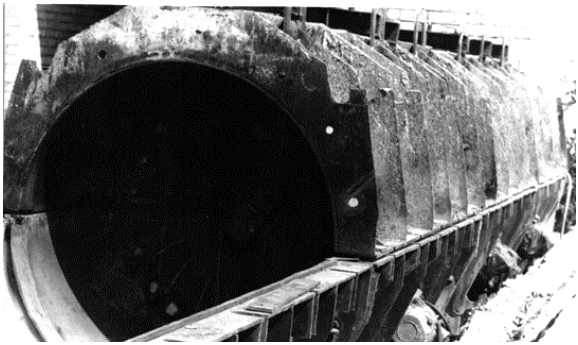

Figure 4.17. Movable end of the pressure mold with a device for sampling compressed concrete of standard sizes

Traditional concrete sampling in accordance with the current state standard could not provide satisfactory results because the concrete in the piers underwent compression, which changed its water-cement ratio and led to structural changes. Reproducing in separate control samples (Figs. 4.18, 4.19) the compression conditions identical to those in the piers during production is difficult. Therefore, it was necessary to develop special measures for quality control of the compressed structures.

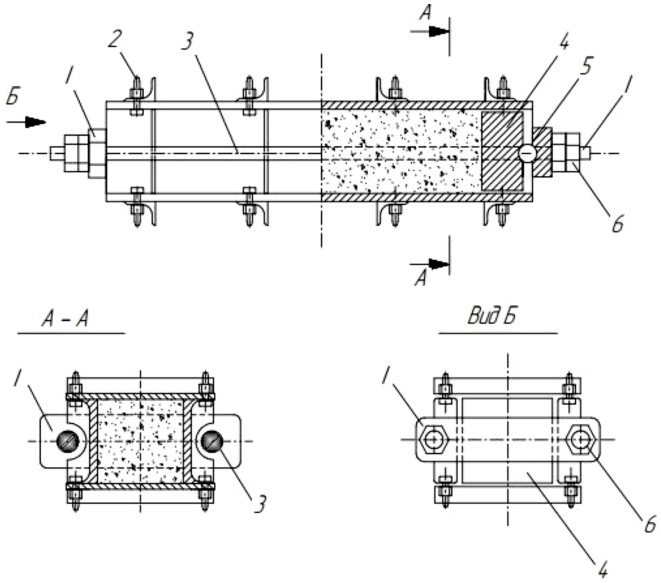

Figure 4.18. Pressure mold for manufacturing compressed samples
1 – traverse; 2 – bolt connection; 3 – tension rod; 4 – plunger; 5 – hinge; 6 – locking nut

Figure 4.19. General view. Pressure mold for manufacturing compressed samples

An overview of the existing concrete sampling methods in domestic practice and abroad did not reveal a sufficiently reliable and acceptable option for the conditions of this production. Non-destructive strength testing methods for critical structures, taking into account the new technology, could not satisfy the consumer. Therefore, a new special device (patent No. 1749040) was developed for sampling directly from the concrete of the compressed pier. For this purpose, a window was provided in the formwork, through which the device was fixed to the mold (see Fig. 20). The cross-section of the design of the concrete sampling device is shown in Fig. 21.

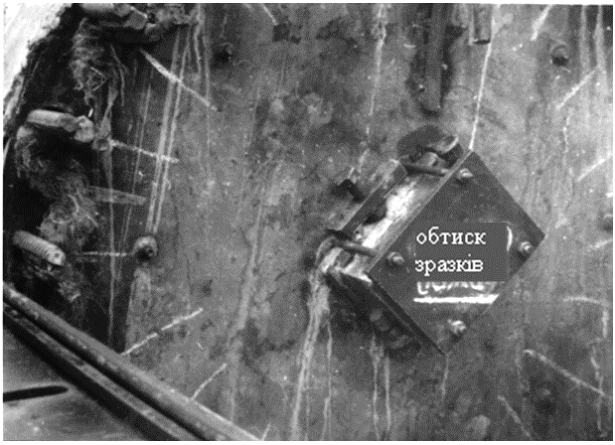

Figure 4.20. End of the pressure mold with a device for sampling concrete of standard sizes

To ensure the reliability of concrete strength control, standard control samples were made simultaneously with the main structure from the same concrete. For this purpose, standard sample molds were fixed to the movable end of the main formwork on a special frame, which was equipped with a splitting wedge. The main form had a window through which the concrete mix was pressed into the standard molds. After the concrete hardened, the standard control samples were separated from the finished structure using the wedge and tested according to the generally accepted method.

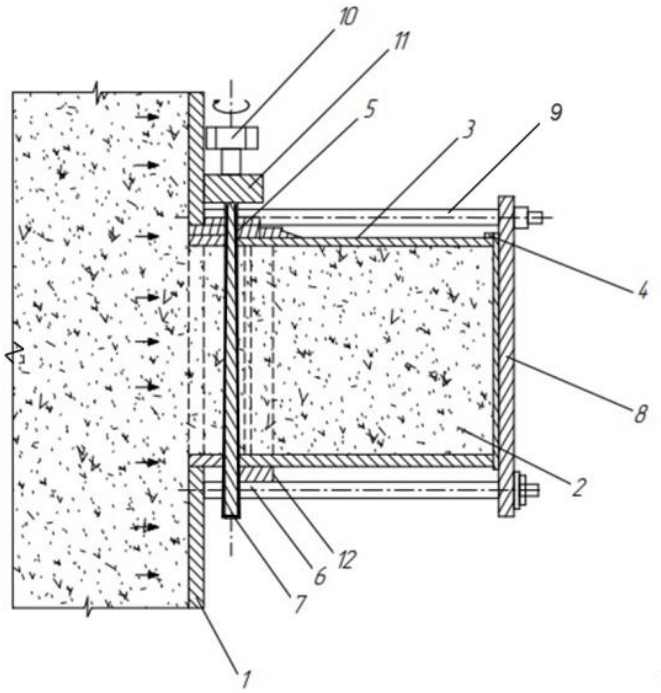

Figure 4.21. Device for sampling concrete of standard sizes
1 – formwork of the structure; 2 – concrete mix; 3 – standard sample mold; 4 – filter; 5 – seal; 6 – frame; 7 – wedge; 8 – plate; 9 – pin; 10 – screw; 11 – bar; 12 – spring

During the manufacturing of piers at the production facility, the required number of cube samples for testing the strength of the compressed concrete was obtained (see Fig. 20). For comparison, samples of the original uncompressed concrete were also made using the standard method. The test results are presented in Table 4.8. Preliminary evaluation of the concrete's tensile strength was carried out directly from the data of the force obtained when detaching the samples from the compressed structure.

After the manufacture of the full-scale piers, a selective quality control of the concrete was performed using the ultrasonic pulse method (Figs. 4.23, 4.24), in accordance with EN 12504-4:2021.

The UK-10 P device was used for measuring the pulse velocity.

Acoustic contact between the concrete and the working surfaces of the ultrasonic transducers was achieved using solidol as the coupling medium.

Figure 4.22. Compressed cube samples and wedge device

Table 4.8

Evaluation of concrete quality of pre-compressed piers using the "mixing" method

Pier Labeling	Ultrasonic Wave Speed v, m/s					Cube Strength f_c, MPa		Strength Improvement, %
	In the Cross-Section of the Pier				In the Cubes Taken from the Pier Concrete	Ordinary Concrete	pre-compressed	
	Startof the Pier Length	First Third	Second Third	end				
СБ-5.92	4510	4461	4455	4474	4454	47.6	65.2	37
СБ-7.22	4487	4445	4474	4493	4443	43.2	62.0	43
СБ-7.22	4504	4474	4447	4466	4442	41.5	61.4	49
СБ-7.22	4496	4493	4440	4459	4440	42.0	59.8	42
СБ-7.22	4508	4476	4456	4476	4452	43.6	63.6	46
СБ-5.92	4491	4459	4449	4493	4448	45.6	64.3	41

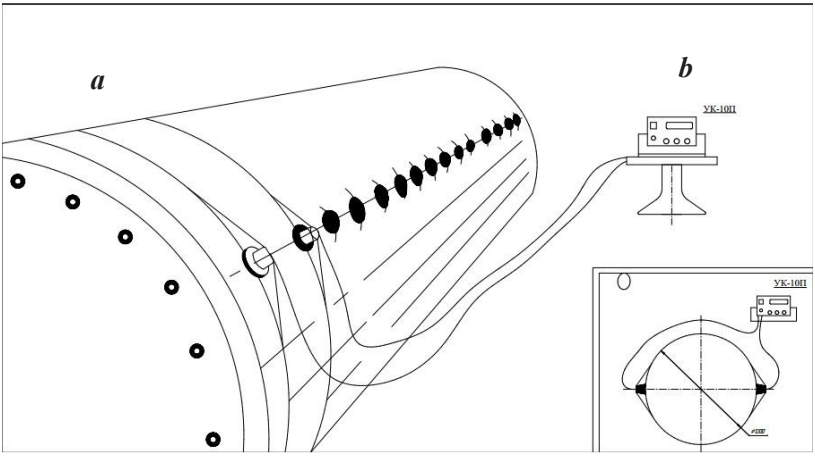

Figure 4.23. Quality Control by Ultrasonic Pulse Method:
a *– Surface sounding,* ***b****– Transverse sounding*

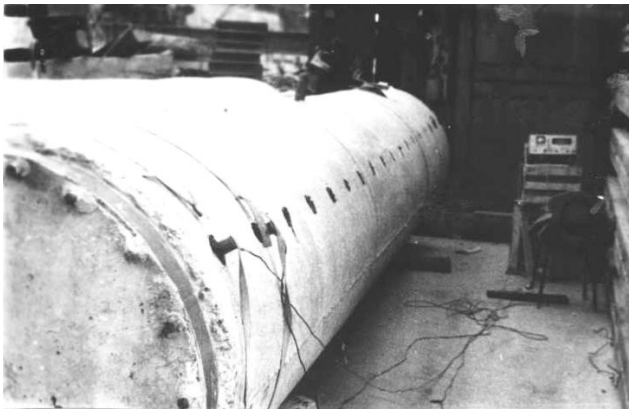

Figure 4.24. General View. Ultrasonic Quality Control

The method of transverse through-sounding of the product was applied.

For this, a marking was applied to the pier surface, and the sounding base was adjusted accordingly.

The ultrasonic wave velocity (V) is determined by the following formula:

$$v = \frac{L}{t - t_1} \cdot 10^3, \tag{4.88}$$

where

L – is the sounding base (in mm);

t – total propagation time of the ultrasonic pulse in the concrete, as measured by the UK-10P device;

The concrete strength at controlled sections of the piers was determined using a pre-established "velocity-strength" relationship for compressed concrete. The results of the measurements of the ultrasonic pulse velocity and the corresponding concrete strength data for the piers are shown in Table 4.8.

From the data in the table, the strengthening effect of the concrete due to compression at 1.5 MPa in the full-scale piers ranged from 37% to 49%. There was a tendency for a slight reduction (up to 7%) in the strengthening effect in the middle section of the structure.

The main reason for this reduction can be attributed to the decreased compaction effect in the middle part of the pier, which is likely caused by friction between moving elements of the formwork and the internal and external friction of the concrete mix during the compression process.

The implementation of the proposed quality control measures for reinforced concrete structures, compressed by the tension of reinforcement during curing, allowed for effective and reliable control of product quality in production conditions.

Observations of the behavior of the compressed piers under service loading at the supports of the elevated approach section of the bridge across the Dnieper River in Kamianske (Figs. 4.25–4.27) demonstrated the absence of defects, confirming the high quality of the piers compressed using the proposed **During–tensioning** method.

Figure 4.25. Operation of the piers compressed using the During-tensioning method for the bridge supports over the Dnieper River in Kamianske

a

b

Figure 4.26. Overall view of the bridge over the Dnieper River in Kamianske:
a – River section, b – Land section

a

b

c

Figure 4.27. Operation of the piers compressed using the During–tensioning method for the bridge supports over the Dnieper River in Kamianske:

a *– general view of the shoreline section,* **b** *– compressed columns,* ***c*** *– fragment of the structure compressed column*

AFTERWORD

Based upon existing methods of prestressed concrete production (post-tensioned and pre-tensioned), where hardened concrete is subjected to tensile forces, an innovative approach has been introduced. This method involves transferring prestress to the freshly laid concrete mix before it hardens.

Following vibrodynamic compaction, the placed mix undergoes compression from the steel stressing force, hardening under pressure. This process enhances mix compaction, removes excess water and air, eliminates macro- and partially micro-defects in the structure, and mitigates destructive processes during concrete hardening. Steel prestressing is retained because, after compacting a specially proportioned concrete mix, a strong and rigid skeleton of solid ingredients forms, securely fixing the stressed steel within this structure.

The technological feasibility of prestressing a freshly laid concrete mix was made possible by the author's invention of specialized formwork that moves during compression, along with devices enabling full or partial prestress transfer.

Extensive experimental research has been conducted, providing reliable data. The analysis of these findings allows for an accurate assessment of the load-bearing capacity of such prestressed structures.

The research has reached the stage of industrial implementation. Currently, large 30-ton bridge elements made using this method–where unset concrete is compressed by the force of steel tensioning (during-tensioning)–are successfully in use in Ukraine.

As a result of comprehensive research and practical application, concrete strength has been increased by 50–70%, while crack resistance remains at conventional levels. This improvement is achieved by compressing the unset concrete mix during the steel tensioning process.

REFERENCES

1. Lund, J. G. E. Beschreibung der Konstruktion und Verwendung von Eisenbetonhohlblocken, armiert nach System Lund. *Beton und Eisen*. 1905, H. 7, S. 143–143, 169–173.
2. Lund, J. G. E. *Prestressed Reinforced Concrete*. US Patent No. 1020578, 1912. First publication, 1907.
3. PISTOR, L. Die Anwendung von Vorspannungen im Stahlbetonbau. *Beton und Eisen*. 1940, H. 11–12, S. 150–154, 160–162.
4. BACH, C. and GRAF, O. *Mitteilungen über Forschungsarbeiten*. VDI, 1910. H. 90–91.
5. WETTSTEIN, K. Die Entwicklung der Wettstein-Betonbretter. *Betonsteinzeitung*. 1948, H. 3, S. 41–45.
6. HEWETT, W. H. *Prestressed Concrete Construction*. US Patent No. 1818254, 1927. Also published in *ACI Journal*, 1923, p. 41.
7. DILL, R. H. US Patent No. 1684663, 1925–1928.
8. FREYSSINET, E. *Une révolution dans les techniques du béton*. Paris: Eyrolles, 1936. 118 p.
9. LENK, K. Spannbetonrohre. *Beton und Eisen*. 1942, H. 15–16, S. 137–144.
10. EMPERGER, F. V. *Stahlbeton mit vorgespannten Zulagen aus höherwertigem Stahl*. Berlin: Verlag Wilhelm Ernst und Sohn, 1939.
11. LÄMMLEIN, A. and BAUER, A. Spannbetonbrücke Emmendingen. *Beton und Stahlbetonbau*. 1950, H. 9, S. 197–203.
12. KLETT, E. Die Spannbetonbrücke der Bundesbahn über den Neckarkanal in Heilbronn. *Beton und Stahlbetonbau*. 1951, H. 7, S. 145–150, 180–184.
13. LEONHARDT, F., STÖHN, W. and GASS, H. Neckarkanalbrücke Obere Badstraße, Heilbronn. *Beton und Stahlbetonbau*. 1951, H. 12, S. 265–270.
14. GUYON, Y. *Béton précontraint: étude théorique et expérimentale*. Vol. 1–2. Paris: Eyrolles / Institut Technique du Bâtiment et des Travaux Publics, 1951–1958.

15. MAGNEL, G. *Prestressed Concrete*. 2nd ed., revised and enlarged. London: Concrete Publications, 1950. 300 p.
16. MÖRSCH, E. Die Ermittlung des Bruchmomentes von Spannbetonbalken. *Beton und Stahlbetonbau*. 1950, H. 7, S. 149–157.
17. LEONHARDT, F. *Spannbeton für die Praxis*. Berlin: Ernst & Sohn, 1955. 588 S.
18. ABELES, P. W. Partial prestressing in England. *Journal of the Prestressed Concrete Institute*. 1963, vol. 8, no. 1.
19. RÜSCH, H. Bruchlast und Bruchsicherheitsnachweis bei Biegungsbeanspruchung von Stahlbeton unter besonderer Berücksichtigung der Vorspannung. *Beton und Stahlbetonbau*. 1950, H. 9, S. 215–220.
20. LIN, T. Y. *Design of Prestressed Concrete Structures*. New York: John Wiley & Sons, 1955. 456 p.
21. PACHOLIK, L. *Prestressed Concrete*. Moscow: Avtotransizdat, 1957. 595 p. (in Russian).
22. KANI, G. *Spannbeton in Entwurf und Ausführung*. Stuttgart: Verlag von Konrad Wittwer, 1955. 573 S.
23. LEONHARDT, F. *Spannbeton für die Praxis*. 3rd ed. Berlin: Wilhelm Ernst & Sohn, 1973. 573 S.
24. KOMENDANT, A. E. *Prestressed Concrete Structures*. New York: McGraw-Hill, 1952. 261 p.
25. FÉDÉRATION INTERNATIONALE DE LA PRÉCONTRAINTE (FIP). *Proceedings of the 5th International Congress of Prestressing*. Paris, 11–18 June 1966. London: Cement and Concrete Association, 1966.
26. FÉDÉRATION INTERNATIONALE DE LA PRÉCONTRAINTE (FIP). *Proceedings of the 7th International Congress of the FIP*. New York, USA, 26 May – 1 June 1974. Vol. 1–2. London: Cement and Concrete Association, 1974.
27. FÉDÉRATION INTERNATIONALE DE LA PRÉCONTRAINTE (FIP). *Proceedings of the Seventh International Congress of the FIP*. New York, 1974. Vol. 1–2. London: Cement and Concrete Association, 1974.
28. FÉDÉRATION INTERNATIONALE DE LA PRÉCONTRAINTE (FIP). *Proceedings of the Eighth International*

Congress of the FIP. London, 30 April – 5 May 1978. Vol. 1. London: Cement and Concrete Association, 1978. 249 p.
29. AJDUKIEWICZ, A. and MAMES, J. *Konstrukcje sprężone*. Warszawa: Arkady, 1984. P. 10–17.
30. GVOZDEV, A. A., DMITRIEV, S. A. and KRYLOV, S. M. *Novoe o prochnosti zhelezobetona* [New Aspects of Reinforced Concrete Strength]. Moscow: Stroyizdat, 1977. 272 p.
31. MIKHAILOV, V. V. *Predvaritel'no-napryazhennye zhelezobetonnye konstruktsii* [Prestressed Reinforced Concrete Structures]. Moscow: Stroyizdat, 1978. 383 p.
32. DMITRIEV, S. A. and KALATUROV, B. A. *Raschet predvaritel'no napryazhennykh zhelezobetonnykh konstruktsii* [Design of Prestressed Reinforced Concrete Structures]. Moscow: Izdatel'stvo literatury po stroitel'stvu, 1956. 508 p.
33. BERG, O. YA. *Fizicheskie osnovy teorii prochnosti betona i zhelezobetona* [Physical Foundations of the Strength Theory of Concrete and Reinforced Concrete]. Moscow: Gosstroyizdat, 1962. 95 p.
34. BERDICHEVSKY, G. I. and TSALALIKHIN, M. S. *Tekhnologicheskie faktory treshchinostoykosti i prochnosti predvaritel'no napryazhennykh zhelezobetonnykh konstruktsii* [Technological Factors of Crack Resistance and Strength of Prestressed Reinforced Concrete Structures]. Moscow: Stroyizdat, 1969. 151 p.
35. BAYKOV, V. N. and SIGALOV, E. E. *Zhelezobetonnye konstruktsii. Obshchii kurs* [Reinforced Concrete Structures: General Course]. Moscow: Stroyizdat, 1985. 762 p.
36. BARASHIKOV, A. YA. *Raschet zhelezobetonnykh konstruktsii na deistvie dlitel'nykh peremennykh nagruzok* [Design of Reinforced Concrete Structures under Long-Term Variable Loads]. Kyiv: Budivelnyk, 1977. 155 p.
37. BARASHIKOV, A. YA. and NOVOTARSKY, I. P. Stress-strain state of bending elements under long-term variable loads of high level. *Stroitel'nye konstruktsii*. 1982, vol. 35, pp. 19–25.
38. BARASHIKOV, A. YA., POLYAKOV, L. P. and YATSENKO, E. A. *Prochnost' i deformativnost' zhelezobetonnykh*

konstruktsii [Strength and Deformability of Reinforced Concrete Structures]. Kyiv: Budivelnyk, 1978. 128 p.
39. BARASHIKOV, A. YA., BUDNIKOVA, YA. M. and KUZNETSOV, Ya. V. *Zhelezobetonnye konstruktsii* [Reinforced Concrete Structures]. Kyiv: Vyshcha Shkola, 1984. 351 p.
40. STOROZHENKO, L. I., PLAKHOTNY, P. I. and CHERNY, A. Ya. *Raschet trubobetonnykh konstruktsii* [Design of Concrete-Filled Tube Structures]. Kyiv: Budivelnyk, 1991. 120 p.
41. MIKHAILOV, K. V. *Provolochnaya armatura dlya predvaritel'no napryazhennogo zhelezobetona* [Wire Reinforcement for Prestressed Reinforced Concrete]. Moscow: Stroyizdat, 1964.
42. RATS, E. G. *Zhelezobeton s elektrotermicheskim natyazheniem armatury* [Reinforced Concrete with Electrothermal Prestressing of Reinforcement]. Moscow: Stroyizdat, 1967.
43. AKHVERDOV, I. N. *Vysokoprochnyi beton* [High-Strength Concrete]. Moscow: Gosstroyizdat, 1961. 162 p.
44. ULITSKY, I. I., KIREEVA, S. V. and FRANSTIL, I. V. *Poteri predvaritel'nogo napryazheniya ot polzuchesti i usadki betona v zhelezobetonnykh konstruktsiyakh* [Prestress Losses Due to Creep and Shrinkage of Concrete in Reinforced Concrete Structures]. Kyiv: State Publishing House for Construction and Architecture Literature, 1962. 207 p.
45. GOLYSHEV, A. B. et al. *Raschet sborno-monolitnykh konstruktsii s uchetom faktora vremeni* [Design of Composite Structures Considering Time Factor]. Kyiv: Budivelnyk, 1969. 220 p.
46. GOLYSHEV, A. B., POLISHCHUK, V. P. and RUDENKO, I. V. Design of reinforced concrete frame systems considering time factor. *Proceedings of UIIVH Conference*. Rivne, 1969, p. 186.
47. ZALESOV, A. S., KODYSH, E. N., LEMYSH, L. L. and NIKITINA, I. K. *Raschet zhelezobetonnykh konstruktsii po prochnosti, treshchinostoykosti i deformatsiyam* [Design of Reinforced Concrete Structures for Strength, Crack Resistance and Deformations]. Moscow: Stroyizdat, 1988. 320 p.
48. GOLYSHEV, L. B. *Proektirovanie zhelezobetonnykh konstruktsii* [Design of Reinforced Concrete Structures]. Kyiv: Budivelnyk, 1990. 544 p.

49. BAYKOV, V. N. and SIGALOV, E. E. *Zhelezobetonnye konstruktsii. Obshchii kurs* [Reinforced Concrete Structures: General Course]. Moscow: Stroyizdat, 1991. 767 p.
50. KUDZIS, A. P. *Zhelezobetonnye i kamennye konstruktsii. Chast' 1* [Reinforced Concrete and Masonry Structures. Part 1]. Moscow: Vysshaya Shkola, 1988. 287 p.
51. KUDZIS, A. P. *Zhelezobetonnye i kamennye konstruktsii. Chast' 2* [Reinforced Concrete and Masonry Structures. Part 2]. Moscow: Vysshaya Shkola, 1988. 287 p.
52. BARASHIKOV, A.Ya., GOLBERG, M. G. and KUSHNAREV, Yu.I. *Spravochnik po raschetu stroitel'nykh konstruktsii na programmiruemykh mikrokalkulyatorakh* [Handbook for Structural Calculations Using Programmable Calculators]. Kyiv: Budivelnyk, 1989. 224 p.
53. GERSHBERG, O. A. *Tekhnologiya betonnykh i zhelezobetonnykh izdelii* [Technology of Concrete and Reinforced Concrete Products]. Moscow: Stroyizdat, 1971. 353 p.
54. MURASHKIN, G. V. *Osobennosti izgotovleniya i proektirovaniya konstruktsii iz betona, tverdeyushchego pod davleniem* [Features of Manufacturing and Design of Structures Made of Pressure-Hardened Concrete]. Kuybyshev, 1985. 258 p.
55. BABICH, E. M. *Konstruktsii iz legkikh betonov na poristykh zapolnitelyakh* [Structures Made of Lightweight Concrete on Porous Aggregates]. Kyiv: Vyshcha Shkola, 1988. 208 p.
56. LUKSHA, L. K. *Prochnost' trubobetona* [Strength of Concrete-Filled Tubes]. Minsk: Vysshaya Shkola, 1977. 96 p.
57. BARASHIKOV, A.Ya., MURASHKO, L. A. and REMINETS, G. M. *Issledovanie deformativnosti zhelezobetonnykh ram* [Investigation of Deformability of Reinforced Concrete Frames]. Kyiv: Budivelnyk, 1974. 86 p.
58. PECHENOV, L. N., DEKHTYAR, A. S. and KOVALSKY, A. P. *Arkhitekturnye konstruktsii grazhdanskikh zdanii: Raschet konstruktsii* [Architectural Structures of Civil Buildings: Structural Design]. Kyiv: Budivelnyk, 1983. 72 p.
59. IOSILEVSKY, L. I. *Dolgovechnost' predvaritel'no napryazhennykh zhelezobetonnykh balochnykh proletnykh stroenii*

mostov [Durability of Prestressed Reinforced Concrete Bridge Girders]. Moscow: Transport, 1967. 281 p.
60. LOPATTO, A. E. *Zhelezobeton v mashinostroenii* [Reinforced Concrete in Mechanical Engineering]. Odessa: Mayak, 1966. 51 p.
61. LOPATTO, A. E. and MAYBORODA, V. F. *Proektirovanie elementov zhelezobetonnykh konstruktsii* [Design of Reinforced Concrete Structural Elements]. Kyiv: Vyshcha Shkola, 1987. 283 p.
62. SEKHNIASHVILI, E. A. *Integral'naya otsenka kachestva i nadezhnosti predvaritel'no napryazhennykh konstruktsii* [Integrated Assessment of Quality and Reliability of Prestressed Structures]. Moscow: Nauka, 1988. 220 p.
63. BONDARENKO, V. M. and SUVORKIN, D. G. *Zhelezobetonnye i kamennye konstruktsii* [Reinforced Concrete and Masonry Structures]. Moscow: Vysshaya Shkola, 1987. 384 p.
64. STEFANOV, B. V. *Tekhnologiya betonnykh i zhelezobetonnykh izdelii* [Technology of Concrete and Reinforced Concrete Products]. Kyiv: Vyshcha Shkola, 1972. 355 p.
65. KLIMOV, Yu.A. *Theory and Calculation of Strength, Crack Resistance and Deformability of Reinforced Concrete Elements under Shear Forces*. Doctoral dissertation. Kyiv, 1992.
66. BABICH, E. M., BLAZHENIN, I. I. and MAKARENKO, L. P. Strength of concrete hardened under triaxial compression. *Beton i Zhelezobeton*. 1966, no. 7, pp. 29–30.
67. BABICH, E. M. *Experimental and Theoretical Investigation of Strength and Deformation Properties of Early-Age Loaded Concrete*. PhD dissertation. Kyiv, 1967.
68. MAKARENKO, L., KASYAN, A. and BABICH, E. Increase in concrete strength. *Budivelni Materialy i Konstruktsii*. 1968, no. 5, pp. 33–35.
69. BABICH, E. M., KRUS, A. M., KOPITMAN, S. M. and BEREGOVICH, V. G. Prestressed piles based on long-term pressed concrete. In: *Proceedings of the XVIII Republican Scientific and Technical Conference*. Rivne, 1969.
70. BABICH, E. M. and MAKARENKO, Zh. P. Investigation of strength and modulus of elasticity of concrete under

triaxial compression. *Stroitel'nye konstruktsii*. 1977, vol. 30, pp. 100–104.
71. COPPERTWAITE, W. C. *Tunnel Shields and the Use of Compressed Air in Subaqueous Works*. London, 1906. 37 p.
72. ROBERTS, E. W. and LEESE, L. E. *Method of Casting Cement or Fibre Cement under Pressure*. London Patent Office, 21 March 1921.
73. FREYSSINET, E. *Method of Accelerating the Hardening of Mortars and Concretes*. London Patent Office, 14 September 1936.
74. VOLKOV, Yu. S. Manufacturing of panels by the Gou-Con pressing system (England). *Beton i Zhelezobeton*. 1972, no. 3, pp. 42–43.
75. *Foreign Equipment for Continuous Forming of Reinforced Concrete Structures*. Moscow: VNIIESM, 1978. pp. 30–35.
76. RYABCHENKO, V. N. and NEPOMNYASHCHY, L. P. Power vibro-rolling. *Na Stroikakh Rossii*. 1960.
77. STANKEVICH, M. K. Concrete press-rolling. *Byulleten Tekhnicheskoi Informatsii*. 1957, no. 3.
78. SATALKIN, A. V. Investigation of properties of pressed concrete. *Proceedings of NIIB*. Leningrad, 1931, vol. 8, pp. 24–25.
79. L'HERMITE, R. and VOLENTA, M. Recherche concernant l'influence de la pression sur la prise des ciments. *Annales de l'Institut Technique du Bâtiment et des Travaux Publics*. 1937, no. 6, p. 51.
80. BOLOMEY, I. Influence du mode de mise en œuvre du béton sur sa résistance. *Travaux*. 1938, no. 70, pp. 437–443.
81. LOKHVITSKII, G. Z. Theory of vibro-pressing of concrete. *Betonnye i zhelezobetonnye konstruktsii* [Concrete and Reinforced Concrete Structures]. Tbilisi, 1984, pp. 7–12.
82. MIKHAILOV, V. V. *Elements of the Theory of Concrete Structure*. Moscow–Leningrad: Gosizdat, 1941. 227 p.
83. KLUS, T., LEESNAR, Y. Physical phenomena in pressed concrete. *Inżynieria i Budownictwo* [Engineering and Construction], 1960, no. 6, p. 23.
84. LAWRENCE, C. D. The properties of cement paste compacted under high pressure. *Research Report 19*. London: Cement and Concrete Association, 1969, pp. 176–191.

85. ROY, D. M., GONDA, G. R., ROBROWSKY, A. Very high strength cement pastes prepared by hot pressing and other high pressure techniques. *Cement and Concrete Research*, 1972, no. 3, pp. 807–820.
86. ROY, D. M., GONDA, G. R. Porosity-strength relation in cementitious materials with very high strengths. *Journal of the American Ceramic Society*, 1973, no. 10, pp. 710–714.
87. BABKOV, V. V., MOKHOV, V. N., ANANENKO, A. A., POLAK, A. F. Structural heterogeneity and strength of porous materials. *Izvestiya VUZov. Stroitelstvo i Arkhitektura* [News of Higher Educational Institutions. Construction and Architecture], 1980, no. 12, pp. 64–69.
88. BABYCH, S., ZHUK, S. Influence of initial and long-term pressing stresses on concrete strength. *Budivelni materialy i konstruktsii* [Building Materials and Structures], 1973, no. 1, pp. 36–37.
89. BALKIN, YA. M. *Pressed Concrete and Analysis of Factors Determining Its Strength*. PhD thesis. Moscow, 1947. 137 p.
90. LESOV, A. E. Some issues of structure, strength and deformation of concrete. In: *Structure, Strength and Deformation of Concrete*. Moscow: Stroyizdat, 1966.
91. ENUKASHVILI, I. R. *Investigation of Technology and Properties of Vibro-Pressed Concrete*. PhD thesis. Tbilisi, 1973. 138 p.
92. MURASHKIN, G. V., TIKHONOV, I. N. Application of high-strength pressure-hardened concrete in prestressed reinforced concrete structures. In: *Proceedings of the XVII Session of the USSR FIP Commission*. Kyiv, 1969, pp. 74–76.
93. MCHEDLOV-PETROSYAN, O., BUNAKOV, A., VORONTSOV, E. Influence of early loading on the strength of cement mortars. *Stroitelnye materialy, izdeliia i konstruktsii* [Building Materials, Products and Structures], 1955, no. 6.
94. SVITONSKII, A. V. *Development and Investigation of Vibrating Technology for Hot Concrete Mixtures*. PhD thesis. Minsk, 1978. 138 p.
95. TSIONSKII, A. L. *Investigation of Concrete Properties and Spiral Reinforcement Tensioning Process Applied to Vibro-Hydropressed Pressure Pipes Production*. PhD thesis. Moscow, 1968. 165 p.

96. ELBAKIDZE, M. G., ENUKASHVILI, I. R. Pressing and vibro-pressing of cement paste, mortar and concrete. *Izvestiya T. NIISGEI im. Vintera* [Proceedings of the Winter Research Institute], Moscow: Energiya, 1971, pp. 79–82.
97. MURASHKIN, G. V. Economic efficiency of using pressure-hardened concrete in columns. *Zhelezobetonnye konstruktsii* [Reinforced Concrete Structures]. Kuibyshev, 1982, pp. 7–21.
98. MURASHKIN, G. V. On the role of pressure duration in physico-mechanical processes of hardening concrete. *Zhelezobetonnye konstruktsii* [Reinforced Concrete Structures]. Kuibyshev, 1984, pp. 5–20.
99. MURASHKIN, G. V. *Features of Manufacturing and Design of Structures Made of Pressure-Hardened Concrete*. Kuibyshev, 1985. 258 p.
100. BABYCH, E. M., MAKARENKO, L. P., TORYANYK, M. S. Properties of high-strength heavy sand and lightweight concretes produced by long-term pressing. In: *Proceedings of the XVII Session of the USSR FIP Commission*. Kyiv, 1969, pp. 51–52.
101. BABYCH, S., KIZYMA, V. Increasing the strength of steam-cured concrete by long-term pressing. *Budivelni materialy i konstruktsii* [Building Materials and Structures], 1970, no. 1, pp. 23–24.
102. TOOSSI, M., HOUDE, J. Evaluating strength variation due to height of concrete members. *Cement and Concrete Research*, 1981, vol. 11, no. 4, pp. 519–529.
103. MATVIENKO, V. M. Production of non-pressure concrete pipes by vibro-pressing method. *Promyshlennost sbornogo zhelezobetona* [Precast Reinforced Concrete Industry], 1978, no. 1, pp. 7–9.
104. MIRIMANOV, G. I. Tensile strength of pressed concrete. *Beton i zhelezobeton* [Concrete and Reinforced Concrete], 1969, no. 8, pp. 23–25.
105. ROY, D. M., GONDA, G. R. Optimisation of strength in cement pastes. In: *Proceedings of the VI International Congress on the Chemistry of Cement*. Moscow, 1974, p. 12.
106. SPASSKAYA, I. A., RADIN, I. A., CHEKHOVSKII, YU. V. Investigation of vibro-pressing process of sand concrete

products. *Promyshlennost sbornogo zhelezobetona* [Precast Reinforced Concrete Industry], 1978, issue 1, pp. 19–21.
107. POPOV, A. I., TSIONSKII, A. L., KHRIPUNOV, V. A. *Production of Reinforced Concrete Vibro-Hydropressed Pressure Pipes*. Moscow: Stroyizdat, 1979. 256 p.
108. BAZHENOV, YU.M., KOMAR, A. G. *Technology of Concrete and Reinforced Concrete Products*. Moscow: Stroyizdat, 1984, pp. 484–498.
109. SHIKHNENKO, I. V. *Short Handbook for Reinforced Concrete Production Engineers*. Kyiv: Budivelnyk, 1989, pp. 224–228.
110. SATALKIN, A. V., SENCHENKO, V. A., KOMOKHOV, A. I. et al. Concrete mixtures for press-rolling and vibro-press-rolling. In: *Automation and Improvement of Processes for Preparation, Placement and Compaction of Concrete Mixes*. Proceedings of NIIZHB, issue 33. Moscow: Stroyizdat, 1964, pp. 271–291.
111. AKHVERDOV, I. P. *Fundamentals of Concrete Physics*. Moscow: Stroyizdat, 1981. 264 p.
112. NAGATAKI, S. On the use of superplasticizers. In: *Proceedings of the Eighth Congress of the Fédération Internationale de la Précontrainte (FIP)*. London, 30 April–May 1978, part 1, pp. 241–249.
113. DONCON, A. I. Mix design for concrete block paving. *Precast Concrete*, 1981, vol. 12, no. 2, pp. 65–75.
114. LYASHKEVICH, I. M. Technology for obtaining high-strength gypsum material by filtration pressing. In: *Technology, Organization and Economics of Construction*. Minsk, 1983, pp. 125–130.
115. KHUSAINOV, I. ZH. On accounting for the influence of compaction method on soil strength. In: *Improving the Quality of Highway Construction in the Non-Chernozem Zone of the RSFSR*. Vladimir, 1981, pp. 104–107.
116. KORZUN, S. I., RUDITSER, R. M. Investigation of physicomechanical properties of vibrated concrete with various pressing regimes and conditions. *Voprosy stroitelstva i arkhitektury* [Issues of Construction and Architecture]. Minsk, 1979, no. 9, pp. 140–145.

117. KORZUN, S. I., RUDITSER, R. M. Rational forming regime for centrifuged reinforced concrete pipes. *Beton i zhelezobeton* [Concrete and Reinforced Concrete], 1983, no. 9, pp. 23–25.
118. SESKIN, I. E., ESMONT, V. A., MURASHKIN, G. V. Deformability of pressure-hardened concrete. *Zhelezobetonnye konstruktsii* [Reinforced Concrete Structures]. Kuibyshev, 1979, pp. 16–32.
119. SESKIN, I. E. *Prestress Losses in Vibro-Hydropressed Pressure Pipes Made of Slag Crushed Stone Concrete, Their Crack Resistance and Water Tightness*. PhD thesis. Kyiv, 1983. 176 p.
120. VARLAMOV, A. A., KRISHAN, A. L., MATVEEV, V. G. Investigation of strength and deformability properties of pressed concrete. In: *Research in Structural Mechanics and Building Structures*. Chelyabinsk, 1985, pp. 141–142.
121. MATVEEV, V. G., KRISHAN, A. L., VARLAMOV, A. A., AMELKIN, G. I. Investigation of bearing capacity of bar elements with compressed concrete structure. In: *Experimental Studies of Engineering Structures*. Novopolotsk, 1986, p. 38.
122. MIRONOV, S. A., KRIVITSKII, M.YA., MALININA, L. A., MALINSKII, E. N., Schastnyi, A. N. *Autoclaved Concretes*. Moscow: Stroyizdat, 1968.
123. MOKHOVA, M. L. *Investigation of Certain Causes of Concrete Strengthening*. Abstract of PhD thesis. Leningrad, 1968. 20 p.
124. GOLYSHEV, A. B., SESKIN, I. E. Prestress losses in vibro-hydropressed pressure pipes. *Zhelezobetonnye konstruktsii* [Reinforced Concrete Structures]. Kuibyshev, 1984, pp. 32–44.
125. MAKARENKO, L. P., BABYCH, E. M. A new method for obtaining high-strength concrete and its properties. *Stroitelnye materialy i stroitelnoe proizvodstvo* [Building Materials and Construction Production]. Leningrad, 1966, pp. 63–65.
126. DAVIS, R., DAVIS, H. Flow of concrete under the action of sustained loads. *Journal of ACI*, March 1931.
127. MAILYAN, D. R. *Investigation of the Influence of Prestressing on Material Properties and Behaviour of Flexible Eccentrically Compressed Reinforced Concrete Columns*. PhD thesis. Rostov-on-Don, 1980. 277 p.

128. MELNIK, R. A. Change in deformability and strength of concrete under long-term compression. *Beton i zhelezobeton* [Concrete and Reinforced Concrete], 1964, no. 3, pp. 8–12.
129. BERG, O. YA., SHCHERBAKOV, E. N., PISANKO, G. M. *High-Strength Concrete*. Moscow: Stroyizdat, 1971. 207 p.
130. AKHVERDOV, I. N. *Issues of the General Theory of Concrete in Connection with Its Structural and Technological Features*. Doctoral dissertation. Tbilisi, 1955. 375 p.
131. AKHVERDOV, I. N., PODMOSTKO, I. V. Change in deformation properties of precompressed concrete. *Doklady Akademii Nauk BSSR* [Proceedings of the Academy of Sciences of the BSSR], 1968, vol. 12, no. 1, pp. 27–30.
132. SATALKIN, A. V. Early loading of concrete and its practical application. In: *Sixth Leningrad Conference on Concrete and Reinforced Concrete*. Leningrad, 1971, pp. 133–140.
133. MAKARENKO, L. P., FENKO, G. A. Reduction in tensile strength of concrete after prolonged compression. *Beton i zhelezobeton* [Concrete and Reinforced Concrete], 1970, no. 7, pp. 18–20.
134. SEMENOV, A. I., ARZHANOVSKII, S. I. Influence of prolonged compression on strength and deformation properties of concrete. *Beton i zhelezobeton* [Concrete and Reinforced Concrete], 1972, no. 1, pp. 34–37.
135. KUDZIS, L. P., GLEBOV, V. I. Influence of long-term compression on mechanical properties of ordinary and polymer-cement centrifuged concretes. *Zhelezobetonnye konstruktsii. Trudy Vilnyusskogo ISI* [Reinforced Concrete Structures. Proceedings of Vilnius Civil Engineering Institute], 1978, no. 9, pp. 19–29.
136. SATALKIN, A. V., SENCHENKO, B. A. *Early Loading of Concrete and Reinforced Concrete in Bridge Construction*. Moscow: Avtotransizdat, 1956. 210 p.
137. SATALKIN, A. V. et al. Concrete mixtures for press-rolling and vibro-rolling. In: *Automation and Improvement of Preparation, Placement and Compaction Processes of Concrete Mixes*. Proceedings of NIIZHB, issue 33. Moscow: Stroyizdat, 1964, pp. 171–191.

138. ZEDGENIDZE, V. A., OPLACHKO, V. M., POLOVETS, V. I. On the bearing capacity of reinforced concrete rods under long-term loading. *Stroitelnye konstruktsii* [Building Structures], issue XVI. Kyiv: Budivelnyk, 1973, pp. 148–152.
139. MELNICHENKO, O. V. *Experimental Investigation of Long-Term Strength of Heavy High-Strength Concretes under Compression*. Abstract of PhD thesis. Kyiv, 1977. 18 p.
140. IVANOV, YU. A., FEDORENKO, M. M. Experimental investigation of strength of flexural reinforced concrete elements made of high-strength concrete. *Stroitelnye konstruktsii* [Building Structures], issue XXVIII. Kyiv: Budivelnyk, 1976, pp. 92–96.
141. GERSHVALD, V. S. Determination of axial prestressing in vibro-hydropressed pressure pipes. *Beton i zhelezobeton* [Concrete and Reinforced Concrete], 1992, no. 11, pp. 14–16.
142. NEVILLE, A. M. *Properties of Concrete*. Moscow: Stroyizdat, 1972. 342 p.
143. LITVYAK, S. I. *Investigation of Stress-Strain State and Bearing Capacity of Reinforced Concrete Beams Reloaded after Long-Term Operational Loading*. PhD thesis. Kyiv, 1973. 167 p.
144. SIROVATKA, L. I. *Bearing Capacity of Flexural and Rigid Eccentrically Compressed Reinforced Concrete Elements with Different Reinforcement Ratios after Long-Term Loading*. PhD thesis. Kyiv, 1984. 189 p.
145. BABENKO, D. V. *Long-Term Resistance of Reinforced Concrete Rods with High Reinforcement Ratio*. Abstract of PhD thesis. Odesa, 1981. 24 p.
146. BATASHEV, V. M., FEDORCHUK, V. I. Strength and deformation properties of high-strength concretes considering load history. In: *Proceedings of the Republican Scientific and Technical Conference "Long-Term Resistance of Concrete and Reinforced Concrete Structures"*. Odesa, 1981, pp. 22–23.
147. ZAITSEV, YU. V. Accounting for long-term concrete resistance in reinforced concrete design. In: *Proceedings of the Scientific and Technical Conference "Long-Term Resistance of Concrete and Reinforced Concrete Structures"*. Odesa, 1981, pp. 6–7.
148. ZAITSEV, YU. V., SHCHERBAKOV, E. N. Verification of concrete strength of prestressed elements under compression

force action. *Beton i zhelezobeton* [Concrete and Reinforced Concrete], 1976, no. 6, pp. 15–17.

149. PROKOPOVICH, I. E. On the theory of creep and long-term resistance of concrete and reinforced concrete structures. In: *Proceedings of the Republican Scientific and Technical Conference "Long-Term Resistance of Concrete and Reinforced Concrete Structures"*. Odesa, 1981, pp. 3–5.
150. KABAILA, A. P., HALL, A. S. Analysis of instability of unrestrained prestressed concrete columns with end eccentricities. In: *ACI Symposium on Concrete Columns*. Special Publication. American Concrete Institute
151. BACHINSKII, V. YA., & AMETOV, YU. G. K otsenke vliyaniya dlitel'nykh protsessov na nesushchuyu sposobnost' izgibaemykh zhelezobetonnykh elementov [On evaluating the influence of long-term processes on the bearing capacity of reinforced concrete bending elements]. *Izvestiya vuzov. Stroitel'stvo i arkhitektura,* 1982, no. 9, pp. 15–20.
152. VASIL'EV, P. I., KONONOV, YU. I., & CHIRKOV, YA. N. Zhelezobetonnye konstruktsii gidrotekhnicheskikh sooruzhenii [Reinforced concrete structures of hydraulic engineering facilities]. Donetsk: Vyshcha shkola, 1982.
153. ZEDGENIDZE, V. A., & POLOVETS, V. I. K voprosu o dlitel'noi nesushchei sposobnosti zhelezobetonnykh balok [On the long-term bearing capacity of reinforced concrete beams]. In: Dlitel'noe soprotivlenie betonnykh i zhelezobetonnykh konstruktsii [Long-term resistance of concrete and reinforced concrete structures], Proceedings of the Republican Scientific and Technical Conference. Odessa, 1981, pp. 86–88.
154. POLOVETS, V. I. Issledovanie nesushchei sposobnosti zhelezobetonnykh balok s obychnoi armaturoi pri dlitel'no deistvuyushchikh nagruzkakh [Investigation of the bearing capacity of reinforced concrete beams with ordinary reinforcement under long-term loading]. Abstract of PhD dissertation. Odessa, 1975.
155. DBN V.2.6-98:2009. Betonni ta zalizobetonni konstruktsii. Osnovni polozhennya [Concrete and reinforced concrete structures. Basic provisions]. Kyiv: Minrehionbud Ukrainy, 2011.

156. VARLAMOV, A. A. *Zhelezobetonnye bruskovye kolonny s dvukhosno-obzhatoi strukturoi betona* [Reinforced concrete bar columns with biaxially compressed concrete structure]. PhD dissertation. Chelyabinsk, 1987.
157. BEKIEV, M. YU., & MAILYAN, L. R. *Raschet izgibaemykh zhelezobetonnykh elementov razlichnoi formy poperechnogo secheniya s uchetom niskhodyashchei vetvi deformirovaniya* [Calculation of reinforced concrete bending elements of various cross-sectional shapes considering descending deformation branch]. Nalchik, 1985.
158. MAILYAN, L. R. *Vliyanie predvaritel'nogo napryazheniya i raspredeleniya armatury na pereraspredelenie usilii v nerazreznykh zhelezobetonnykh balkakh* [Influence of prestressing and reinforcement distribution on force redistribution in continuous reinforced concrete beams]. Abstract of PhD dissertation. Leningrad, 1980.
159. SERYKH, R. L., CHISTYAKOVA, E. A., & KRAMAR', V. G. 27-ya sessiya Evropeiskogo komiteta po betonu [27th session of the European Committee for Concrete]. Beton i zhelezobeton, 1991? no.5, pp. 24–25.
160. MALAKHOVA, A. N., MATKOV, N. G., & LOKOTKOV, M. B. (1990). Avtomatizatsiya eksperimental'nykh issledovanii zhelezobetonnykh konstruktsii [Automation of experimental studies of reinforced concrete structures]. *Beton i zhelezobeton,* no. 10, pp. 25–27.
161. BACHINSKII, V. YA., BAMBURA, A. N., & VATAGIN, S. S. Svyaz' mezhdu napryazheniyami i deformatsiyami betona pri kratkovremennom neodnorodnom szhatii [Relationship between stresses and strains in concrete under short-term non-uniform compression]. *Beton i zhelezobeton*, 1984? no. 10, pp. 18–19.
162. BACHINSKII, V. YA., BAMBURA, A. N., VATAGIN, S. S., & ZHURAVLEVA, N. V. (1985). *Metodicheskie rekomendatsii po opredeleniyu parametrov diagrammy "σ-ε" betona pri kratkovremennom szhatii* [Methodological recommendations for determining parameters of the concrete stress–strain diagram under short-term compression]. Kyiv: NIISK.
163. VATAGIN, S. S. Svyaz' mezhdu napryazheniyami i deformatsiyami betona v szhatoi zone zhelezobetonnykh elementov.

Integral'naya otsenka raboty rastyanutogo betona [Relationship between stresses and strains in the compressed zone of reinforced concrete elements. Integral evaluation of tensile concrete performance]. PhD dissertation. Kyiv, 1987.

164. UZUN, I. A. Realizatsiya diagramm deformirovaniya betona pri odnorodnom i neodnorodnom napryazhennykh sostoyaniyakh [Implementation of concrete deformation diagrams under uniform and non-uniform stress states]. *Beton i zhelezobeton,* 1991, no. 8, pp. 19–20.
165. STOLYAROV, YA. V. Vvedenie v teoriyu zhelezobetona [Introduction to reinforced concrete theory]. Moscow: Stroiizdat, 1947.
166. EVGRAFOV, G. K. O raschete zhelezobetonnykh mostov po teorii predel'nykh sostoyanii [On the calculation of reinforced concrete bridges according to limit state theory]. *Tekhnika zheleznykh dorog*, 1947, no. 12.
167. BAIKOV, V. N., GORBATOV, V. S., & DMITROV, Z. A. Postroenie zavisimosti mezhdu napryazheniyami i deformatsiyami szhatogo betona po sisteme normiruemykh pokazatelei [Construction of the relationship between stresses and strains in compressed concrete according to a standardized indicator system]. *Izvestiya vuzov. Stroitel'stvo i arkhitektura,* 1977, no. 6.
168. ROGOVOI, S. I. *Eksperimental'no-teoreticheskie issledovaniya zhelezobetonnykh elementov s kosvennym setchatym armirovaniem* [Experimental and theoretical studies of reinforced concrete elements with indirect mesh reinforcement]. Abstract of PhD dissertation. Moscow, 1981.
169. KRASNOVSKII, R. O. et al. Analiticheskoe opisanie diagrammy deformirovaniya betona pri kratkovremennom szhatii [Analytical description of the concrete deformation diagram under short-term compression]. *Trudy VNIIFTRI*, 1976, no. 26.
170. PROKOPOVICH, A. A. K opredeleniyu zavisimosti "σ-ε" s nispadayushchim uchastkom betona pri szhatii [On determining the "σ–ε" relationship with descending branch for compressed concrete]. In: *Zhelezobetonnye konstruktsii* [Reinforced concrete structures]. Kuibyshev: KGU, 1979.

171. ZAIKIN, A. I. *Issledovanie nesushchei sposobnosti i deformativnosti vnetsentrenno szhatykh s malymi* ekscentrisitetami elementov iz betonov vysokoi prochnosti [Study of bearing capacity and deformability of eccentrically compressed high-strength concrete elements with small eccentricities]. Abstract of PhD dissertation. Leningrad, 1972.
172. KARPENKO, N. I., MUKHAMEDIEV, T. A., & PETROV, A. N. Iskhodnye i transformirovannye diagrammy deformirovaniya betona i armatury [Initial and transformed deformation diagrams of concrete and reinforcement]. In: *Napryazhenno-deformirovannoe sostoyanie betonnykh i zhelezobetonnykh konstruktsii* [Stress-strain state of concrete and reinforced concrete structures]. Moscow: NIIZhB, 1986, pp. 7–25.
173. KARPENKO, N. I., & MUKHAMEDIEV, T. A. Opredelenie krivizny i udlineniya sterzhnevykh elementov s treshchinami [Determination of curvature and elongation of cracked bar elements]. *Beton i zhelezobeton*, 1981, no. 2, pp. 17–18.
174. KARPENKO, N. I., & ERYSHEV, V. A. Issledovanie deformatsii zhelezobetonnykh balochnykh plit na vetvyakh razgruzki [Investigation of deformation of reinforced concrete beam slabs on unloading branches]. In: *Prochnostnye i deformativnye kharakteristiki elementov betonnykh i zhelezobetonnykh konstruktsii* [Strength and deformation characteristics of concrete and reinforced concrete structural elements]. Moscow: NIIZhB, 1981, pp. 106–128.
175. KARPENKO, N. I. Metodika konechnykh prirashchenii dlya rascheta deformatsii zhelezobetonnykh elementov pri znakoperemennoi nagruzke [Finite increment method for calculating deformations of reinforced concrete elements under alternating load]. In: Sovershenstvovanie konstruktivnykh form, metodov rascheta i proektirovanie zhelezobetonnykh konstruktsii [Improvement of structural forms, calculation methods and design of reinforced concrete structures]. Moscow: NIIZhB, 1983, pp. 3–11.
176. BAMBURA, A. N., BACHINSKII, V. YA., ZHURAVLEVA, N. V., & PESHKOVA, I. N. *Metodicheskie rekomendatsii po utochnennomu raschetu zhelezobetonnykh elementov s uchetom polnoi diagrammy szhatiya betona* [Methodological

recommendations for refined calculation of reinforced concrete elements considering the complete concrete compression diagram]. Kyiv: NIISK, 1987.

177. LEMYSH, L. L. Raschet zhelezobetonnykh konstruktsii s ispol'zovaniem polnykh diagramm betona i armatury [Calculation of reinforced concrete structures using full stress–strain diagrams of concrete and reinforcement]. *Beton i zhelezobeton,* 1991, no. 7, pp. 21–23.
178. CHEKANOVICH, M. G. *Nekotorye osobennosti izgotovleniya i rascheta zhelezobetonnykh konstruktsii, prednapryagaemykh putem natyazheniya armatury na svezheulozhennyi beton* [Some features of manufacturing and calculation of reinforced concrete structures prestressed by tensioning reinforcement on fresh concrete]. Kyiv, 1988.
179. RASSKAZOV, A. O., & CHEKANOVICH, M. G. Chastichno prednapryazhennye konstruktsii s peredachei sil natyazheniya armatury na svezheulozhennuyu betonnuyu smes' [Partially prestressed structures with transfer of reinforcement tension forces to fresh concrete mix]. In: *Konstruktsii iz chastichno prednapryazhennogo betona* [Structures made of partially prestressed concrete]. Bratislava, 1988, p. 58.
180. RASSKAZOV, A. O., & CHEKANOVICH, M. G. Kachestvo i dolgovechnost' zhelezobetonnykh konstruktsii, prednaprya-gaemykh putem natyazheniya armatury na svezheulozhennyi beton [Quality and durability of reinforced concrete structures prestressed by tensioning reinforcement on fresh concrete]. In: *Puti povysheniya kachestva, nadezhnosti i dolgovechnosti konstruktsii inzhenernogo naznacheniya* [Ways to improve quality, reliability and durability of engineering structures]. Khabarovsk, 1988, pp. 37–39.
181. RASSKAZOV, A. O. AND CHEKANOVYCH, M. H. Sposob izgotovleniya predvaritel'no napryazhennykh zhelezobetonnykh konstruktsiy, uluchshayushchiy ikh kachestvo [Method for manufacturing prestressed reinforced concrete structures improving their quality]. *Avtomobil'ni dorohy i dorozhnye budivnytstvo*, 1988, issue 43, pp. 62–65.
182. CHEKANOVYCH, M. H. Armaturnyy element dlya napryazhenno-armirovannykh zhelezobetonnykh konstruktsiy

[Reinforcement element for prestressed reinforced concrete structures]. In: *Modelirovanie i optimizatsiya tekhnologicheskikh protsessov i elementov konstruktsiy sooruzheniy inzhenernogo naznacheniya*. Khabarovsk, 1989, pp. 23–24.

183. RASSKAZOV, A. O., CHEKANOVYCH, M. H. Osobennosti predvaritel'nogo napryazheniya zhelezobetonnykh konstruktsiy pri formovanii [Features of prestressing reinforced concrete structures during forming]. In: *Modelirovanie i optimizatsiya tekhnologicheskikh protsessov i elementov konstruktsiy sooruzheniy inzhenernogo naznacheniya*. Khabarovsk, 1989, pp. 22–23.
184. CHEKANOVYCH, M., CHEKANOVYCH, O. Smart reinforced concrete structures. In: *Proceedings of the fib Symposium "Keep Concrete Attractive"*, Budapest, 23–25 May 2005, pp. 201–206.
185. CHEKANOVYCH, M. G. A new method of prestressing concrete structures. In: *Proceedings of the 13th FIP Congress "Challenges for Concrete in the Next Millennium"*, 1998, pp. 23–29.
186. Chekanovych, M. H., 1995. *Metodyka rozrakhunku mitsnosti obtysnenykh za sposobom na sumish zalizobetonnykh elementiv* [Methodology for strength calculation of reinforced concrete elements compressed by prestressing on fresh concrete mix]. Kherson. Deposited manuscript no. 2524-UK 95, State Scientific and Technical Library of Ukraine.
187. BABICH, E. M., KRUS', A. M., KOPYTMAN, S. M., BEREGOVICH, V. G. Predvaritel'no napryazhennye svai na osnove dlitel'no pressovannogo betona [Prestressed piles based on long-term pressed concrete]. In: *Materialy XVII Respublikanskoy konferentsii UIIVKh*. Rovno, 1969, p. 186.
188. BABYCH, YE. AND ZHUK, YE. Vplyv velychyny napruhy pochatkovoho i tryvaloho presuvannya na mitsnist' betonu [Influence of initial and long-term pressing stress on concrete strength]. *Budivel'ni materialy i konstruktsiyi*, 1973, no. 1, pp. 36–37.
189. BLYSHCHYK, N. P. Osnovy teorii pressovaniya i vakuumirovaniya betonnykh smesey [Fundamentals of the theory of pressing and vacuum processing of concrete mixtures].

In: *Tekhnologiya bezvibratsionnogo formirovaniya zhelezobetonnykh izdeliy*. Minsk, 1979.

190. CHEKANOVYCH, M. H. *Nesucha zdatnist' zalizobetonnykh elementiv, obtysnenykh shlyakhom natyahu armatury na svizhoukladenu betonnu sumish* [Load-bearing capacity of reinforced concrete elements compressed by prestressing reinforcement on fresh concrete mix]. Abstract of PhD thesis. Kyiv, 1993, 18 p.
191. SEMIRNENKO, YU. I. *Rehulyuvannya napruzhenoho stanu v zalizobetonnykh balkakh* [Regulation of stress state in reinforced concrete beams]. PhD thesis. Sumy, 1998, 172 p.
192. ZALESOV, A. S., KLIMOV, YU. A. *Prochnost' zhelezobetonnykh konstruktsiy pri deystvii poperechnykh sil* [Strength of reinforced concrete structures under transverse forces]. Kyiv: Budivel'nyk, 1989.
193. IONOV, Yu. K. *Oborudovanie dlya formirovaniya zhelezobetonnykh izdeliy* [Equipment for forming reinforced concrete products]. Kyiv: Budivel'nyk, 1969.
194. LEMYSH, L. L. Raschet zhelezobetonnykh konstruktsiy s ispol'zovaniem polnykh diagramm szhatiya betona i armatury [Calculation of reinforced concrete structures using complete compression diagrams of concrete and reinforcement]. *Beton i zhelezobeton*, 1991, no. 7, pp. 21–23.
195. LEONHARDT, F. *Spannbeton für die Praxis*. 3rd ed. Berlin–München–Düsseldorf: Ernst und Sohn, 1973, p. 246.
196. MATVEEV, V. G. Issledovanie osnovnykh fiziko-mekhanicheskikh svoystv pressovannogo betona [Investigation of the main physico-mechanical properties of pressed concrete]. In: *Prochnost', nadezhnost' i dolgovechnost' konstruktsiy*. Magnitogorsk: MGMI, 1992, pp. 48–53.
197. CHEKANOVYCH, M. H. Vysokoefektyvni zalizobetonni konstruktsiyi [Highly efficient reinforced concrete structures]. In: *Materialy VI Vseukrayins'koyi naukovo-praktychnoyi internet-konferentsiyi "Budivel'ni materialy, konstruktsiyi ta sporudy tret'oho tysyacholittya"*. Kherson: KhDAEU, 2023, pp. 27–31.
198. PROTSENKO, P. V., VERTELOV, K. M., PUSHKAR', N. I. *Formirovanie konstruktsiy vibronagnetatel'nym sposobom*

[Formation of structures by vibro-injection method]. Moscow: Stroyizdat, 1988.
199. CHEKANOVYCH, M. and Chekanovych, O. Smart reinforced concrete structures. In: *Keep Concrete Attractive. Proceedings of the fib Symposium*, 2005, vol. 2, pp. 1009–1014. Scopus author profile.
200. CHEKANOVYCH, M. H. Eksperymental'ni doslidzhennya mitsnosti ta deformatyvnosti rehulyovanoyi balky Chekanovycha [Experimental investigations of strength and deformability of the regulated Chekanovych beam]. *Tavriys'kyy naukovyy visnyk. Seriya: Tekhnichni nauky*, 2022, pp. 71–82.
201. CHEKANOVYCH, M. H. Utochnennya rozrakhunku zalizobetonnykh elementiv shtuchnykh sporud [Refinement of calculation of reinforced concrete elements of artificial structures]. *Avtomobil'ni dorohy i dorozhnye budivnytstvo*, 1993, issue 51, pp. 107–111.
202. CHEKANOVYCH, M. H. Trubobetonni konstruktsiyi, zmitsneni pozdovzhnim poperednim obtyskom [Concrete-filled tube structures strengthened by longitudinal prestressing compression]. *Zbirnyk naukovykh prats' Poltavs'koho natsional'noho tekhnichnoho universytetu im. Yu. Kondratyuka. Seriya: Haluzeve mashynobuduvannya, budivnytstvo*, 2014, no. 3, pp. 221–226.
203. CHEKANOVYCH, M. Stress-strain state of reinforced concrete beams strengthened with a flexible rod-roller system. *AIP Conference Proceedings*, 2023, pp. 65–69. Scopus author profile.
204. TOOSSI, M., HOUDE, J. Evaluating strength variation due to height of concrete members. *Cement and Concrete Research*, 1981, no. 11 (4), pp. 519–529.
205. LAWRENCE, C. O. The properties of cement paste compacted under high pressure. *Research Report 19, Cement and Concrete Association*. London, 1969, pp. 176–191.
206. ROY, D. M., GONDA, G. R., AND ROBROWSKY, A. Very high strength cement pastes prepared by hot pressing and other high pressure techniques. *Cement and Concrete Research*, 1972, no. 3, pp. 807–820.

207. MATVEEV, V. G. Issledovanie osnovnykh fiziko-mekhanicheskikh svoystv pressovannogo betona [Investigation of the main physical and mechanical properties of pressed concrete]. In: *Prochnost', nadezhnost' i dolgovechnost' konstruktsiy* [Strength, reliability and durability of structures]. Inter-university collection. Magnitogorsk: MGMI, 1992, pp. 48–53.
208. CHEKANOVYCH, M. H. Vysokoefektyvni zalizobetonni konstruktsiyi [High-efficiency reinforced concrete structures]. In: *Materialy VI Vseukrayins'koyi naukovo-praktychnoyi internet-konferentsiyi "Budivel'ni materialy, konstruktsiyi ta sporudy tret'oho tysyacholittya"* [Proceedings of the 6th All-Ukrainian Scientific-Practical Internet Conference "Building Materials, Structures and Constructions of the Third Millennium"]. Kherson: KhDAEU, 2023, pp. 27–31.
209. PROTSENKO, P. V., VERTELOV, K. M., PUSHKAR', N. I. *Formirovanie konstruktsiy vibronagnetatel'nym sposobom* [Formation of structures by vibro-pressure injection method]. Moscow: Stroyizdat, 1988.
210. CHEKANOVYCH, M. AND CHEKANOVYCH, O. Smart reinforced concrete structures. In: *Keep Concrete Attractive. Proceedings of the fib Symposium*, 2005, vol. 2, pp. 1009–1014. Budapest.Scopus author profile.
211. CHEKANOVYCH, M. H. Experimental investigations of strength and deformability of the regulated Chekanovych beam. *Tavriys'kyy naukovyy visnyk. Seriya: Tekhnichni nauky* [Taurian Scientific Bulletin. Technical Sciences Series], 2022, pp. 71–82.
212. CHEKANOVYCH, M. H. Utochnennya rozrakhunku zalizobetonnykh elementiv shtuchnykh sporud [Refinement of calculation of reinforced concrete elements of artificial structures]. *Avtomobil'ni dorohy i dorozhnye budivnytstvo* [Highways and Road Construction], 1993, issue 51, pp. 107–111.
213. CHEKANOVYCH, M. H. Concrete-filled tube structures strengthened by longitudinal prestressing compression. *Zbirnyk naukovykh prats' Poltavs'koho natsional'noho tekhnichnoho universytetu im. Yu. Kondratyuka. Seriya: Haluzeve mashynobudu-*

vannya, budivnytstvo [Collection of Scientific Works of Poltava National Technical University], 2014, no. 3, pp. 221–226.
214. CHEKANOVYCH, M. Reinforced concrete structures with during-tensioning the concrete mix. Kherson State Agrarian and Economic University. Odesa: Oldi+. 2024. 146 p.
215. Toossi, M. and Houde, I., 1981. Evaluating strength variation due to height of concrete members. *Cement and Concrete Research*, no. 11 (4), pp. 519–529.
216. LAWRENCE, C. O. The properties of cement paste compacted under high pressure. *Research Report 19, Cement and Concrete Association*. London, 1969, pp. 176–191.
217. ROY, D. M., GONDA, G. R. AND ROBROWSKY, A. Very high strength cement pastes pepared by hot pressing and other high-pressure techniques. *Cement and Concrete Research*, 1972, no. 3, pp. 807–820.
218. AGOUZAL, E. et al. *Projection-based model order reduction for prestressed concrete with an application to the standard section of a nuclear containment building*. 2024.
219. AGRAWAL, A. et al. *From concrete mixture to structural design – a holistic optimization procedure in the presence of uncertainties.* 2023.
220. ELLIOTT, K. S., MAGILL, M. Precast Prestressed Concrete for Building Structures. *Boca Raton*: CRC Press / Taylor & Francis, 2023. DOI: 10.1201/9781003319450.
221. ZHANG, W., ZENG, J., LI, Z., LIU, Y. *Research on the load-bearing capacity of a new prestressed concrete prefabricated foundation with high lifting resistance.* Buildings, 2024, vol. 14, no. 12, art. 3743. DOI: 10.3390/buildings14123743.
222. WANG, J., YANG, W. Plastic properties of continuous beams of prestressed reinforced concrete with high-strength steel reinforcement. *Applied Sciences*, 2024, vol. 14, no. 2, art. 507. DOI: 10.3390/app14020507.
223. YANG, J., ZHANG, J., LI, H. Durability evaluation of precast prestressed concrete frame structures in chloride environment. *Materials*, 2023, vol. 16, no. 20, art. 6666. DOI: 10.3390/ma16206666.

224. MCGINNIS, M. J. et al. *Experimental and numerical investigation of the bending, shear, and punching shear behavior of recycled aggregate concrete precast/prestressed hollow core slabs*. 2024.
225. TIAN, X. et al. *Flexural behavior and design of prestressed ultra-high performance concrete (UHPC) beams: failure mode and ductility.* 2024.
226. WU, L. et al. *Peridynamic modeling for impact failure of wet concrete considering the influence of saturation*. 2022.
227. ZHAI, K., XU, H., WANG, Y., SHEN, D. Mechanical behavior of prestressed concrete cylinder pipes strengthened with prestressed carbon fiber under secondary loading. *Advances in Structural Engineering*, 2025.

Наукове видання

ЧЕКАНОВИЧ Мечислав Геннадійович

ЗАЛІЗОБЕТОННІ КОНСТРУКЦІЇ З НАТЯГОМ АРМАТУРИ НА БЕТОННУ СУМІШ

Монографія

Дизайн обкладинки В. Савельєва
Технічне редагування О. Гринюк
Верстка Ю. Семенченко

Підписано до друку 06.07.2026 р.
Формат 60×84/16. Папір офсетний.
Цифровий друк. Гарнітура Times.
Ум. друк. арк. 9,30. Наклад 300.
Замовлення № 0526-022.

Видавництво та друк: Олді+
65101, м. Одеса, вул. Інглезі, 6/1,
тел.: +38 (095) 559-45-45, e-mail: office@oldiplus.ua
Свідоцтво ДК № 7642 від 29.07.2022 р.

Замовлення книг:
тел.: +38 (050) 915-34-54, +38 (068) 517-50-33
e-mail: book@oldiplus.ua